

University of Windsor

Scholarship at UWindor

Electronic Theses and Dissertations

Theses, Dissertations, and Major Papers

2013

Characterization of SCF Ubiquitin-Ligase Subunits in Arabidopsis

Mohammad Haj Dezfulian
University of Windsor

Follow this and additional works at: <https://scholar.uwindsor.ca/etd>

Recommended Citation

Dezfulian, Mohammad Haj, "Characterization of SCF Ubiquitin-Ligase Subunits in Arabidopsis" (2013).
Electronic Theses and Dissertations. 4759.
<https://scholar.uwindsor.ca/etd/4759>

This online database contains the full-text of PhD dissertations and Masters' theses of University of Windsor students from 1954 forward. These documents are made available for personal study and research purposes only, in accordance with the Canadian Copyright Act and the Creative Commons license—CC BY-NC-ND (Attribution, Non-Commercial, No Derivative Works). Under this license, works must always be attributed to the copyright holder (original author), cannot be used for any commercial purposes, and may not be altered. Any other use would require the permission of the copyright holder. Students may inquire about withdrawing their dissertation and/or thesis from this database. For additional inquiries, please contact the repository administrator via email (scholarship@uwindsor.ca) or by telephone at 519-253-3000ext. 3208.

Characterization of SCF Ubiquitin-Ligase Subunits in Arabidopsis

by

Mohammad Haj Dezfulian

A Dissertation

Submitted to the Faculty of Graduate Studies
through the Department of Biological Sciences
in Partial Fulfillment of the Requirements for
the Degree of Doctor of Philosophy at the
University of Windsor

Windsor, Ontario, Canada

2013

© 2013 Mohammad Haj Dezfulian



Library and Archives
Canada

Published Heritage
Branch

395 Wellington Street
Ottawa ON K1A 0N4
Canada

Bibliothèque et
Archives Canada

Direction du
Patrimoine de l'édition

395, rue Wellington
Ottawa ON K1A 0N4
Canada

Your file Votre référence
ISBN: 978-0-494-79306-0

Our file Notre référence
ISBN: 978-0-494-79306-0

NOTICE:

The author has granted a non-exclusive license allowing Library and Archives Canada to reproduce, publish, archive, preserve, conserve, communicate to the public by telecommunication or on the Internet, loan, distribute and sell theses worldwide, for commercial or non-commercial purposes, in microform, paper, electronic and/or any other formats.

The author retains copyright ownership and moral rights in this thesis. Neither the thesis nor substantial extracts from it may be printed or otherwise reproduced without the author's permission.

In compliance with the Canadian Privacy Act some supporting forms may have been removed from this thesis.

While these forms may be included in the document page count, their removal does not represent any loss of content from the thesis.

AVIS:

L'auteur a accordé une licence non exclusive permettant à la Bibliothèque et Archives Canada de reproduire, publier, archiver, sauvegarder, conserver, transmettre au public par télécommunication ou par l'Internet, prêter, distribuer et vendre des thèses partout dans le monde, à des fins commerciales ou autres, sur support microforme, papier, électronique et/ou autres formats.

L'auteur conserve la propriété du droit d'auteur et des droits moraux qui protègent cette thèse. Ni la thèse ni des extraits substantiels de celle-ci ne doivent être imprimés ou autrement reproduits sans son autorisation.

Conformément à la loi canadienne sur la protection de la vie privée, quelques formulaires secondaires ont été enlevés de cette thèse.

Bien que ces formulaires aient inclus dans la pagination, il n'y aura aucun contenu manquant.

Canada

Characterization of SCF Ubiquitin-Ligase Subunits in Arabidopsis

by

Mohammad Haj Dezfulian

APPROVED BY:

Dr. Edward M. Golenberg
Wayne State University, Department of Biological Sciences

Dr. Panayiotis O. Vacratsis
Department of Chemistry & Biochemistry

Dr. Andrew D. Swan
Department of Biological Sciences

Dr. Lisa A. Porter
Department of Biological Sciences

Dr. William L. Crosby
Department of Biological Sciences

Dr. William P. Anderson, Chair of Defense
Department of Political Sciences

6 February 2013

DECLARATION OF PREVIOUS PUBLICATION

This thesis includes 1 original paper that has been previously published in peer-reviewed journals, as follows:

Thesis Chapter	Publication title/full citation	Publication status
Chapter 2	Dezfulian MH, Soulliere DM, Dhaliwal RK, Sareen M, Crosby WL (2012) The <i>SKP1-Like</i> Gene Family of Arabidopsis Exhibits a High Degree of Differential Gene Expression and Gene Product Interaction during Development. PLoS ONE 7(11): e50984. doi:10.1371/journal.pone.0050984	Published

I certify that I have obtained a written permission from the copyright owner(s) to include the above-published material in my thesis. I certify that the above material describes work completed during my registration as a graduate student at the University of Windsor.

I declare that, to the best of my knowledge, my thesis does not infringe upon anyone's copyright nor violate any proprietary rights and that any ideas, techniques, quotations, or any other material from the work of other people included in my thesis, published or otherwise, are fully acknowledged in accordance with the standard referencing practices. Furthermore, to the extent that I have included copyrighted material that surpasses the bounds of fair dealing within the meaning of the Canada Copyright Act, I certify that I have obtained a written permission from the copyright owner(s) to include such material(s) in my thesis.

I declare that this a true copy of my thesis, including any final revisions, as approved by my thesis committee and the Graduate Studies office, and that this thesis has not been submitted for a higher degree to any other University or Institution.

DECLARATION OF CO-AUTHORSHIP

I hereby declare that this thesis incorporates material that is result of joint research, as follows:

This thesis incorporates the outcome of a joint research undertaken in collaboration with Danielle M. Soulliere, Rajdeep Dhaliwal, and Madhulika Sareen under the supervision of Dr. William L. Crosby. The collaboration is covered in Chapter 2 of the thesis. In all cases, the key ideas, primary contributions, experimental designs, data analysis and interpretation, were performed by the author, and the contribution of co-authors was primarily through the provision of performing experiments.

I am aware of the University of Windsor Senate Policy on Authorship and I certify that I have properly acknowledged the contribution of other researchers to my thesis, and have obtained written permission from each of the co-authors to include the above materials in my thesis.

I certify that, with the above qualification, the thesis, and the research to which it refers, is the product of my own work.

ABSTRACT

The *Arabidopsis thaliana* genome encodes several families of polypeptides that are known or predicted to participate in the formation of the SCF-class of E3-ubiquitin ligase complexes. One such gene family encodes the Skp1-like class of polypeptide subunits, where 21 genes have been identified and are known to be expressed in *Arabidopsis*. The complexity of this family of *Arabidopsis* Skp1-like – or *ASK* – genes, together with the close structural similarity among its members, raises the prospect of significant functional redundancy among select paralogs. We have assessed the potential for functional redundancy within the *ASK* gene family by analyzing an expanded set of criteria that define redundancy with higher resolution. The criteria used include quantitative expression of locus-specific transcripts using qRT-PCR, assessment of the sub-cellular localization of individual ASK:YFP auto-fluorescent fusion proteins expressed *in vivo*, as well as the *in planta* assessment of individual ASK-F-box protein interactions using BiFC. The results indicated significant functional divergence of steady-state transcript abundance and protein-protein interaction specificity involving ASK proteins in a pattern that is poorly predicted by sequence-based phylogeny. The information emerging from this and related studies was used to functionally characterize using an RNAi approach complemented by phenotypical analysis. The observation of diverse phenotypes not only argues a high level of sub-functionalization has occurred throughout the *ASK* gene family, but also underscores the breadth of functions that this gene family plays throughout plant development.

Transport Inhibitor Response (TIR1), is a member of a family of five Auxin-signaling F-box proteins (AFBs) and has been shown to act as the receptor for auxin

binding and activation of the SCF^{TIR1} complex, leading to targeted protein degradation events involved in auxin perception. We provide evidence for homo-dimerization of TIR1 protein *in planta* together with a role for TIR1 homo-dimerization in the degradation of Aux/IAA proteins as part of the auxin-signaling pathway.

DEDICATION

To my parents, Rahman Dezfulian and Shahnaz Maftooh.

Thank you for a wonderful life.

ACKNOWLEDGEMENTS

First and foremost, I would like to thank my supervisor and mentor Dr. Bill Crosby for giving me this wonderful opportunity to be a part of this lab and for constantly challenging me to expand my knowledge and perspective in science while giving me confidence, guidance, and intellectual freedom. It has truly been an unforgettable learning experience and I will forever cherish the past couple of years. The enlightening discussions, his wealth of knowledge, intellectual freedom bestowed upon me, availability when times were busy, unconditional support, positive attitude and especially the many laughs are all greatly appreciated. I could not have asked for a more understanding or patient advisor. I am deeply indebted to him.

I thank my MSc and PhD committee members Drs. Lisa Porter, Andrew Swan, Panayotis Vacratis and Trevor Pitcher for their unwavering support, enthusiasm, valuable discussions and advice throughout my stay at Windsor. I have learned so much from them. I would like also to thank Dr. Michael Crawford for serving on the comprehensive examination committee and to extend my great gratitude to Dr. Edward Golenberg for agreeing to serve as my external examiner.

I would like to thank my great friend and colleague, Espanta Jalili. Thank you sincerely for all your help in and outside of the lab, for encouraging me to strive to be a better scientist and believing in me. I could have not asked for a better friend.

A special thanks to Danielle Soulliere and Don Karl Roberto. They have been truly instrumental in my scientific endeavors. I could have not achieved much was it not for all their help. I am forever grateful for their help and truly appreciate it.

I would like to thank the members of the Crosby lab for their constant support, help and companionship: Claudia DiNatale, Marta Franczak, Elizabeth Montclam, Rajdeep Dhaliwal, Kerry Khoo, Madhulika Sareen, Mrinal Pal, Seth Munholland, Evgeni Gentchev, Bledi Elshani, Jean Liew, Kim Chipman and Matthew Links. Thank you for being great friends and making my stay in the lab pleasant and joyful.

Thank you everyone for all of the wonderful memories.

TABLE OF CONTENTS

DECLARATION OF PREVIOUS PUBLICATION	iii
DECLARATION OF CO-AUTHORSHIP	iv
ABSTRACT	v
DEDICATION	vii
ACKNOWLEDGEMENTS	viii
LIST OF TABLES	xi
LIST OF ILLUSTRATIONS	xii
LIST OF ABBREVIATIONS AND NOMENCLATURE	xv
CHAPTER 1: General Introduction	1
BIBLIOGRAPHY	50
CHAPTER 2: The <i>SKP1-like</i> Gene Family of Arabidopsis Exhibits a High Degree of Differential Gene Expression and Gene Product Interaction During Development	63
INTRODUCTION	64
MATERIALS AND METHODS	68
RESULTS	78
DISCUSSION	100
BIBLIOGRAPHY	109
CHAPTER 3: Functional Characterization of <i>Arabidopsis SKP1-like</i> Genes	115
INTRODUCTION	116
MATERIALS AND METHODS	120
RESULTS	125
CONCLUSION	144
BIBLIOGRAPHY	147
CHAPTER 4: Dimerization of the E3 SCF^{TIR1} Ligase is Essential for Auxin Signaling	150
INTRODUCTION	151
RESULTS AND DISCUSSION	153
CONCLUSION	173
MATERIALS AND METHODS	175
BIBLIOGRAPHY	177
VITA AUCTORIS	179

LIST OF TABLES

Table 2.1.	Gene names and locus identifiers for genes used in this study.	69
Table 2.2.	Primers used for stop codon removal in Gateway® vectors.	70
Table 2.3.	Plasmid constructs generated in this study.	72
Table 2.4.	Oligonucleotide primers used for qRT-PCR analyses.	76
Table 3.1.	21-nt amiRNA fragments designed against select <i>ASK</i> genes.	121
Table 3.2.	Primers used for genotyping of transgenic plants.	122
Table 3.3.	Oligonucleotide primers used for qRT-PCR analyses.	124
Table 3.4.	amiRNA expression vectors generated throughout this study.	126

LIST OF ILLUSTRATIONS

Figure 1.1.	Crystal structure of ubiquitin.	6
Figure 1.2.	Alignment of ubiquitin protein sequences from different species.	7
Figure 1.3.	General schematic of protein ubiquitination.	8
Figure 1.4.	Ubiquitination patterns serve different functions.	10
Figure 1.5.	Conformation of polyubiquitin chains.	12
Figure 1.6.	Mode of action of RING- and HECT-domain-containing E3 ligases.	14
Figure 1.7.	Crystal of RBX1.	15
Figure 1.8.	Formation of distinct RING-E3 ligases.	17
Figure 1.9.	The SCF-class of E3 ubiquitin ligases.	20
Figure 1.10.	Crystal structure of Arabidopsis and human SKP1.	23
Figure 1.11.	Schematic of the three different classes of F-box proteins.	25
Figure 1.12.	TIR1 is an auxin receptor.	28
Figure 1.13.	Schematic diagram of CUL1 NEDDylation/RUBylation.	30
Figure 1.14.	Oligomerization of SCF ligases.	33
Figure 1.15.	The chemical structure of indole-3-acetic acid	39
Figure 1.16.	COI1 is a jasmonate receptor.	41
Figure 1.17	Gibberellin-mediated degradation of DELLA proteins.	43
Figure 2.1.	Relationship of the <i>ASK</i> gene family in Arabidopsis.	79
Figure 2.2.	Real-time expression analysis of the Arabidopsis <i>ASK</i> gene family.	81
Figure 2.3.	Pearson-based hierarchical clustering of <i>ASK</i> gene expression.	82
Figure 2.4.	Relative organ-specific abundance of cDNAs for select <i>ASK</i> genes.	83
Figure 2.5.	Hierarchical clustering of <i>ASK</i> gene expression.	86

Figure 2.6.	Confocal imaging and sub-cellular localization of ASK proteins in transgenic Arabidopsis.	88
Figure 2.7.	Confocal imaging and sub-cellular localization of YFP:ASK protein fusions in transgenic Arabidopsis.	89
Figure 2.8.	Expression and localization of YFP:ASK8 fusion protein in transgenic Arabidopsis.	91
Figure 2.9.	Confocal imaging and sub-cellular localization of CFP fusion proteins in <i>N. benthamiana</i> .	92
Figure 2.10.	Interaction profile of select ASK and F-Box proteins as assessed using BiFC.	94
Figure 2.11.	Sub-cellular localization of BiFC signals.	95
Figure 2.12.	Interaction profile map of select ASK and F-box proteins.	96
Figure 2.13.	Protein expression verification of the split-YFP fragments in the BiFC assay.	99
Figure 2.14	<i>ASK</i> gene chromosomal location.	105
Figure 3.1.	mRNA transcript abundance for <i>ASK1</i> and <i>ASK2</i> in various mutant backgrounds.	129
Figure 3.2	Phenotypic characterization of <i>ask1/ask2</i> mutant lines.	130
Figure 3.3.	mRNA transcript abundance for <i>ASK3</i> and <i>ASK4</i> in various mutant backgrounds.	133
Figure 3.4.	mRNA transcript abundance for <i>ASK7</i> , <i>ASK8</i> , <i>ASK9</i> and <i>ASK10</i> in various mutant backgrounds.	135
Figure 3.5.	Phenotypic characterization of <i>ask7/8/9/10</i> mutant lines.	137
Figure 3.6.	mRNA transcript abundance for <i>ASK11</i> and <i>ASK12</i> in various mutant backgrounds.	139
Figure 3.7.	Phenotypic characterization of <i>ask11/12</i> mutant lines.	140
Figure 3.8.	mRNA transcript abundance for <i>ASK20</i> and <i>ASK21</i> in various mutant backgrounds.	143

Figure 4.1.	Arabidopsis Aux/IAA protein abundance is regulated by the SCF ^{TIR1} E3 ligase in <i>N. benthamiana</i> .	155
Figure 4.2.	BiFC-based evaluation of homo-dimerization potential of SCF ^{TIR1} components in <i>N. benthamiana</i> .	157
Figure 4.3.	Nuclear and cytoplasmic localization of TIR1 following transient expression in <i>N. benthamiana</i> leaves.	158
Figure 4.4.	Validation of TIR1 homo-dimerization using Co-IP and Y2H	159
Figure 4.5.	TIR1 homo-dimerization is independent of ASK1 homo-dimerization.	162
Figure 4.6.	TIR1 homo-dimerization is independent of Aux/IAA binding.	164
Figure 4.7.	Cys140 and Gly142 mediate TIR1 homo-dimerization.	168
Figure 4.8.	TIR1 homo-dimerization is essential for efficient degradation of Aux/IAA proteins.	170
Figure 4.9.	S-nitrosylation results in an increase in TIR1 protein stability.	172

LIST OF ABBREVIATIONS AND NOMENCLATURE

aa	amino acids
ABRC	Arabidopsis Biological Resource Center
AFB	Auxin F-Box
AFR	Attenuated Far-red Response
Akt	AKT kinase-transforming protein
Ala, A	alanine
amiRNA	artificial ribonucleic acid
APC/C	Anaphase Promoting Complex/Cyclosome
ARF	Auxin Response Factors
ASK	Arabidopsis SKP1-Like
ATP	adenosine triphosphate
ATPase	Adenosine Triphosphate enzyme
Aux/IAA	Auxin/Indolic Acetic Acid
Bar	bialaphos
BiFC	bimolecular fluorescence complementation
bp, Mbp	base pair, mega base pair
BTB	Broad Complex-Tramtrack-Bric-a-Brac
CaMV	cauliflower mosaic virus
CAND1	Cullin-Associated and Neddylation-Disassociated
CASH domain	Carbohydrate-binding proteins and Sugar Hydrolases
Cbf3	Centromere DNA-binding protein complex
CDH1	CDC20 Homolog of CDC twenty 1
CDK	cyclin-dependent kinase
cDNA	complementary deoxyribonucleic acid
CHX	cycloheximide
Co-IP	co-immunoprecipitation
COI1	Coronatine Insensitive 1
Col-0	Arabidopsis Columbia ecotype
COP9	Constitutive Photomorphogenic
CUL1	Cullin1
Cys, C	cysteine
D-box	destruction box
E2-Rad6	radiation damage in protein 6
E2-Ube2W	Ubiquitin-conjugating enzyme E2 W
E3-Rad18	radiation damage in protein 18
EBF	Ethylene Binding F-box
EDTA	ethylenediaminetetraacetic acid
EID1	Empfindlicher im Dunkelroten Licht 1
ETO	Ethylene Overproducer 1
ETP1	EIN2-Targeting Protein1
EYFP	enhanced yellow fluorescent protein
FANDC2	Fanconi anemia group D2 protein
FBL	F-box LRR domain containing protein
FBW	F-Box WD domain containing protein

Fbw7	F-box and WD repeat domain-containing 7
FBX2	F-box only protein 2
FKF1	Flavin Binding, Kelch Repea F-box
GFP	Green Fluorescent Protein
GID1	GA Insensitive DWARF1A
Glu, E	glutamate
Gly, G	glycine
GPS	Global Protein Stability
HECT	Homologous to E6-AP Carboxy Terminus
His, H	histidine
IAA	indole-3-acetic acid
JA-Ile	jasmonyl-isoleucine
JAZ	JA-ZIM domain-containing
kD	kiloDalton
KRP	Kip-Related Protein
Leu, L	leucine
LFY	Leafy
LOV	Light-Oxygen-Voltage
LRR	leucine-rich repeats
Lys, K	lysine
MAX2	More Axillary Branches 2
Met, M	methionine
miRNA	micro ribonucleic acid
MNE	mean number of elements
mRNA	messenger ribonucleic acid
MS	Murashige and Skoog
NEDD4	Neural Precursor Developmentally Down-regulated protein 4
NEDD8	Neural Expressed Developmentally Down-regulated protein 8
NLS	nuclear localization signal
NO	nitrous oxide
nt	nucleotide
ORF	Open Reading Frame
PCNA	Proliferating Cell Nuclear Antigen
PCR	polymerase chain reaction
PI	propidium iodide
PIF	Phytochrome Interacting Factor
qRT-PCR	quantitative reverse transcriptase-polymerase chain reaction
RAV proteins	Regulator of V-ATPase in vacuolar membrane protein
RBX1	RING-Box Protein 1
RFP	Red Fluorescent Protein
RING	Really Interesting New Gene
RNA	ribonucleic acid
RNAi	RNA interference
RUB	Related to Ubiquitin
SCF	SKP1/CUL1/F-box protein
SDS	sodium dodecyl sulfate

SE	standard error
Ser, S	serine
SIGnAL	Salk Institute Genomic Analysis Laboratory
siRNA	small interfering ribonucleic acid
SKP1	S-phase Kinase-associated Protein 1
SKP2A	S-phase Kinase-associated Protein 2A
SLY1	Sleepy1
SNP	sodium nitroprusside
SNY1	Sneezy1
T-DNA	transfer deoxyribonucleic acid
TAIR	The Arabidopsis Information Resource
Thr, T	threonine
TIR1	Transport Inhibitor 1
TRIS	tris(hydroxymethyl)aminomethane
Tyr, Y	tyrosine
UBD	Ubiquitin Binding Domain
UFO	Unusual Floral Organs
Val, V	valine
WD	tryptophan-aspartate repeat-containing domain
Y2H	yeast 2-hybrid
YFP	Yellow Fluorescent Protein
ZTL	Zeitlupe

CHAPTER 1

General Introduction

Arabidopsis thaliana

Advances in the field of molecular biology in the past 30-40 years have resulted in an unprecedented level of insight into the molecular mechanisms governing complex biological processes. At the forefront of these discoveries has been *Arabidopsis thaliana*, a dicot plant species and member of the family *Cruciferae* (mustards), which has been utilized extensively as a model organism to study the function and specific roles of plant genes in the context of plant growth and development. This plant model species is widely used in plant research on the merits of its small stature, large seed set, short generation time (8 weeks), self-compatibility, and relatively small genome (125 Mbp) [1].

Arabidopsis has served as a productive system in which to gain insight in our basic understanding of cell homeostasis and organism development. The benefits of such studies in *Arabidopsis* arise from a combination of the technical benefits of *Arabidopsis* for plant research, combined with a vast array of genetic and genomic resources available for this model plant species [1–3]. These findings have been extrapolated to other non-plant model species, for instance in aspects of our understanding of the development of multi-cellular organisms from single cells or how signals in an organism's environment are integrated during the organism's growth and development. *Arabidopsis* has also contributed significantly (albeit indirectly) to human health as it relates to improving food security through an understanding of plant pathogenesis and productivity, or as a result of contributions *Arabidopsis* has made through the elucidation of the function and contribution of evolutionarily-conserved plant developmental and pathways [4].

Due to the relatively recent divergence of flowering plants from a common ancestor around 150 million years ago [5,6], *Arabidopsis* can be considered to be related

to many of angiosperm plants extant today, making it an ideal model candidate in the realm of plant science.

Plants uniquely face many challenges with respect to changes in their biotic and abiotic environment. Given their sessile nature, plants must adapt to rapid and significant changes (such as changes in temperature or the presence of a pathogen) all without the ability to evade threatening conditions, as is possible with animals. Hence, plants must integrate internal and environmental cues and must respond in such a way to ensure reproductive survival and success. The prominence of this integration can also be visualized by the fact that the plant embryo, unlike animal embryos, contains no adult organs, thus all patterning and post-embryonic development proceeds in close association with the environment. This unique feature of plants should allow for a distinct adaptive strategy different from that observed in the animal kingdom. The adaptive capacity of plants in response to their environment is thought to be achieved through rapid changes to the metabolome and proteome [7,8] but precisely how this process is controlled has been under much speculation and debate. With the availability of the *Arabidopsis* genomic sequence in 2000, and subsequent genomic comparison studies between *Arabidopsis* and other model systems, it was clear that the *Arabidopsis* genome contained a high proportion of genes associated with post-translational protein turnover [9,10]. With the availability of the genome sequence of other plants species, [11–13] a similar pattern was observed suggesting that protein degradation may be a fundamental regulatory attribute of the plant adaptive strategy, and essential for underlying patterning and developmental responses in complex sessile organisms such as plants. However, this hypothesis has not been experimentally verified to date due to technical difficulties associated with assessing

protein degradation in plants. In support of this view, unbiased genetic surveys have connected targeted protein degradation mechanisms with almost every aspect of environmental response and developmental pattern in plants [14–19]. The relatively large number of ubiquitin-associated proteins found in eukaryotes (4% of the entire protein coding repertoire in humans and 6.5% in Arabidopsis) indicates a diverse array of cellular functions in which ubiquitin is involved [23,25–27]

Ubiquitin

Ubiquitin is a small, 8.5-kD polypeptide comprised of 76 amino acids (aa) possessing a mostly rigid structure, characterized by a unique β -grasp fold (**Figure 1.1**) [20]. Ubiquitin's sequence is highly conserved from yeast to humans and Arabidopsis with only four conserved aa substitutions observed suggesting a high degree of evolutionary selective pressure [21], in the regulation of growth and development of multi-cellular organisms (**Figure 1.2**).

Ubiquitination

Ubiquitination is a process of covalent post-translational modification whereby ubiquitin moieties are covalently conjugated via lysine residues within the target protein. Ubiquitination is achieved through the sequential action of three protein complexes as enzymes; an E1 (ubiquitin-activating enzyme), E2 (ubiquitin-conjugating enzyme) and E3 (ubiquitin ligase enzyme) [21–23]. Ubiquitination is initiated generally by ATP-mediated activation of ubiquitin resulting in a thioester bond between ubiquitin and E1 [23]. Activated ubiquitin is subsequently transferred from E1 to E2. The final step of ubiquitination is achieved through the coordinated action of E2 and E3 enzyme resulting in the formation of an iso-peptide bond between the C-terminal tail of ubiquitin's

terminal glycine residue and the ϵ -amino group of a lysine residue found within the substrate [23]. E3s can bind substrates directly or through an intermediate protein, thus determining the specificity of the reaction (**Figure 1.3**). Although ubiquitin is generally conjugated via lysine residues, ubiquitination has also been shown to occur at the N-terminal amino group of substrate proteins and in rare occasions at cysteine and serine residues [24,25].

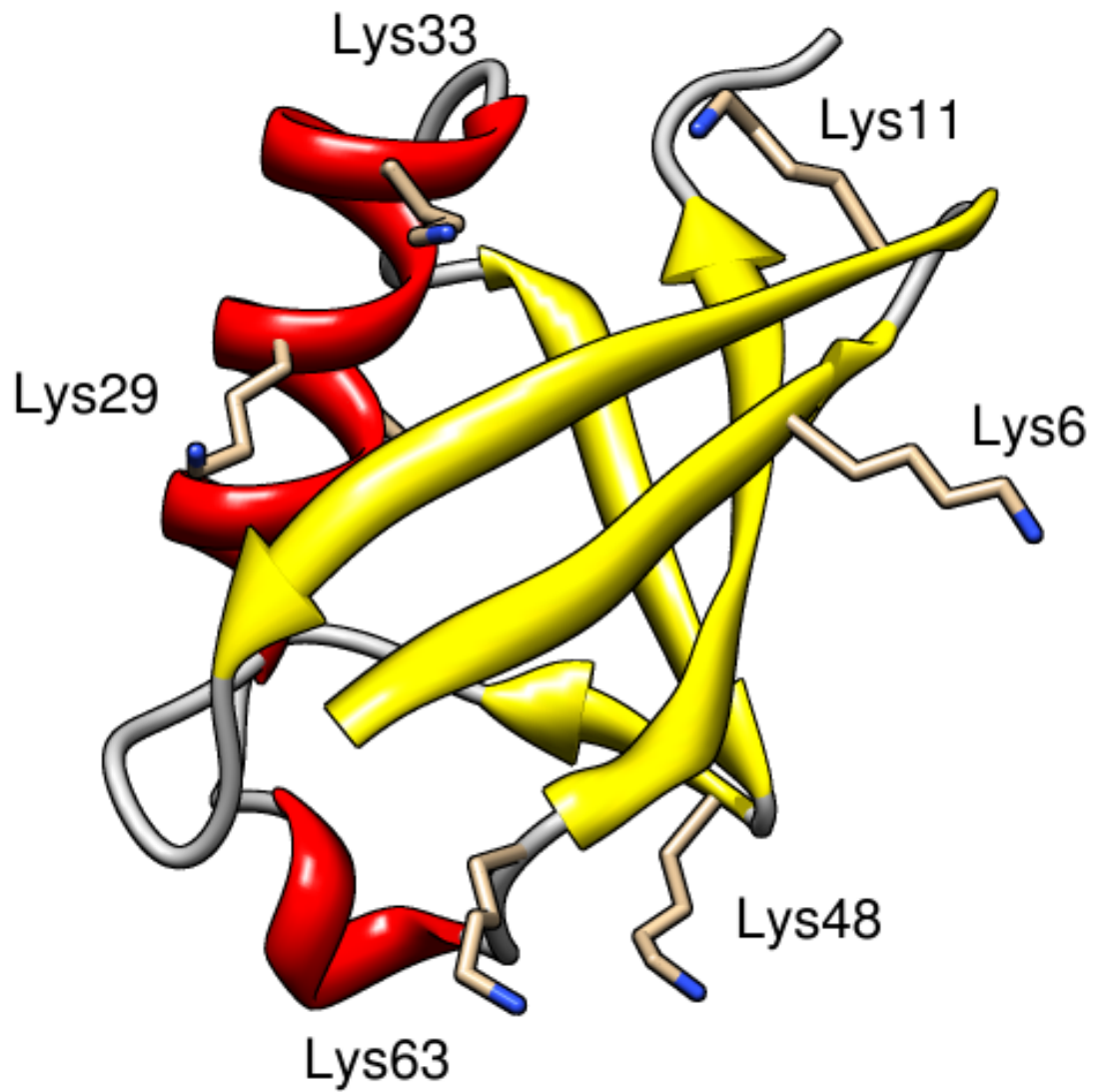


Figure 1.1. Crystal structure of ubiquitin.

Ubiquitin is a small, 8.5-kD protein comprised of 76 amino acids (aa) possessing a mostly rigid structure, composed of 4 β -strands and two helix structures. Ubiquitin proteins across all species have 7 conserved lysine residues essential for mediating ubiquitin-ubiquitin interactions.

```

Danio_rerio          MQIEVKTLLTGGKTTILEVEPPSDTIENVKAKIQDKEGIPPDQRLLIFAGKQLEDGRLLSDYNIQKESTLHLVLRIRGG 76
Mus_musculus        MQIEVKTLLTGGKTTILEVEPPSDTIENVKAKIQDKEGIPPDQRLLIFAGKQLEDGRLLSDYNIQKESTLHLVLRIRGG 76
Drosophila_melanogaster MQIEVKTLLTGGKTTILEVEPPSDTIENVKAKIQDKEGIPPDQRLLIFAGKQLEDGRLLSDYNIQKESTLHLVLRIRGG 76
Homo_Sapiens        MQIEVKTLLTGGKTTILEVEPPSDTIENVKAKIQDKEGIPPDQRLLIFAGKQLEDGRLLSDYNIQKESTLHLVLRIRGG 76
Arabidopsis_thaliana MQIEVKTLLTGGKTTILEVESSDIDNVKAKIQDKEGIPPDQRLLIFAGKQLEDGRLLADYNIQKESTLHLVLRIRGG 76
Oryza_sativa         MQIEVKTLLTGGKTTILEVESSDIDNVKAKIQDKEGIPPDQRLLIFAGKQLEDGRLLSDYNIQKESTLHLVLRIRGG 76
Saccharomyces_cerevisiae MQIEVKTLLTGGKTTILEVESSDIDNVKSKIQDKEGIPPDQRLLIFAGKQLEDGRLLSDYNIQKESTLHLVLRIRGG 76
*****:****:*****:*****:*****:*****:*****:*****:*****:*****:*****:*****

```

Figure 1.2. Alignment of ubiquitin protein sequences from different species.

Alignment of the ubiquitin protein sequences from different species indicates that Ubiquitin is highly conserved protein with minimal amino acid substitutions.

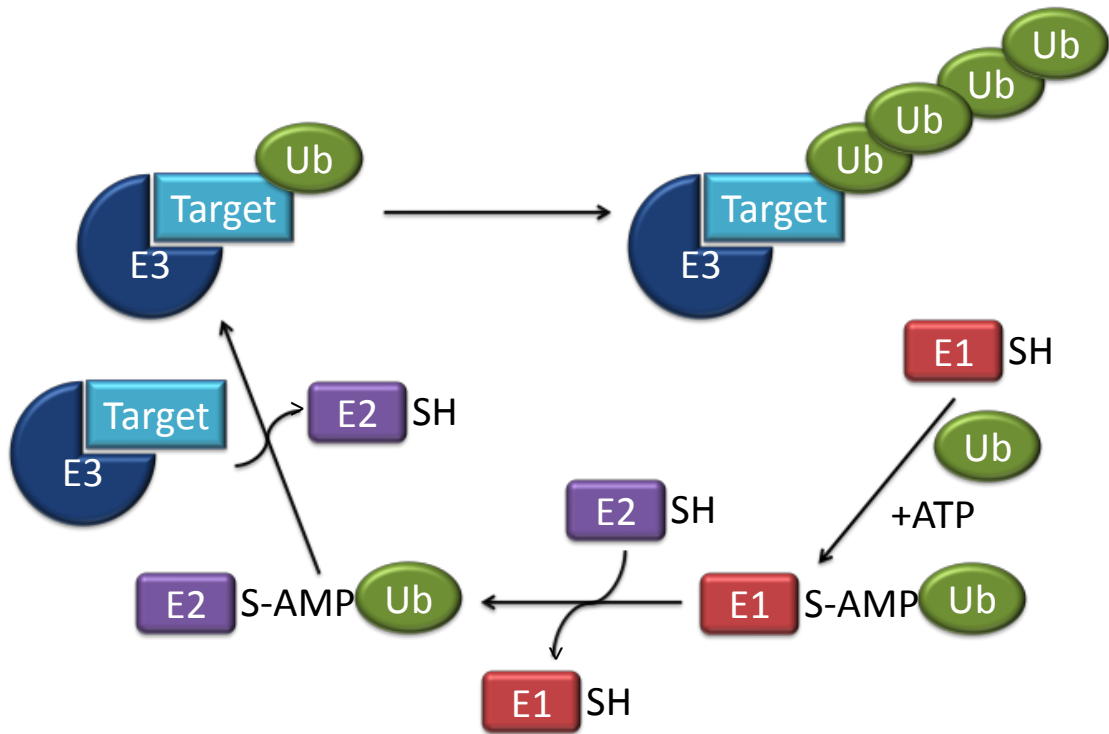


Figure 1.3. General schematic of protein ubiquitination.

In an ATP-dependant manner, ubiquitin is initially activated by the E1 enzyme. Activated ubiquitin is then transferred from E1 to the E2 enzyme. E3 ligases are responsible for the recognition and selection of the substrate protein. Once E3 binds to the substrate, the E2 enzyme is recruited by the E3. Ubiquitin is then transferred from the E2 enzyme to the substrate. The repetition of the above sequence of events allows for the formation of a ubiquitin chain on the protein.

Unlike most other enzymatic processes inside the cell whereby a single enzyme is sufficient for the carrying out a reaction (e.g. protein phosphorylation by kinases), the requirement of three enzymes (E1, E2, and E3) for the ubiquitin-based modification of target proteins has been one of the many challenges complicating the study of ubiquitination as a post-translational regulatory mechanism.

Following the attachment of an initial ubiquitin moiety to a 'target' protein, two distinct paths can be taken: either the protein remains mono-ubiquitinated (**Figure 1.4A**) or the covalently linked ubiquitin is subjected to poly-ubiquitination (**Figure 1.4B**). Poly-ubiquitination is the result of the formation of new iso-peptide bonds between the first ubiquitin moiety and that of additional ubiquitin moieties, either through the N-terminus of the first ubiquitin or within one of its seven lysine residues (Lys6, Lys11, Lys27, Lys29, Lys33, Lys48 and Lys63) [23,25–27]. Substrates harboring all probable linkage types have been identified *in vivo* in several species such as yeast and humans [23,25,28,29]. Poly-ubiquitin chains can be homogenous (the same lysine residues are used for ubiquitin chain formation) or heterogeneous (different lysine residues are used throughout the chain) resulting in a diverse array of conformations and corresponding molecular functions.

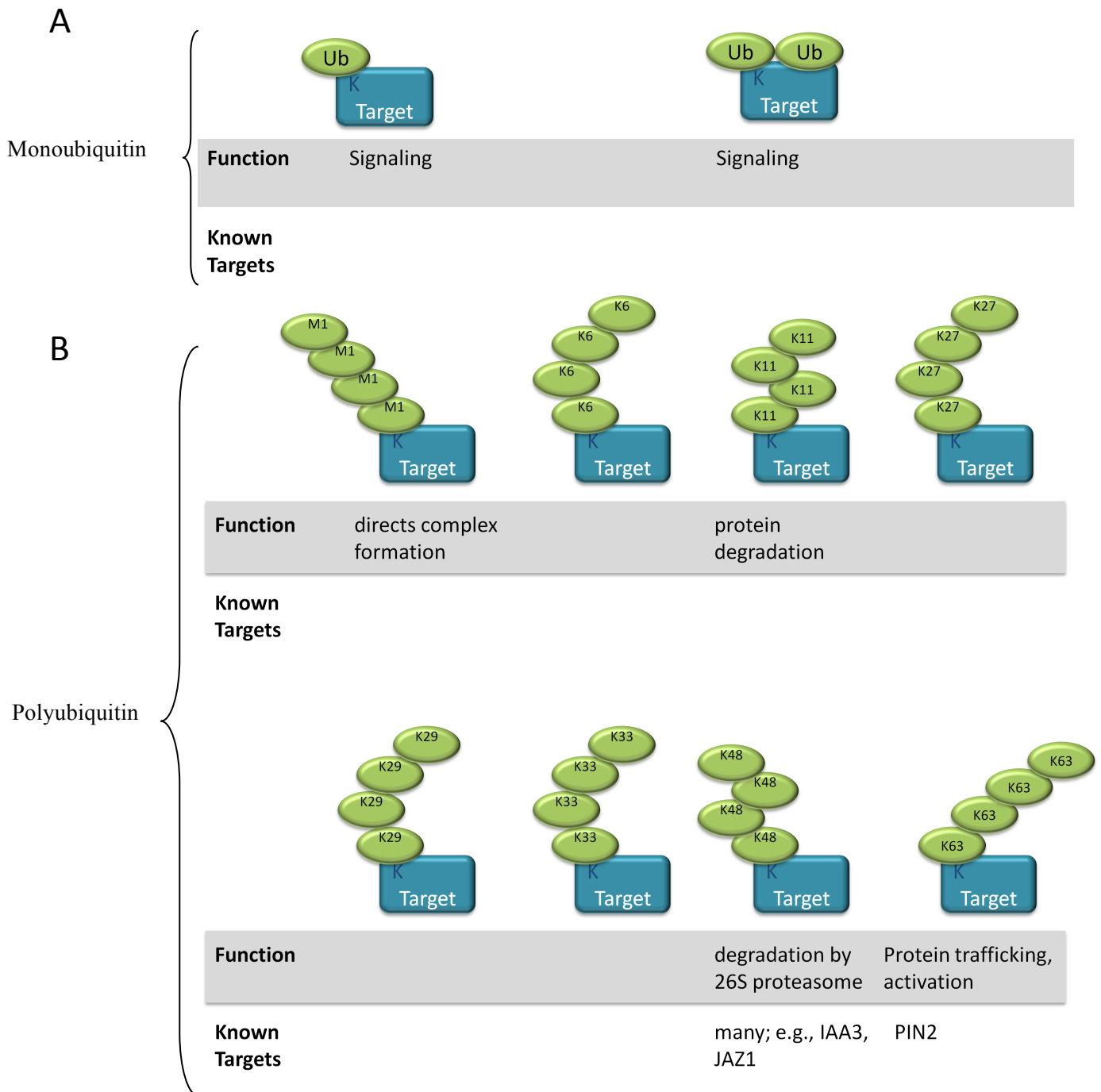


Figure 1.4. Ubiquitination patterns serve different functions.

Ubiquitin binds to a lysine residue within the substrate protein. Proteins can undergo either mono-ubiquitination (mono- or multi-mono-ubiquitination) or poly-ubiquitination. Several known proteins that are subjected to some of these different types of polyubiquitination are provided in this figure.

Little is known about the molecular basis of Ub chain formation and elongation. Based on recent observations, E2 and E3 enzymes collectively dictate the type and the length of the ubiquitin chains to be formed on a target substrate [25,29–31]. Mono-ubiquitination of proteins has been shown to be mainly involved in trafficking and endosomal sorting of proteins [25,32,33].

Mono-ubiquitination or poly-ubiquitination of target proteins is achieved either solely by the catalytic activity of the E2 enzyme (FANCD2 ubiquitination via E2-Ube2W) [34], or in some instances is the result of E3 ligase-mediated inhibition of the conjugative activity of the E2 enzyme (e.g. the ubiquitination of PCNA via E2-Rad6 and E3-Rad18) [35].

With the exception of Lys48 and Lys63 homogenous poly-ubiquitin chains, the function of the remaining linkage classes is not clearly understood. The Lys48-linked chains adopt a closed conformation and have been shown to signal the targeted proteins for degradation via the 26S proteasome (**Figure 1.5A**) [36,37]. Alternatively, Lys63-linked chains adopt an open configuration and mainly act in a non-proteolytic manner for the recruitment of proteins for trafficking and localization (**Figure 1.5B**) [36,37]. Lys11-linked chains also adopt a closed conformation but have a relatively flexible structure compared to that of Lys48 chains (**Figure 1.5C**) [38]. Lys11 chains are primarily produced by the Anaphase Promoting Complex (APC/C) and are involved in mitotic degradation of proteins via the 26S proteasome [39].

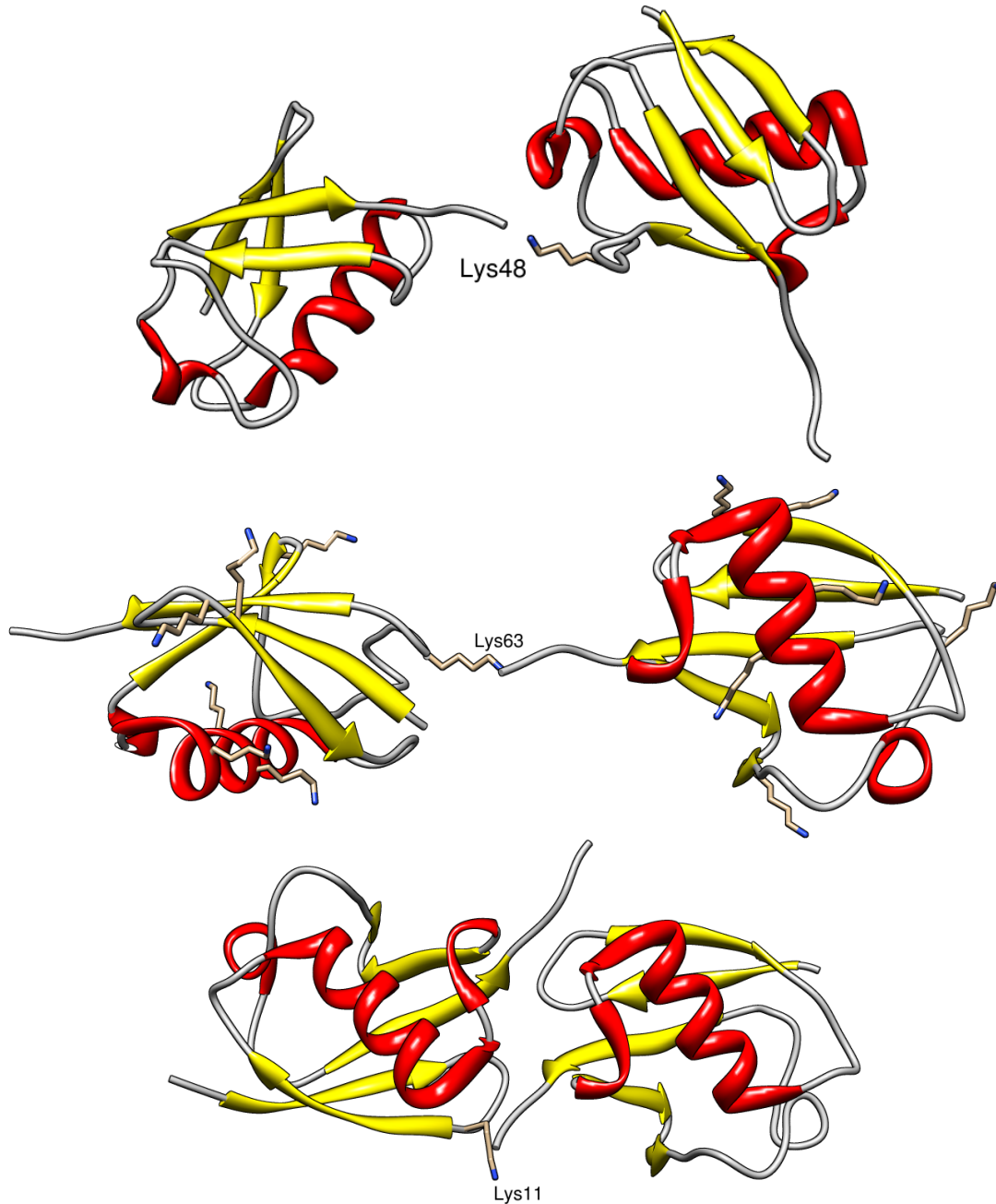


Figure 1.5. Conformation of polyubiquitin chains.

The availability of different lysine residues allows poly-ubiquitin chains to acquire different structural conformations. In the more open structures (K48, K63) the hydrophobic patches are more exposed as opposed to chains that take the closed conformation (K11) where hydrophobic patches are buried within the protein.

The molecular structures and mechanisms underlying the function of the E2 conjugating enzyme, or ubiquitin transfer by E3 ligases, is not yet fully understood. The E3 ligases have been classified into two groups based on their discrete roles in the determination and specificity of substrate ubiquitination and chain formation [40].

The first class of E3 ligases is comprised of the RING-Box containing E3 ligases (RING-E3), where the type and formation of the chain is solely dictated by the type of E2 ligase bound to the RING-E3 ligase [41]. The second group of E3 ligases bear a HECT domain (Homologous to E6-AP Carboxy Terminus) and a catalytic cysteine (Cys) residue that is involved in the transfer of activated ubiquitin from E2 to the HECT-E3 ligase [40,42]. The attachment of the activated ubiquitin to the HECT domain confers on the HECT-E3 ligase the ability to form the ubiquitin chain on the substrate protein (**Figure 1.6**) [42].

RING-E3 Ligases

RING-E3 ligases are conserved across all *eukaryotae* from yeast, humans, and plants. Despite their relatively high abundance, many aspects of structure-function and regulation of these enzymes are poorly understood. An initial description of the RING domains was reported in 1991 by Freemont and co-workers [43]. Subsequently, characterization of the three dimensional structure of the RING domain revealed that buried within its core were conserved Cys and His residues that play an essential role in maintaining the overall structure of the protein through their ability to bind two zinc atoms buried within the core of the RING domain (**Figure 1.7**) [44].

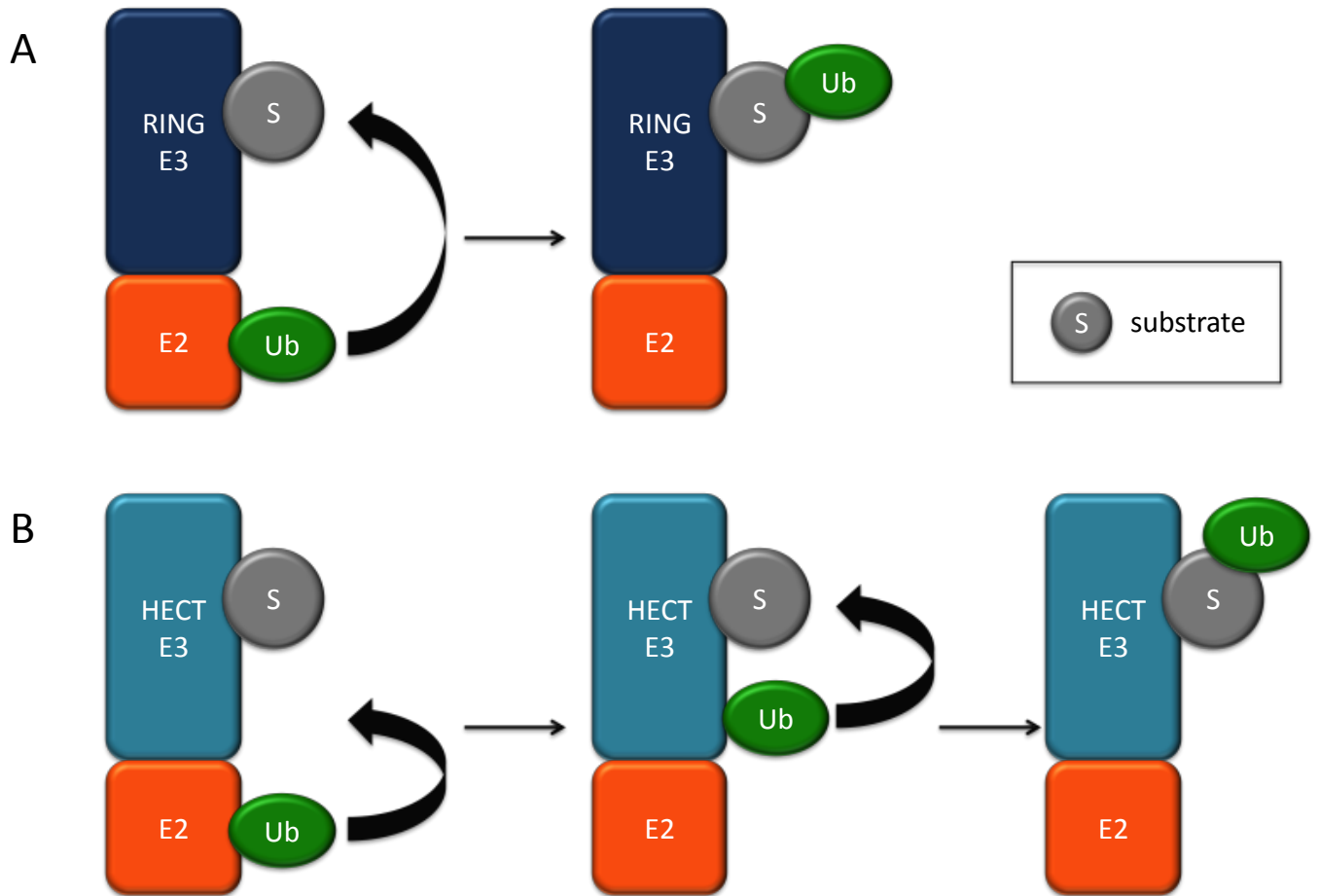


Figure 1.6. Mode of action of RING- and HECT-domain-containing E3 ligases.

E3 ligases are generally categorized into two main classes, the RING and HECT ligases.

A. The RING class comprises the largest class of E3 ligases. Within the RING class the E2 enzyme binds to the RING domain and the activated ubiquitin is transferred directly to the lysine residue on the substrate. **B.** The HECT class possesses a domain that allows for the transfer of the activated ubiquitin from the E2 enzyme to the E3 and then the substrate protein.

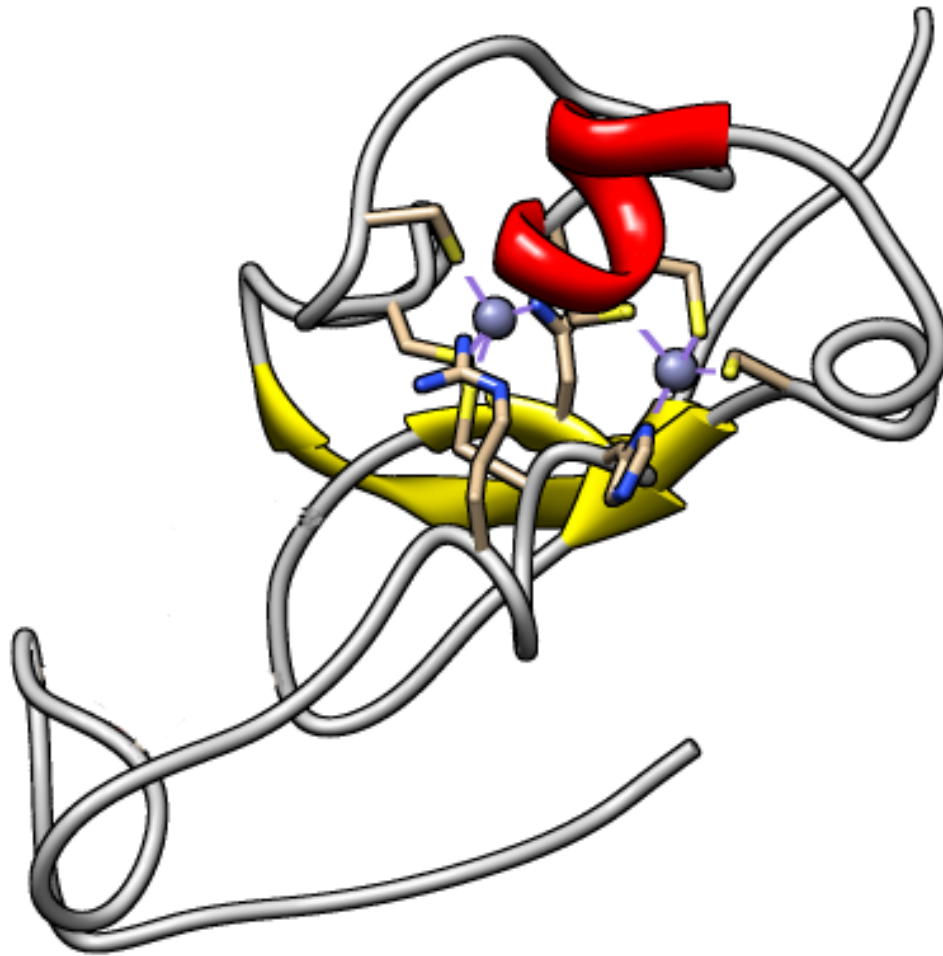


Figure 1.7. Crystal of RBX1.

RING domain-containing proteins are found in most eukaryote species. RING domains are composed of 7 Cys and one His residue (C-X₂-C-X_[9-39]-C-X_[1-3]-H-X_[2-3]-C-X₂-C-X_[4-48]-C-X₂-C). The RING domain in RBX1 protein is responsible for the recruitment of the E2 ligase. All RING domains bind two zinc ions (depicted in purple).

Although the initial connection between the RING domain and ubiquitination was not made until 1999, based on genetic and biochemical studies it was assumed early-on that the RING domain potentially mediates ubiquitination [45].

The first concrete evidence connecting the RING domain and ubiquitination was made by three laboratories who independently showed that a RING domain protein, RBX1, could assemble as part of the SCF sub-class of E3 ubiquitin ligases [46,46,47]. It was later shown that the RING domain mediates ubiquitination by binding to the E2 enzyme, bringing the E2 enzyme in close proximity to the substrate binding subunit of the E3 ligase [48,49].

In some classes of E3 ligases the RING domain co-resides in a single polypeptide with the substrate-binding domain, whereas the majority of E3 ligases have distinct and dedicated subunits that mediate substrate-binding and E2-ligase recruitment, thus allowing for a greater diversity of substrate-binding specificity and Ub chain formation, with a correspondingly more complex role(s) in post-translational protein regulation (**Figure 1.8**) [49]. Of interest is the Cullin-class of E3 ligase complexes, which all share the same RING-domain subunit protein component in RBX1, but possesses different classes of substrate-binding proteins in the form of F-box and BTB-domain subunit proteins [45,49]. It should also be noted that not all RING-Box-containing proteins have explicit E2-binding or E3 ligase activity. However, the majority of RING-Box-containing proteins are believed to be associated with the ubiquitination process [49,50].

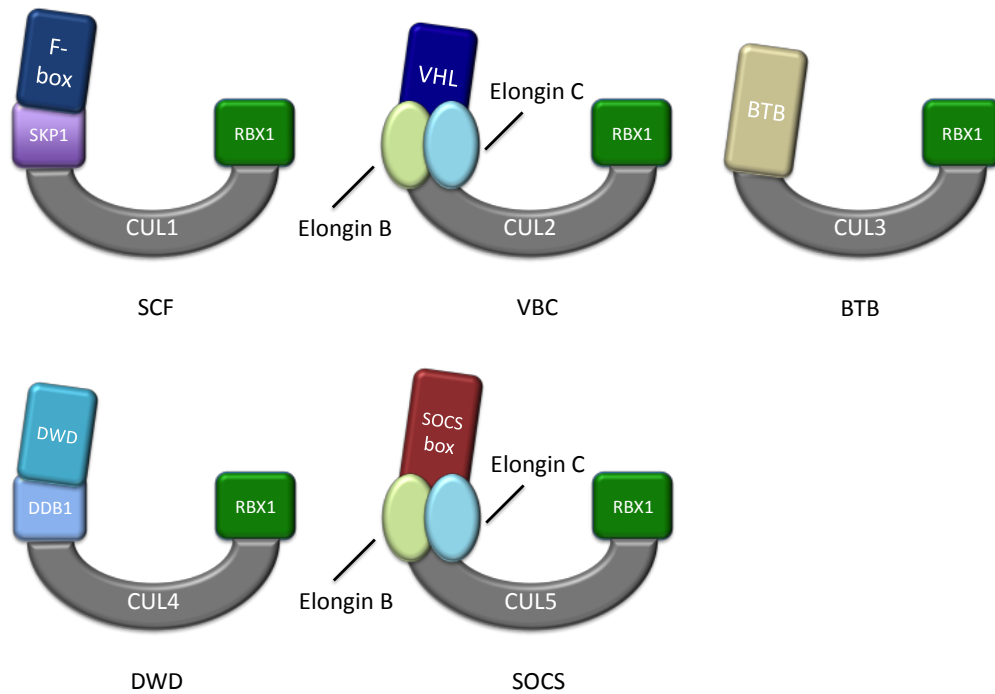


Figure 1.8. Formation of distinct RING-E3 ligases.

The RING E3 ligases are categorized into 5 distinct classes. All E3 ligases can bind to the RBX1 protein. Although distinct Cullin proteins functions as the backbone of the complex, all have a high level of sequence identity at their C-terminus (RING binding domain). With the exception of the BTB class, all other classes have an adaptor subunit connecting the backbone of the complex to the substrate recognition subunit. The adaptor subunit is variable among different classes: SKP1, which binds to CUL1; Elongin B and C, which bind to CUL2 and CUL5; and DDB1, which binds CUL4. In the BTB class, one end of BTB acts as the substrate recognition subunit while the other end is responsible for recognition of the CUL3 protein. F-box, VHL, BTB, DWD and SOCS-box proteins act as substrate recognition subunits for CUL1-, CUL2-, CUL3-, CUL4- and CUL5-based E3 ligases, respectively.

SCF-ligase

SCF-ligases are the largest class of E3 ligases and are believed to be responsible for the targeting of up to 20% of ubiquitinated proteins [50,51]. This class of E3 ligase complexes has been shown to be minimally comprised of 4 subunits: RBX1, CUL1, SKP1 and an F-Box protein, where RBX1 is responsible for the recruitment of the E2 ligase, CUL1 acts as a scaffold for the assembly of SCF ligase, SKP1 acts as an adaptor connecting CUL1 to the F-box protein, and the F-box protein dictates the target specificity of the E3 through substrate selection. (**Figure 1.9**) [52]. The greater part of SCF-ligase function is thought to be the control of protein abundance via ubiquitination and subsequent 26S proteasome-mediated degradation [53]. Although a substantial amount of information has been provided for regulation of the cell cycle, transcription and many other processes via proteasome-bound SCF ligase-mediated protein abundance regulation, the possibility of substrate ubiquitination events mediated by the SCF-ligase which are not subjected to proteasome bound degradation cannot be excluded at this juncture.

CULLIN

Cullin proteins act as scaffolds for the assembly of the CUL-E3 ligase complexes. To date, 7 Cullin proteins have been characterized [53,54]. . While all share the ability to bind to the RBX proteins, each Cullin subunit is distinguished by its ability to directly or indirectly associate with different sets of substrate-binding proteins (**Figure 1.8**). For example, CUL1 exclusively participates in the formation of the SCF-ligase by binding SKP1 via its N-terminus, as well as interacting with RBX1 via its highly conserved C-terminus[55]. A distinguishing characteristic of CUL1 proteins is the rigidity of the

structure and its long, crescent-like shape, although the functional significance of the observed molecular topology has yet to be assessed. It is known that RBX1 alone cannot activate an E2-ligase but, rather, requires an interaction with CUL1 [56]. Hence, CUL1 in conjugation with RBX1 is responsible for the activation of the E2-ligase.

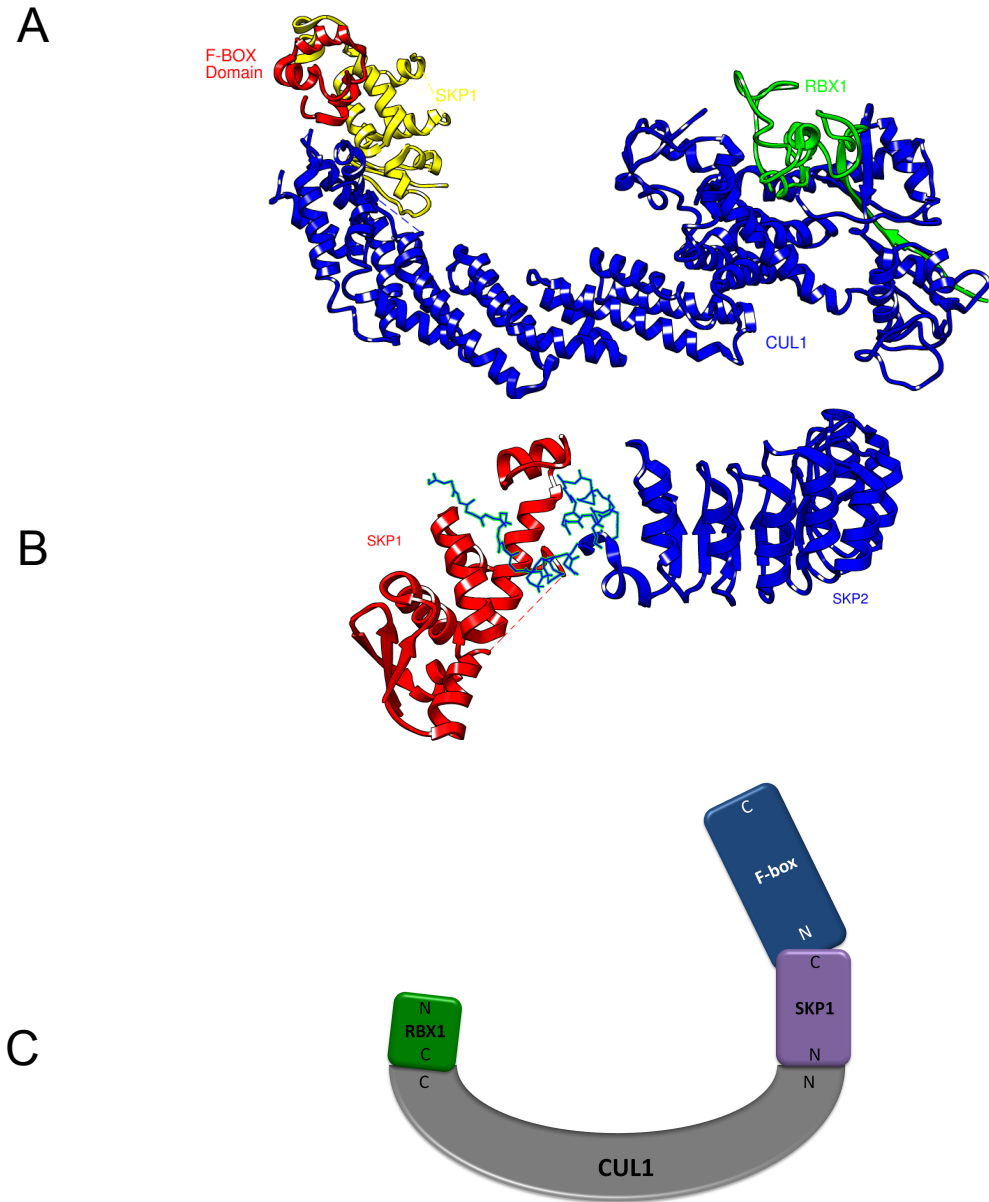


Figure 1.9. The SCF-class of E3 ubiquitin ligases.

The SCF class is composed of four subunits (F-Box, SKP1, CUL1, RBX1). F-box proteins are responsible for recognition and selection of the substrate and bind via their F-box domain (depicted by the stick model in **B**) to SKP1.

SKP1

SKP1 is a small and highly conserved protein of about 160 aa residues (**Figure 1.10**) [57,58]. Various studies have shown that SKP1 associates as a subunit component of different E3 ligase complexes, thus establishing an essential role for SKP1-like proteins in cellular growth and development. For example, protein interaction studies involving both immune co-precipitation pull-down and yeast 2-hybrid (Y2H) approaches have shown that SKP1 associates with a diverse array of proteins such as RAV proteins to form a vacuole ATPase [59] or Cbf3 binding proteins as part of the kinetochore complex [60].

The unusually large number of proteins that SKP1 can associate with, along with the lack of different isoforms, indicates a diverse role for SKP1-like proteins in post-translational regulation [57–60]. SKP1 has been best characterized as the adaptor protein mediating the interaction of the F-box protein with other components of the SCF-ligase **Figure 1.9**. SKP1 recognizes and binds to a semi-conserved 40-aa F-box domain within F-box proteins thus connecting the F-box protein to the remaining subunits comprising the SCF class of E3 ligases. [61].

Our lab's historical interest in the SKP1 protein pre-dates an understanding of the role SKP1 in the structure and function of SCF-ligases. During the course of characterizing the function of mutant alleles of the *Unusual Flower Organs (UFO)* locus (def flowering mutant termed), we showed that the protein product of the *UFO* locus interacted with two proteins (UIP1 and UIP2) [62] that were later defined as Arabidopsis SKP1-like proteins, ASK1 and ASK2, which bore strong primary sequence similarity to yeast the SKP1 protein shown to be involved in yeast cell cycle regulation [63]. In 1999,

following the functional characterization of the F-box domain by others, plus the finding that SKP1 and SKP2 are both subunit components of E3 SCF-ligases [61,63], it was deduced that UFO was an F-box protein that interacted with Skp1-like subunits in a putative E3 Ub ligase complex [62]. There followed an undertaking to annotate the *ASK* gene content of the Arabidopsis genome, with the finding that a total of 21 *ASK* genes are expressed in the Arabidopsis genome. As one aspect of this thesis, I have undertaken a functional analysis of members of this gene family as a contribution to our understanding of why this gene family has been so highly expanded during the course of Arabidopsis evolution.

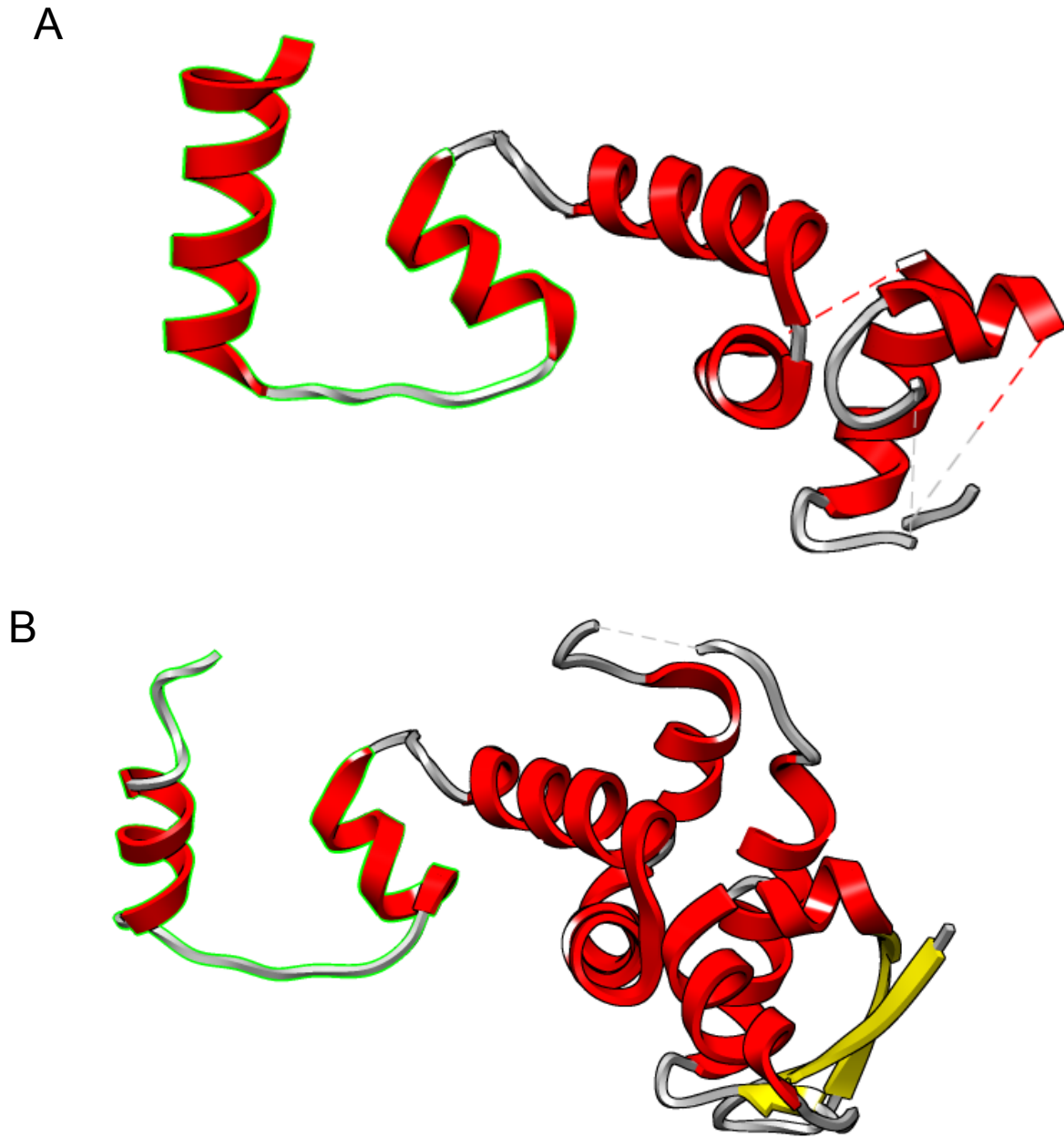


Figure 1.10. Crystal structure of Arabidopsis and human SKP1.

SKP1 is a highly conserved protein among different species. **A.** Crystal structure of the human SKP1. **B.** Crystal structure of Arabidopsis SKP1. All SKP1 proteins display a U-shaped structure (highlighted), which is responsible for recognition and covering of the hydrophobic F-box domain. Of the 200 or so interacting partners identified the majority were two highly similar proteins, which were termed UFO Interacting Proteins 1 and 2.

F-box proteins

F-box proteins are the principal substrate-recognition components of the SCF-ligase [57,61,65]. All F-box proteins possess a semi-conserved stretch of 40-50 aa's denoted as the F-box domain [61]. The name F-box was derived from Cyclin F, the first F-box protein to be characterized. The F-box domain is composed of three highly hydrophobic helices that mediate interaction with SKP1-like proteins [57,65]. The most C-terminal helix of SKP1 is sandwiched between the two N-terminal helices of the F-box protein via an extensively hydrophobic interaction, thus concealing the F-box protein's hydrophobic patch [57,65]. F-box proteins transiently bind to their substrates via various modular domains found within their C-terminus [66,67] and are categorized into three distinct classes based on their substrate-binding domain [68]. F-box proteins that possess a WD-40 domain or leucine-rich repeats (LRRs) are classified as FBW and FBL respectively, and comprise the two largest classes of F-box proteins. FBO is the third class of F-box proteins which contain various C-terminal domains (such as Kelch repeats or CASH domains) or no known motifs (**Figure 1.11**) [69].

Regulation of the SCF ligase

Given the broad-based and essential role that the SCF family of E3-ligases plays in the regulation of cellular processes, stringent regulation of SCF-ligase subunit expression, compartmentalization and assembly is likely. Most regulatory mechanisms identified to date are manifest at primarily the post-translational level and include a plethora of different modifications, from regulation of SCF oligmerization to phosphorylation-dependent binding of substrates [70–73].

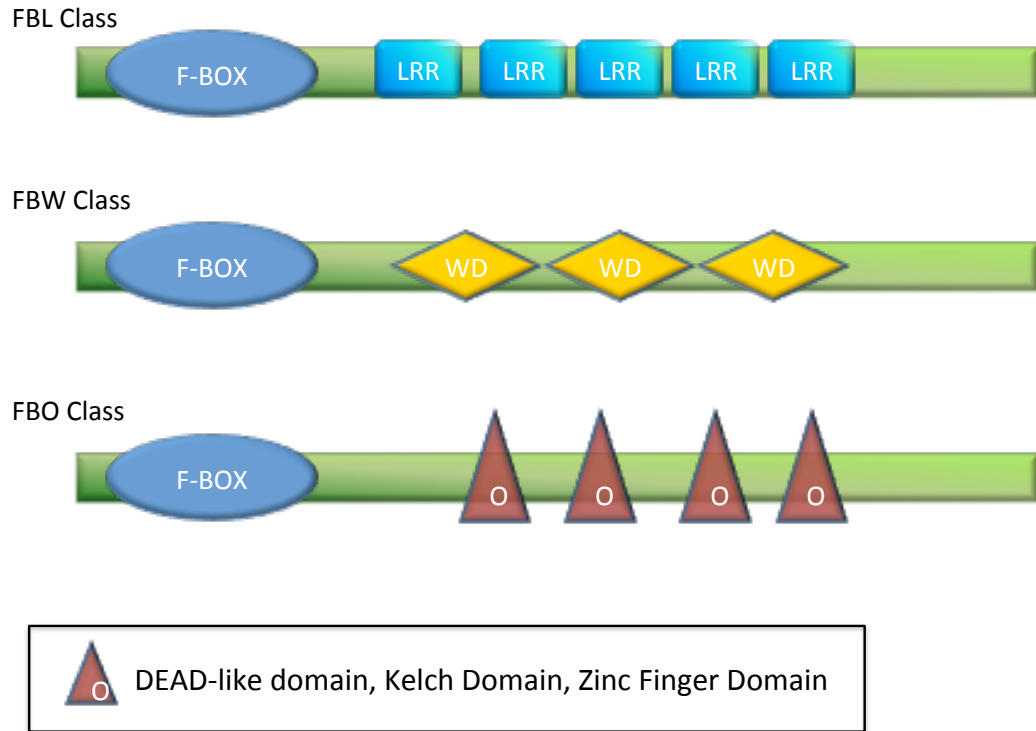


Figure 1.11. Schematic of the three different classes of F-box proteins.

All F-box proteins possess a degenerate F-box domain, which mediates the interaction of the F-box protein with the remainder of the SCF ligase. The F-box proteins use various protein interaction domains for the recognition of different substrates. F-box proteins that possess a WD-40 domain or leucine-rich repeats (LRRs) are respectively called FBW and FBL, and comprise the two largest classes of F-box proteins. FBO is the third class of F-box protein, which contains either various types of domains (such as Kelch repeats or CASH domains) or no known motif.

Post-translation modification of substrates

The selection of substrates for ubiquitination by the SCF ligase is usually achieved via post-translational modification. Chief among these is protein phosphorylation [73,74] of target proteins as a requirement for their binding and selection by the F-box protein. A classic example is the cell cycle regulator p27, which is recognized by the SCF^{SKP2} ligase and subjected to ubiquitin-mediated degradation only after the phosphorylation of Thr187 [75,76]. Although the vast majority of proteins recognized by the SCF-ligases are subjected to phosphorylation, other forms of post-translational modification of substrate proteins have also been reported. For example, the glycosylation of Pre-integrin 1 is required for recognition by the SCF^{FBX2} ligase [77,78]. Despite the essentiality of substrate modification for recognition by the SCF-ligase for the majority of reported substrates, it appears that such modifications are not mandatory. For instance, in the auxin-signaling pathway, SCF^{TIR1} recognition of IAA proteins is not mediated by any form of post-translation modification of the target, but rather by the direct binding of the auxin effector molecule to the subunit F-box protein, TIR1 [77–79].

Regulation of SCF ligases

Regulation of SCF-ligase function can also be achieved via post-translational modification of the E3 ligase at the level of each individual substrate. These forms of regulation are categorized into two principal classes: ubiquitin- or phosphorylation-based modification.

Phosphorylation-based regulation

The F-box protein SKP2 is phosphorylated at Ser64 and Ser72 by two kinases, Akt and Cdk2, respectively [79–81]. These phosphorylation sites are in close proximity to the destruction box motif (D-box) of SKP2. This D-box is responsible for the recognition

and binding of SKP2 to APC^{Cdh1}, ultimately controlling the stability of SKP2 in a 26s proteasome-dependent manner [79,82,83]. The phosphorylation of SKP2 at Ser64 and Ser72 prevents Cdh1 binding, resulting in SKP2's increased stability and abundance [79,84].

High-throughput phospho-proteomics screens have shown that mouse and human SKP1 is also subjected to phosphorylation at a residue that is conserved among its orthologs [79,85,86]. Although the functional significance of this phosphorylation event is not known, the close proximity of the phosphorylation site to the F-box binding region suggests a potential involvement of phosphorylation in F-box binding.

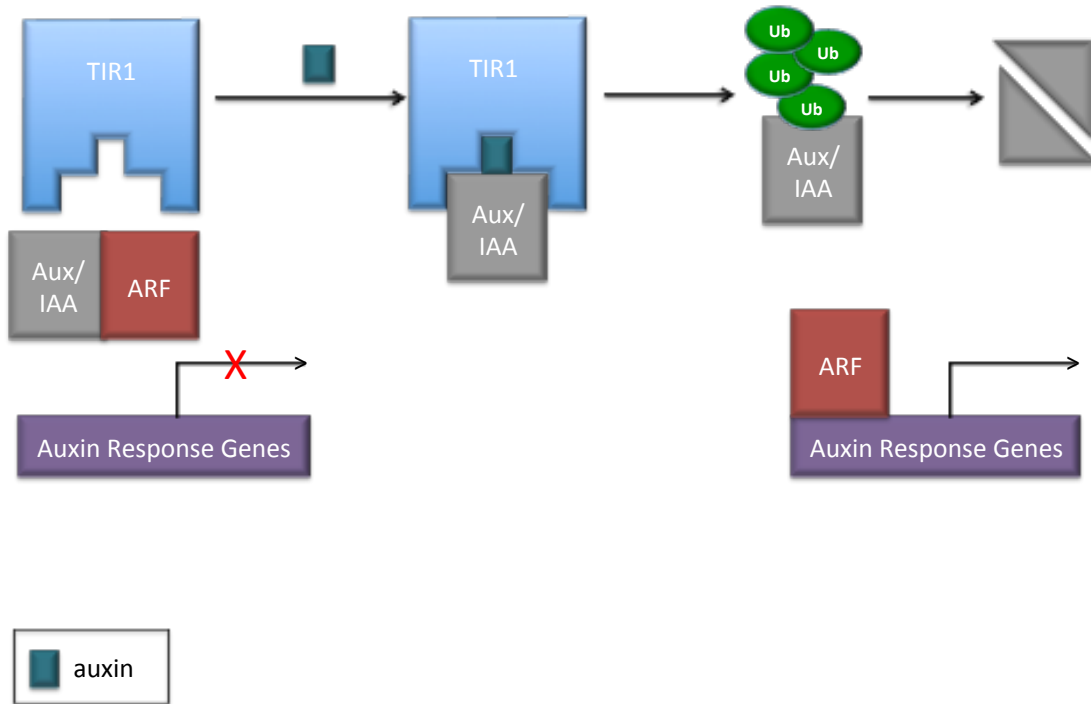


Figure 1.12. TIR1 is an auxin receptor.

The TIR1/AFB family of F-box proteins is the only characterized auxin receptor. The auxin molecule is responsible for enhancing the interaction between the F-box proteins and the Aux/IAA transcriptional inhibitors. The recruitment of Aux/IAA proteins to the $SCF^{TIR1/AFB}$ complex promotes Aux/IAA ubiquitination and degradation. This leads to expression of the auxin response gene under the action of ARFs.

Ubiquitin and ubiquitin-like modifications

Subunit components of the SCF ligase can be regulated via auto-ubiquitination or through modification by the ubiquitin-like protein, Nedd8 [87–90]. For example, F-box proteins have been shown to be subjected to ubiquitination via the same E2 ligase that conjugates ubiquitin to the substrate [91]. This form of auto-ubiquitination is only seen when the F-box protein is not bound to a substrate, suggesting that F-box proteins are stabilized in the presence of substrate protein, and are subjected to proteasome-mediated degradation in the absence of an F-Box-substrate interaction (**Figure 1.13**) [92].

NEDD8-based modification is the most well studied form of SCF regulation [88,90,92]. Nedd8 and ubiquitin share 58% identity and function in a similar manner [93,94]. The NEDDylation of target proteins is achieved via the sequential function of three enzyme complexes also known as E1, E2 and E3. E1 activates Nedd8 while E2 is responsible for conjugation of Nedd8, and finally, E3 is responsible for the selection of the substrate [88,90]. It should be noted here that NEDDylation and ubiquitination require an independent set of E1 and E2 complexes, however no unique E3 ligase responsible exclusively for NEDDylation has so far been identified [95]. It is hypothesized that the same set of E3 ligases responsible for ubiquitination are also utilized for NEDDylation. The CUL1 subunit of the SCF E3 ligase has been shown to be NEDDylated [89–91,93–95]. This NEDDylation occurs at a highly conserved lysine residue within the CUL1 C-terminus, in close proximity to the RBX1 binding site (**Figure 1.13**).

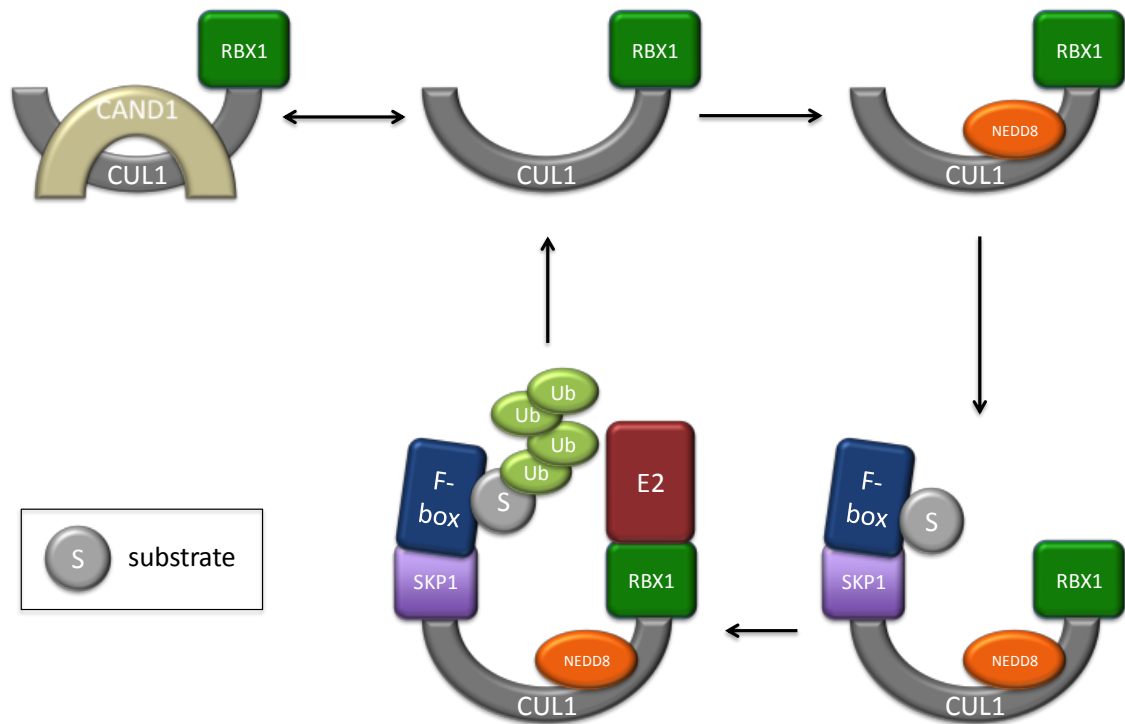


Figure 1.13. Schematic diagram of CUL1 NEDDylation/RUBylation.

NEDDylation/RUBylation of Cullin proteins provides a means of regulation for the RING E3 ligases. CAND1 binds to CUL1 in a competitive manner opposing SKP1 binding to CUL1, thus impeding the formation of a complete SCF ligase. The conjugation of the NEDD8 protein to CUL1 promotes the disassociation of CAND1, which in turn is hypothesized to allow the recruitment of the SKP1-F-box complex. NEDD8 is thought to be detached through the collaborative function of the COP9 signalosome and a deubiquitination enzyme.

The NEDDylation of CUL1 has been shown to be essential for the ubiquitination of select SCF target proteins [88,89,96]. A mutation in the conserved lysine residue of CUL1 results in the accumulation of SCF ligase substrates such as IAA proteins and p27 [97,98]. It is assumed that NEDDylation provides the flexibility that RBX1 needs for the recruitment and retention of E2-ligases [95]. Although the essentiality of subunit NEDDylation for selected target selection and ubiquitination by SCF-ligases has been shown, the extent to which target ubiquitination is generally dependent on CUL1 NEDDylation has not been fully examined. NEDDylation has also been shown to control SCF-ligase homeostasis, where the NEDDylated form of CUL1 – although active – is highly unstable [95,96,98]. De-NEDDylation of CUL1 is mediated by COP9 signalosome, which prevents the degradation of the protein ultimately resulting in the increased stability of CUL1 [99,100]. CAND1 (Cullin-Associated and NEDDylation-Disassociated) binds to unneddylated CUL1 and prevents CUL1 NEDDylation, maintaining the protein in an inactive form [100,101]. The crystal structure of CAND1 in complex with CUL1 has shown that CAND1 wraps around the length of CUL1 thus covering Nedd8 and SKP1 binding sites [100,101]. Although it is known that CAND1 is displaced by the COP9 signalosome, the mechanism by which this is achieved is not understood.

Oligomerization of the complex

Most RING-E3 ligases have been shown to form higher-order structures through hetero- or homo-oligomerization (**Figure 1.14**) [102–104]. The functional significance or the structural determinates of these dimerization events has yet to be fully characterized. Various hypotheses have been put forward for the functional significance of these

oligomerization structures including increased stability of the E3 ligase through the covering of surface- exposed hydrophobic patches, enhanced affinity and efficient ubiquitination of substrate proteins (either through requirement and joint function of two E2 ligases on a single substrate) or aiding in the exposure of inaccessible ubiquitination sites [102,104,105]. The homo-dimerization of the SCF-ligase is thought to be mediated solely via the F-box protein [102,106–108]. To date, all F-box proteins that have been shown to dimerize are all part of the WD-40 class of F-box proteins and contain a short dimerization domain (D-domain). The dimerization of the WD-class of F-box proteins has been shown to be imperative for the functionality of the SCF^{CDC4} [106–109]. Mutations abolishing the ability of the yeast F-box protein Cdc4 to undergo dimerization results in poor ubiquitination of substrate proteins and an inability to rescue the phenotype presented by Cdc4 deletion mutants of yeast [105]. Homo-dimerization of Fbw7 is influenced by the phosphorylation of a Ser residue located close to the D-domain, providing a means for regulated dimerization [110]. In cancerous cells, mutations in Fbw7 more commonly occur within the D-domain than in any other region of the protein, emphasizing the functional significance of Fbw7 homo-dimerization in the transformed state [111]. F-box proteins that do not possess a dimerization domain such as the FBL and FBO classes, are thought to function solely as monomers, although no experimental data has been provided to support this hypothesis [50].

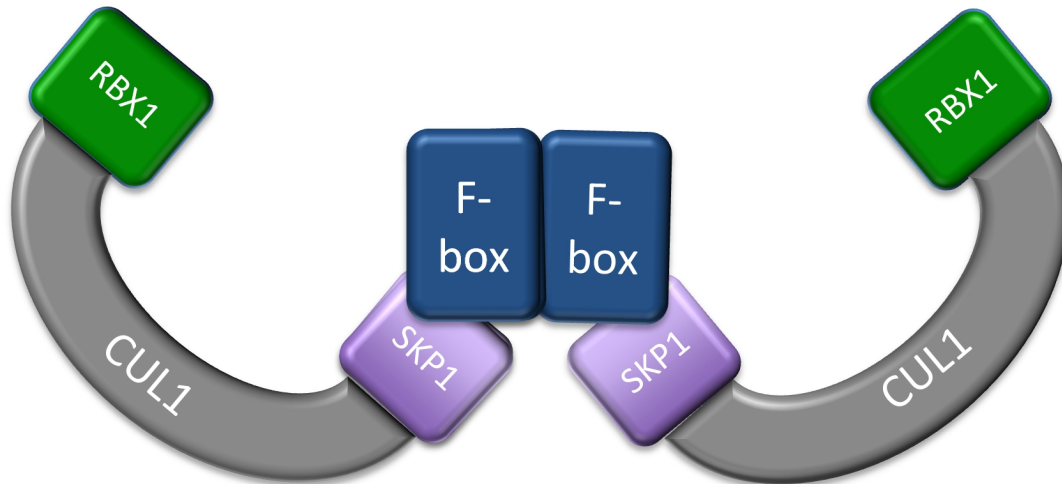


Figure 1.14. Oligomerization of SCF ligases.

SCF dimerization has been shown to be mediated via their substrate recognition subunit, the F-box protein. Although the functional relevance of this dimerization is not clearly understood, it has been shown that dimerization of select F-box proteins is essential for substrate recognition and ultimately ubiquitination and degradation of said substrate mediated by the SCF ligase. It is hypothesized that the availability of two E2 ligases within close proximity of the substrate can result in a more efficient ubiquitination of the substrate than the presence of a single E2. There is also the possibility that F-box homodimerization increases its affinity for the substrate.

Ubiquitination in Arabidopsis

Following the sequencing and subsequent annotation of the Arabidopsis genome, it was evident that genes known or predicted to participate in the post-translational ubiquitination machinery are highly elaborated in the Arabidopsis genome. It is estimated that nearly 6% of the protein-coding capacity of the genome is involved in the selection and ubiquitination of the proteome, with nearly 1400 proteins thought to act as potential E3 ligases [112,113]. Interestingly, in yeast roughly 150 genes (or 2.5% of the genome) are dedicated to this same process. Along with phylogenetic-based genomic studies, unbiased genetic surveys have also emphasized the importance of the ubiquitin machinery in plant growth and development [114–117]. These studies have shown that almost every aspect of plant growth and development including cell cycle, hormone signaling, environmental response and the like are regulated by the ubiquitination machinery [113,115–117].

In the Arabidopsis genome, the F-box protein family constitutes the largest E3 Ub ligase subunit family with at least 700 F-box proteins known to be expressed, in contrast to the human and yeast genome that encode for only 68 and 12 F-box proteins, respectively[118]. Furthermore, the third largest gene family in Arabidopsis is the RING-domain containing protein family with 480 members [113], which is an order of a magnitude more complex than the corresponding gene set in yeast and humans comprised of 48 and ~120 members, respectively [118]. Sheer numbers indicates that in comparison to other non-plant model species such as *S. cerevisiae*, *C. elegans*, *D. melanogaster*, *D. rerio*, *M. musculus* and even *H. sapiens*, ubiquitination-associated genes are highly expanded in Arabidopsis [118]. It should be noted that this elevated level of gene

complexity is not unique to *Arabidopsis* and can be found in other plant species such as *Oryza sativa*, *Populus trichocarpa* and *Zea mays*, all of which possess a large number of genes dedicated to the ubiquitination machinery [12].

Several hypotheses have been postulated as to the evolutionary benefits that may accrue from the expansion of the ubiquitination machinery for the plant adaptive strategy, however none have been experimentally substantiated. One possible explanation is that plants are transparent to their environment and rely on post-translational mechanisms to rapidly modify their cellular processes in response to changes in their environment [118]. This hypothesis can be validated by comparing the collection of ubiquitinated proteins – or the “ubiquitome” – of the plant prior to and following exposure to environmental changes. Another possibility for the expansion of this genes family arises from a comparison of the number of ubiquitination-related genes in the genomes of herbaceous versus woody plants, where woody plants contain a smaller repertoire of ubiquitination-related genes. The larger numbers in herbaceous plants could be an indirect result of the rapid life-cycle that the plant must undergo within a single growth and reproductive season. This suggestion is supported by the number of genes in a model species that possesses a shorter life cycle, such as *C. elegans* (21 *SKP1* and 326 F-box genes) is in sharp contrast to lone *SKP1* and ~ 70 F-box proteins expressed in humans and mice [118]. Another possibility could be that the high number of genes is merely the result of polyploidy through whole-genome duplications - a common evolutionary feature within the plant kingdom. However, if one accepts this hypothesis, the retention of such a large family of genes during plant evolution must also be explained. For instance, although there are 200 pseudo-F-box proteins in *Arabidopsis*, there are 700 functional F-box genes

that have been annotated within the genome. A counterargument that can be made for the retention of such a high number of ubiquitination related genes might be the neo-functionalization of a number of genes within the family. While the literature lacks any experimental evidence supporting this hypothesis, one could recognize this as a viable alternative. To test this hypothesis one would have to compare the expansion and retention of phylogenetic clades. For instance, if one assumed that neo- or sub-neo-functionalization is occurring within a certain clade associated with the new function that clade should exhibit signs of rapid evolution relative to the clades that are associated with the retained functions.

SCF-ligase in Arabidopsis

The Arabidopsis genome expresses 5 of the 7 known Cullin subunit proteins (Cul1, Cul2, Cul3A, Cul3B and Cul4) found in humans and yeast [113,119], all of which are able to assemble as part of Cullin-based E3 ligases and play an essential role during plant growth and development [119,120,120]. Arabidopsis CUL1 has been extensively shown to assemble as part of Arabidopsis SCF-ligases. Unlike the other components of the SCF ligase, one and two genes encode CUL1 and RBX1, respectively [119,120]. Other subunit components of the SCF-ligase in Arabidopsis such as ASK1 (Arabidopsis SKP1-like protein) and F-box proteins are encoded by large gene families comprising 21 and 700 genes, respectively, accounting for almost 2.5% of the coding capacity of the genome [118]. The large number of SCF-related genes allows for the assembly of a combinatorially diverse set of SCF-ligase complexes, providing the means for the targeting of a complex spectrum of different proteins for ubiquitination. Signifying the importance of this complex throughout the plant development are the severe

developmental defects associated with loss-of-function alleles of genes encoding broadly functional SCF components such as *ASK1*, *ASK2*, *RBX1*, *RBX2* and *CUL1* [117,120–122].

SCF ligases and hormone regulation

Plant hormones are small molecules synthesized by plants that have a broad impact on plant growth and development. Plant hormones include such compounds as auxin, jasmonic acid, cytokinin, abscisic acid, gibberellin, ethylene and brassinosteroid [123]. Over the past 20 years, genetic studies have elucidated pathways that lead to the biosynthesis and regulation of these hormones including how these hormones exert their effects. Interestingly, a common theme among most of these hormones is the utilization of the ubiquitination machinery – more specifically, the SCF-ligase class of E3 Ub ligases – to control the abundance of specific activators and repressors of hormone-signaling pathways [124]. Moreover, some can even initiate substrate binding through their direct binding to components of the SCF-ligase [124,125]. I describe here, in some detail, the mechanism and function of several of these hormones and how they interplay with the SCF ligase machinery.

Auxin signaling

The plant hormone auxin, or indole-3-acetic acid (IAA), is a small amphipathic molecule (175.184 MW) (**Figure 1.15**) that has a central role in plant growth and development [123]. Auxin signaling is achieved through the regulation of a set of transcription factors known as auxin response factors (ARFs) which act as either negative or positive regulators of auxin response genes [123,125]. A family of five auxin F-box (AFB) proteins has been extensively characterized to act as co-receptors for the IAA

molecule [125–128]. The binding of IAA enhances the affinity of these AFBs for Aux/IAA transcription factors, which act as negative regulators of ARFs. In the presence of auxin, Aux/IAA proteins are targeted for ubiquitin-mediated degradation via the 26S proteasome. The Arabidopsis genome expresses 5 AFB and 29 Aux/IAA proteins. While no experimental data has been provided, it has been suggested that the combination of the different AFB and Aux/IAA proteins along with diverse set of affinities observed between the two groups of proteins provides a means for auxin to play diverse roles during growth and development [128,129]. At this juncture, the possibility that auxin could have additional unidentified receptors cannot be excluded and further experimental data is required to validate the above hypothesis.

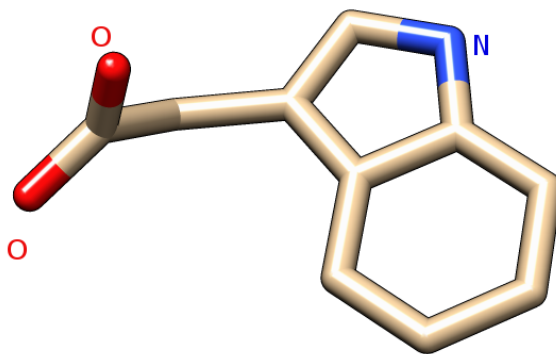


Figure 1.15. The chemical structure of indole-3-acetic acid.

The plant hormone auxin, or indole-3-acetic acid (IAA), is a small amphipathic molecule (175.184 MW).

Jasmonate signaling

Jasmonates are a group of small molecules composed of jasmonic acid and its derivatives, which are responsible for the mediation of biotic and abiotic responses in plants [123]. *COI1* encodes an F-box protein that is structurally similar to AFB, and was one of the first components discovered in the jasmonate signaling pathway [116,123,130,131]. The jasmonate signaling pathway is now known to be highly reminiscent of the auxin-signaling pathway in several respects. Jasmonate ZIM domain-containing (JAZ) proteins act as negative regulators of jasmonate signaling through their interaction with MYC2 transcription factors. MYC2 transcription factors have been shown to act as direct effectors of jasmonate response genes. The JAZ proteins are targeted for degradation via SCF^{COI1} in the presence of jasmonic acid thus allowing MYC2 transcription factors to coordinate the expression of jasmonic acid response genes (**Figure 1.16**) [131]. Structural studies have revealed that jasmonic acid binds directly to COI1 and in turn increases the affinity of COI1 for JAZ proteins [130]. To date, COI1 is the sole identified receptor for jasmonic acid, although the broad range of functions that jasmonate can play suggests that additional receptors remain to be discovered.

Gibberellin signaling

Gibberellin is a plant steroid-based plant hormone that can regulate a diverse set of functions in plants, such as cell division and timing of flowering [123]. DELLA proteins have been shown to act as negative regulators of gibberellin signaling through their direct interaction with a set of transcription factors, PIF3 and PIF4 [125].

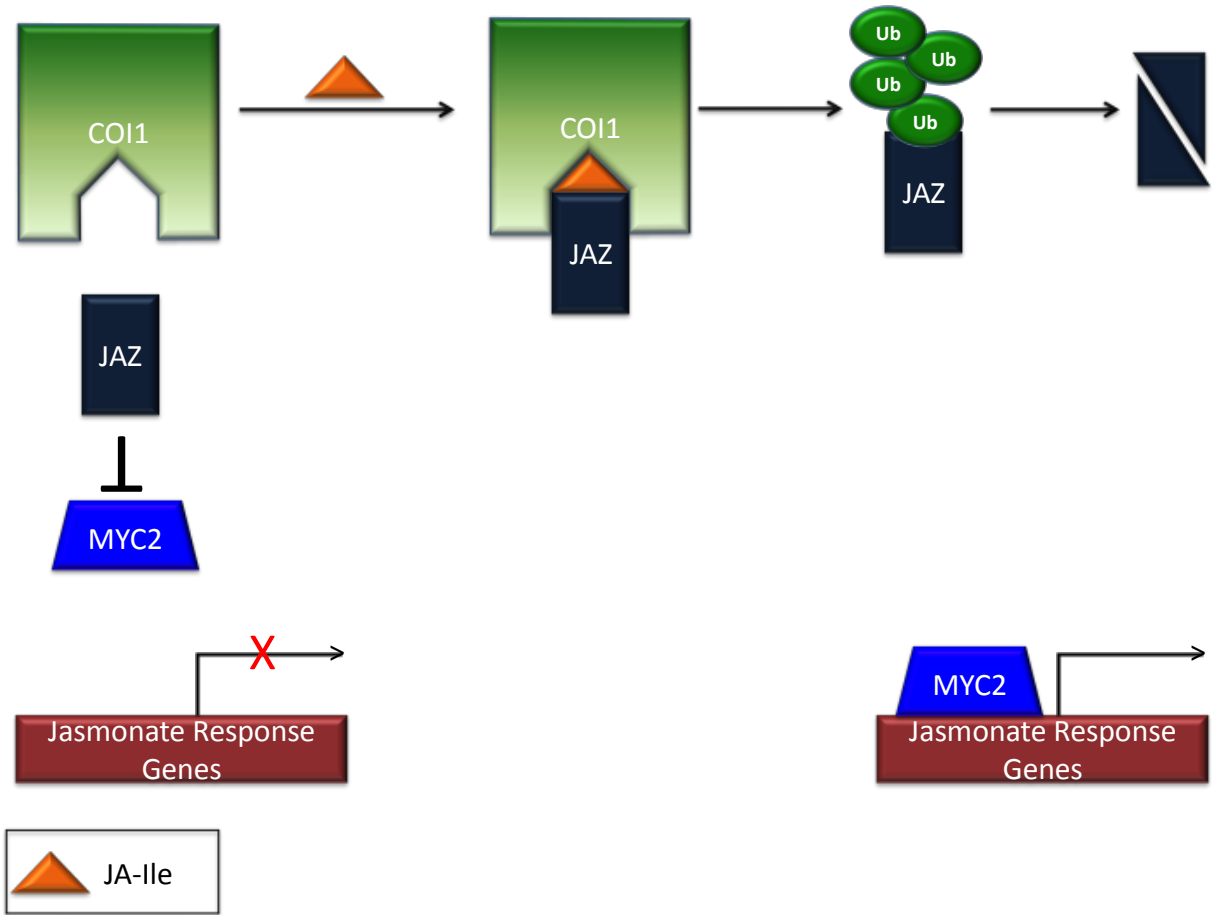


Figure 1.16. COI1 is a jasmonate receptor.

COI1 is the main receptor for the jasmonate (JA) molecule. The binding of jasmonyl-isoleucine (JA-Ile) to COI1 enhances the recruitment of JA response inhibitors, the JAZ proteins. Binding of JAZ proteins to SCF^{COI1} results in the ubiquitination and degradation of these JAZ proteins, resulting in the derepression of the MYC2 transcription factor.

PIF3 and PIF4 are responsible for the activation of expression of gibberellin response genes [125]. DELLA proteins are subjected to proteasome-mediated degradation via the SCF ligase harboring the F-box proteins SLEEPY1 (SLY1) or SNEEZY1 (SNY1) in the presence of gibberellin [125,132]. Unlike auxin and jasmonate, gibberellin does not directly bind to the F-box proteins but rather to a different protein, GID1. GID1 acts as co-factor and mediator between SLY1/SNY1 and the DELLA proteins (**Figure 1.17**) [125,132]. The mode of GID1 action resembles that of CKS1 in SCF^{SKP2}, which is responsible for the degradation of p27 in the regulation of cell cycle progression [133].

SCF-ligase and other hormones

The SCF ligase has also been shown to regulate other hormone signaling pathways, such as strigolactone signaling mediated by the F-box protein MAX2, or the ethylene-signaling pathway. In the latter case, not only are F-box proteins involved in controlling signaling (EBF1 and EBF2), but also in the regulation of ethylene synthesis (ETO1 and ETL1) [125,134].

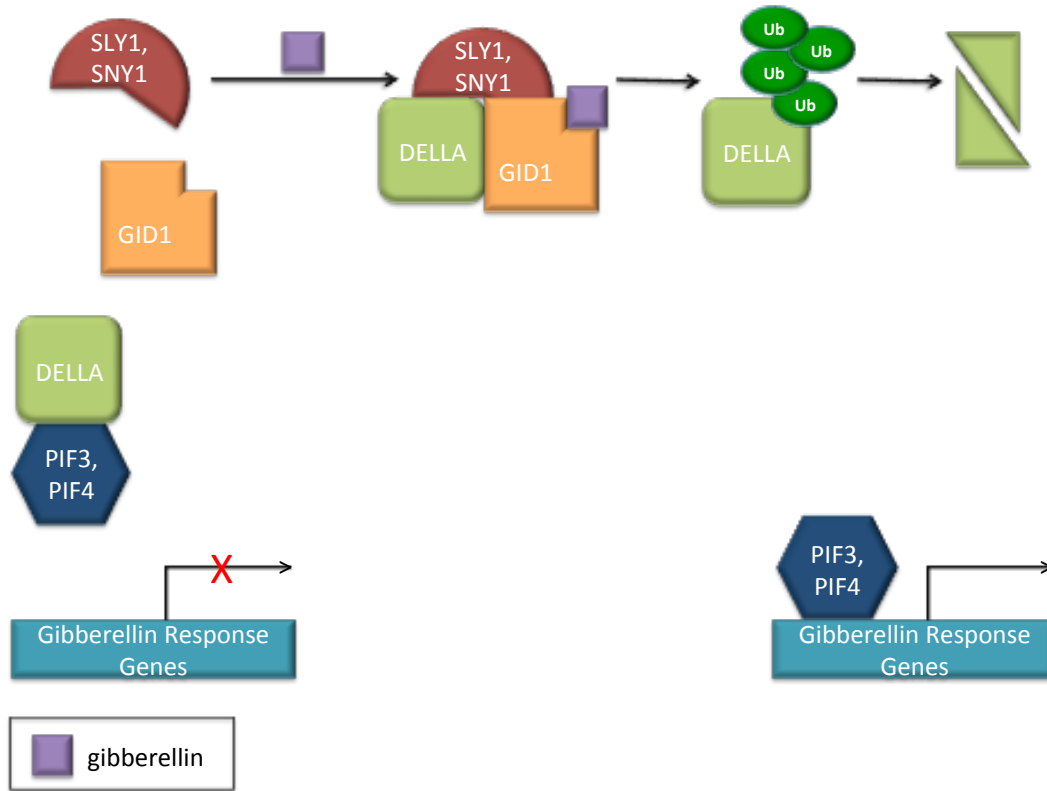


Figure 1.17. Gibberellin-mediated degradation of DELLA proteins.

GID1 acts as the main gibberellin receptor. The binding of gibberellin enhances the formation of a complex between GID1 and the DELLA protein. This interaction promotes the recognition and subsequent poly-ubiquitination of DELLA proteins by SCF^{SLY1/SNY2}. DELLA proteins are subsequently degraded, releasing PIF proteins that bind DNA and act as transcription factors.

Plant morphogenesis and the SCF-ligase

Forward genetic screens have functionally connected diverse aspects of plant morphogenesis with key components of the SCF ligase machinery in Arabidopsis. As described earlier, the UFO protein is an F-box protein that regulates both homeotic and caudal functions supporting normal growth and development during florogenesis. Phenotypic analysis of *ufo* mutant plants has revealed de-regulation of the spatial pattern of cell division in early floral meristems. UFO has been suggested to target LEAFY (LFY) for degradation, thus acting as a negative regulator of the B-class of flower homeotic genes [135].

FBL17 is a male germline-specific F-box protein that allows the haploid cells of flowering plants to undergo a division and produce twin sperm cells. This cell division is mediated by the degradation of the cyclin-dependent kinase inhibitors, KRP6 and KRP7, following transient expression of FBL17 in male germline cells [136].

Several F-box proteins, such as ZTL and FK1, also tightly regulate the plant circadian clock. These F-box proteins possess a common LOV domain that is involved in plant responses to blue light. ZTL and FK1 are responsible for the degradation of key circadian regulators, TOC1 and PRR5. It is believed that the oscillating levels of these proteins, achieved through combined expression and degradation, allows the plants to respond and measure the photoperiod and distinguish between the various seasons [134,137].

Identification of ubiquitinated proteins

Due to the rapid degradation of ubiquitinated proteins and transient interaction between E3 ligases and their substrates, identification of ubiquitinated proteins has been

of utmost difficulty [138]. Early approaches in identification of targets for various E3 ligases relied mostly on genetic studies. Recent advancements in mass spectroscopy and various affinity purification methods have greatly assisted in the global identification of post-translational modifications [139], proteome-wide profiling of ubiquitinated proteins still remains a challenge. Nevertheless, proteome-wide profiling of ubiquitinated proteins still remains a challenge. This challenge is more pronounced in the Arabidopsis-ubiquitin community where only a small number of the ubiquitinated proteins (~200) have been identified, only a handful of which have been fully characterized. In part due to their importance to our understanding of ubiquitination as a post-translational aspect of gene expression regulation, I review here the various methods that have been employed to identify ubiquitinated proteins in both the Arabidopsis community and beyond.

One of the first attempts at the identification of ubiquitinated proteins was made by expressing an epitope-tagged ubiquitin in a yeast ubiquitin null background [141]. A similar study was done in mammalian cells using His-tagged ubiquitin. Both methods were successful in identifying ~100 and ~50 ubiquitinated proteins, respectively [141,142]. This method has been further optimized and has allowed for the identification of 750 ubiquitinated proteins in mammalian cells [142]. A similar approach in Arabidopsis using His-tagged ubiquitin resulted in only 54 ubiquitinated proteins being identified [143]. Although purification of ubiquitinated proteins using tagged ubiquitin has its advantages such as the ability to purify purification of proteins under denaturing conditions. Nevertheless, it is widely accepted that application of a tagged form of ubiquitin can interfere with its function - a problem more evident with the linear form of ubiquitin chains. Furthermore, it has been shown that the over-expression of ubiquitin can

cause mild dominant-negative phenotypes in the cells and organisms studied - likely due to the competition between over-expressed and endogenous ubiquitin, especially in organisms where multiple loci are dedicated to the expression of ubiquitin genes such as in *Arabidopsis* and mammalian cells [142–144].

To overcome problems associated with the utilization of tagged ubiquitin several labs have used alternative methods of enrichment employing Ubiquitin Binding Domains (UBD) to enrich for ubiquitinated proteins [145,146]. UBDs vary in their binding affinity for ubiquitin and its different ubiquitin moieties [147]. Enrichment using UBDs has allowed for the identification of ubiquitinated proteins under native conditions. Employing UBDs in purification of ubiquitinated proteins in mammalian cells coupled with mass spectroscopy-based characterization has led to identification of 300 ubiquitinated proteins [148]. A similar approach in *Arabidopsis* cell extracts purified 294 proteins, only 54 of which bore a ubiquitin signature [145]. One explanation for the identification of only a small number of ubiquitinated proteins could be that *Arabidopsis* cell lines were employed instead of whole plant tissues. A second study utilized *Arabidopsis* seedlings, which identified a comparable number of ubiquitinated proteins suggesting that the inability to identify a large number of ubiquitinated proteins reflects the limitations of the techniques and not the sample used [149].

One of the limitations hindering the utility of ubiquitin antibodies for purification purposes has been their low affinity towards ubiquitinated proteins. To overcome this problem two different approaches have been utilized. In one approach, the unique Gly-Gly-Lys signature of ubiquitinated proteins following trypsin digestion has been exploited to develop a unique antibody against this remnant peptide [150]. This antibody

was used to characterize several hundred novel ubiquitinated proteins in mammalian cells [150]. One disadvantage associated with this antibody approach is that it cannot distinguish between ubiquitin modification and ubiquitin-like modifications such as NEDDylation [51]. Secondly, for reasons not yet fully understood, the antibody developed was unable to identify the majority of known ubiquitinated proteins present in the extract. The application of this antibody approach has so far yet to be reported in Arabidopsis.

Other studies have taken a different approach to tackle the problem associated with the low affinity of the ubiquitin antibodies. Through the exploitation of phage-display libraries exposed to various ubiquitin chain peptides, high-affinity ubiquitin chain-specific antibodies were developed [151]. The high affinity of these antibodies has been experimentally verified but has not yet been employed in a mass spectroscopy-based proteomic screen.

Genetics-based assays have been used as an alternative approach towards profiling the ubiquitome of mammalian cells. This approach has been spearheaded by the Elledge lab and is known as Global Protein Stability (GPS) profiling [139,139,151,152]. GPS profiling examines, in real-time, the changes in the stability of proteins under various treatments. GPS profiling relies on a fluorescent reporter system whereby two fluorescent proteins, GFP-ORF and RFP, are produced from a single transcript. The relative ratio of GFP/RFP is an indirect measure of protein stability. This method has been employed in mammalian cells and has led to the identification of 294 Cullin substrates using various NEDDylation inhibitors and dominant-negative forms of Cullin proteins [139].

An alternative to proteomic- and genetics-based approaches is the utilization of protein arrays. Protein arrays populated with over 5000 proteins have been employed for the identification of NEDD4 E3 ligase substrates [153]. The single-subunit nature of HECT-based E3 ligase along with an extensive knowledge of the mode of action of this class of E3 ligases has allowed for a relatively easy recapitulation of the ubiquitination behavior *in vitro*. In this way, NEDD4 ubiquitination was reconstituted in the presence of the appropriate E1 and E2 enzymes on the protein array, which led to the identification of 154 ubiquitinated proteins [153]. Due to the multi-subunit nature of SCF ligases, along with the large number of Skp1 and F-box proteins, which can assemble as part of the SCF ligase, reconstitution of this class of E3 ligase activity *in vitro* is not easily achieved [Personal communication, Judy Callis], thus a similar approach cannot be readily exploited for the SCF-ligase.

Summary

Our understanding of the ubiquitin machinery in Arabidopsis has been greatly expanded in the past decade and has resulted in an appreciation for ubiquitination-related processes as a major contributor to the regulation of plant growth and development. Although forward genetic screens have associated ubiquitination to almost every aspect of plant biology, further elucidation of the underlying molecular processes will require more targeted, reverse-genetic approaches combined with more effective methods for the identification of ubiquitinated proteins. Arising from the central role of post-translational ubiquitination in various aspects of plant biology, furthering our understanding of ubiquitin biology and regulation could help us elucidate the evolutionary benefits that plants have gained by acquiring such a vast array of genes devoted to the ubiquitination. Furthermore as a prominent translational model species, Arabidopsis, our study of ubiquitination events can not only further our understating of various aspects of growth and development but can also result in diverse approaches for the improvement of agriculture ultimately advancing human health.

BIBLIOGRAPHY

1. The Arabidopsis Genome Initiative (2000) Analysis of the genome sequence of the flowering plant *Arabidopsis thaliana*. *Nature* 408: 796-815.
2. Yamada K, Lim J, Dale JM, Chen H, Shinn P, Palm CJ, Southwick AM, Wu HC, Kim C, Nguyen M, Pham P, Cheuk R, Karlin-Newmann G, Liu SX, Lam B, Sakano H, Wu T, Yu G, Miranda M, Quach HL, Tripp M, Chang CH, Lee JM, Toriumi M, Chan MMH, Tang CC, Onodera C, Deng JM, Akiyama K, Ansari Y, Arakawa T, Banh J, Banno F, Bowser L, Brooks S, Carninci P, Chao Q, Choy N, Enju A, Goldsmith AD, Gurjal M, Hansen NF, Hayashizaki Y, Johnson-Hopson C, Hsuan VW, Iida K, Karnes M, Khan S, Koesema E, Ishida J, Jiang PX, Jones T, Kawai J, Kamiya A, Meyers C, Nakajima M, Narusaka M, Seki M, Sakurai T, Satou M, Tamse R, Vaysberg M, Wallender EK, Wong C, Yamamura Y, Yuan S, Shinozaki K, Davis RW, Theologis A, Ecker JR (2003) Empirical Analysis of Transcriptional Activity in the Arabidopsis Genome. *Science* 302: 842-846.
3. Alonso JM, Stepanova AN, Leisse TJ, Kim CJ, Chen H, Shinn P, Stevenson DK, Zimmerman J, Barajas P, Cheuk R (2003) Genome-wide insertional mutagenesis of *Arabidopsis thaliana*. *Science Signalling* 301: 653.
4. Jones AM, Chory J, Dangl JL, Estelle M, Jacobsen SE, Meyerowitz EM, Nordborg M, Weigel D (2008) The Impact of *Arabidopsis* on Human Health: Diversifying Our Portfolio. *Cell* 133: 939-943.
5. Blanc G, Hokamp K, Wolfe KH (2003) A recent polyploidy superimposed on older large-scale duplications in the Arabidopsis genome. *Genome research* 13: 137-144.
6. Blanc G, Wolfe KH (2004) Functional divergence of duplicated genes formed by polyploidy during Arabidopsis evolution. *The Plant Cell Online* 16: 1679-1691.
7. Walley JW, Dehesh K (2010) Molecular mechanisms regulating rapid stress signaling networks in Arabidopsis. *Journal of integrative plant biology* 52: 354-359.
8. Külheim C, Agren J, Jansson S (2002) Rapid regulation of light harvesting and plant fitness in the field. *Science* 297: 91-93.
9. Kuroda H, Takahashi N, Shimada H, Seki M, Shinozaki K, Matsui M (2002) Classification and expression analysis of Arabidopsis F-box-containing protein genes. *Plant and Cell Physiology* 43: 1073-1085.
10. Gagne JM, Downes BP, Shiu SH, Durski AM, Vierstra RD (2002) The F-box subunit of the SCF E3 complex is encoded by a diverse superfamily of

genes in Arabidopsis. Proceedings of the National Academy of Sciences 99: 11519-11524.

11. Goff SA, Ricke D, Lan TH, Presting G, Wang R, Dunn M, Glazebrook J, Sessions A, Oeller P, Varma H (2002) A draft sequence of the rice genome (*Oryza sativa* L. ssp. japonica). *Science* 296: 92-100.
12. Jain M, Nijhawan A, Arora R, Agarwal P, Ray S, Sharma P, Kapoor S, Tyagi AK, Khurana JP (2007) F-box proteins in rice. Genome-wide analysis, classification, temporal and spatial gene expression during panicle and seed development, and regulation by light and abiotic stress. *Plant Physiology* 143: 1467-1483.
13. Vogel JP, Garvin DF, Mockler TC, Schmutz J, Rokhsar D, Bevan MW, Barry K, Lucas S, Harmon-Smith M, Lail K (2010) Genome sequencing and analysis of the model grass *Brachypodium distachyon*. *Nature* 463: 763-768.
14. Devoto A, Nieto-Rostro M, Xie D, Ellis C, Harmston R, Patrick E, Davis J, Sherratt L, Coleman M, Turner JG (2002) COI1 links jasmonate signalling and fertility to the SCF ubiquitin-ligase complex in Arabidopsis. *Plant Journal* 32: 457-466.
15. Dharmasiri N, Dharmasiri S, Estelle M (2005) The F-box protein TIR1 is an auxin receptor. *Nature* 435: 441-445. 10.1038/nature03543.
16. Dieterle M, Zhou YC, Scñfer E, Funk M, Kretsch T (2001) EID1, an f-box protein involved in phytochrome a-specific light signaling. *Genes and Development* 15: 939-944.
17. Harmon FG, Kay SA (2003) The F Box Protein AFR Is a Positive Regulator of Phytochrome A-Mediated Light Signaling. *Current Biology* 13: 2091-2096.
18. Hepworth SR, Klenz JE, Haughn GW (2006) UFO in the Arabidopsis inflorescence apex is required for floral-meristem identity and bract suppression. *Planta* 223: 769-778.
19. Imaizumi T, Tran HG, Swartz TE, Briggs WR, Kay SA (2003) FKF1 is essential for photoperiodic-specific light signalling in Arabidopsis. *Nature* 426: 302-306. 10.1038/nature02090.
20. Vijay-Kumar S, Bugg CE, Wilkinson KD, Vierstra RD, Hatfield PM, Cook WJ (1987) Comparison of the three-dimensional structures of human, yeast, and oat ubiquitin. *Journal of Biological Chemistry* 262: 6396-6399.
21. Varshavsky A (1997) The ubiquitin system. *Trends in biochemical sciences* 22: 383-387.

22. Harper JW, Tan MKM (2012) Ubiquitin Pathway Proteomics. *Molecular & Cellular Proteomics* .
23. Hershko A, Ciechanover A (1998) The ubiquitin system. *Annual review of biochemistry* 67: 425-479.
24. Cadwell K, Coscoy L (2005) Ubiquitination on nonlysine residues by a viral E3 ubiquitin ligase. *Science Signalling* 309: 127.
25. Pickart CM (2001) Mechanisms underlying ubiquitination. *Annual review of biochemistry* 70: 503-533.
26. Petroski MD, Deshaies RJ (2005) Function and regulation of cullin-RING ubiquitin ligases. *Nature Reviews Molecular Cell Biology* 6: 9-20.
27. Deshaies RJ, Joazeiro CAP (2009) RING domain E3 ubiquitin ligases. *Annual review of biochemistry* 78: 399-434.
28. Pickart CM, Fushman D (2004) Polyubiquitin chains: polymeric protein signals. *Current opinion in chemical biology* 8: 610-616.
29. Hochstrasser M (2006) Lingering mysteries of ubiquitin-chain assembly. *Cell* 124: 27-34.
30. Jin L, Williamson A, Banerjee S, Philipp I, Rape M (2008) Mechanism of ubiquitin-chain formation by the human anaphase-promoting complex. *Cell* 133: 653-665.
31. Petroski MD, Deshaies RJ (2005) Mechanism of lysine 48-linked ubiquitin-chain synthesis by the cullin-RING ubiquitin-ligase complex SCF-Cdc34. *Cell* 123: 1107-1120.
32. Haglund K, Di Fiore PP, Dikic I (2003) Distinct monoubiquitin signals in receptor endocytosis. *Trends in biochemical sciences* 28: 598.
33. Hicke L (2001) Protein regulation by monoubiquitin. *Nature Reviews Molecular Cell Biology* 2: 195-201.
34. Scaglione KM, Zavodszky E, Todi SV, Patury S, Xu P, Rodriguez-Lebrin E, Fischer S, Konen J, Djarmati A, Peng J (2011) Ube2w and ataxin-3 coordinately regulate the ubiquitin ligase CHIP. *Molecular Cell* 43: 599-612.
35. Parker JL, Ulrich HD (2009) Mechanistic analysis of PCNA poly-ubiquitylation by the ubiquitin protein ligases Rad18 and Rad5. *The EMBO journal* 28: 3657-3666.

36. Willis MS, Patterson C (2006) Into the heart: the emerging role of the ubiquitin-proteasome system. *Journal of molecular and cellular cardiology* 41: 567-579.
37. Tenno T, Fujiwara K, Tochio H, Iwai K, Morita EH, Hayashi H, Murata S, Hiroaki H, Sato M, Tanaka K (2004) Structural basis for distinct roles of Lys63 and Lys48 linked polyubiquitin chains. *Genes to Cells* 9: 865-875.
38. Bremm A, Freund SMV, Komander D (2010) Lys11-linked ubiquitin chains adopt compact conformations and are preferentially hydrolyzed by the deubiquitinase Cezanne. *Nature structural & molecular biology* 17: 939-947.
39. Ye Y, Rape M (2009) Building ubiquitin chains: E2 enzymes at work. *Nature reviews Molecular cell biology* 10: 755-764.
40. Ardley H, Robinson P (2005) E3 ubiquitin ligases. *Essays Biochem* 41: 15-30.
41. Tyers M, Willems AR (1999) One ring to rule a superfamily of E3 ubiquitin ligases. *Science* 284: 601-604.
42. Verdecia MA, Joazeiro CAP, Wells NJ, Ferrer JL, Bowman ME, Hunter T, Noel JP (2003) Conformational flexibility underlies ubiquitin ligation mediated by the WWP1 HECT domain E3 ligase. *Molecular Cell* 11: 249-259.
43. Freemont PS, Hanson IM, Trowsdale J (1991) A novel cysteine-rich sequence motif. *Cell* 64: 483-484.
44. Borden KL, Boddy MN, Lally J, O'reilly NJ, Martin S, Howe K, Solomon E, Freemont PS (1995) The solution structure of the RING finger domain from the acute promyelocytic leukaemia proto-oncoprotein PML. *The EMBO journal* 14: 1532.
45. Deshaies RJ (1999) SCF and Cullin/Ring H2-based ubiquitin ligases. *Annual review of cell and developmental biology* 15: 435-467.
46. Seol JH, Feldman RMR, Zachariae W, Shevchenko A, Correll CC, Lyapina S, Chi Y, Galova M, Claypool J, Sandmeyer S (1999) Cdc53/cullin and the essential Hrt1 RING E2 subunit of SCF define a ubiquitin ligase module that activates the E2 enzyme Cdc34. *Genes & Development* 13: 1614-1626.
47. Freemont PS (2000) Ubiquitination: RING for destruction? *Current Biology* 10: R84-R87.
48. Ulrich HD, Jentsch S (2000) Two RING finger proteins mediate cooperation between ubiquitin-conjugating enzymes in DNA repair. *The EMBO journal* 19: 3388-3397.

49. Petroski MD, Deshaies RJ (2005) Function and regulation of cullin-RING ubiquitin ligases. *Nature reviews Molecular cell biology* 6: 9-20.
50. Deshaies RJ, Joazeiro CAP (2009) RING domain E3 ubiquitin ligases. *Annual review of biochemistry* 78: 399-434.
51. Merlet J, Burger J, Gomes JE, Pintard L (2009) Regulation of cullin-RING E3 ubiquitin-ligases by NEDDylation and dimerization. *Cellular and molecular life sciences* 66: 1924-1938.
52. Willems AR, Schwab M, Tyers M (2004) A hitchhiker's guide to the cullin ubiquitin ligases: SCF and its kin. *Biochimica et biophysica acta* 1695: 133.
53. Bosu DR, Kipreos ET (2008) Cullin-RING ubiquitin ligases: global regulation and activation cycles. *Cell division* 3: 7.
54. Hotton SK, Callis J (2008) Regulation of cullin RING ligases. *Annu Rev Plant Biol* 59: 467-489.
55. Zheng N, Schulman BA, Song L, Miller JJ, Jeffrey PD, Wang P, Chu C, Koeppe DM, Elledge SJ, Pagano M (2002) Structure of the Cul 1-Rbx 1-Skp 1-F box-Skp 2 SCF ubiquitin ligase complex. *Nature* 416: 703-709.
56. Seol JH, Feldman RMR, Zachariae W, Shevchenko A, Correll CC, Lyapina S, Chi Y, Galova M, Claypool J, Sandmeyer S (1999) Cdc53/cullin and the essential Hrt1 RING-H2 subunit of SCF define a ubiquitin ligase module that activates the E2 enzyme Cdc34. *Genes & Development* 13: 1614-1626.
57. Schulman BA, Carrano AC, Jeffrey PD, Bowen Z, Kinnucan ERE, Finnin MS, Elledge SJ, Harper JW, Pagano M, Pavletich NP (2000) Insights into SCF ubiquitin ligases from the structure of the Skp1-Skp2 complex. *Nature* 408: 381-386.
58. Bai C, Sen P, Hofmann K, Ma L, Goebel M, Harper JW, Elledge SJ (1996) SKP1 connects cell cycle regulators to the ubiquitin proteolysis machinery through a novel motif, the F-box. *Cell* 86: 263.
59. Yamanaka A, Yada M, Imaki H, Koga M, Ohshima Y, Nakayama KI (2002) Multiple Skp1-Related Proteins in *Caenorhabditis elegans*: Diverse Patterns of Interaction with Cullins and F-Box Proteins. *Current Biology* 12: 267-275.
60. Connelly C, Hieter P (1996) Budding yeast SKP1 encodes an evolutionarily conserved kinetochore protein required for cell cycle progression. *Cell* 86: 275.

61. Bai C, Sen P, Hofmann K, Ma L, Goebel M, Harper JW, Elledge SJ (1996) SKP1 connects cell cycle regulators to the ubiquitin proteolysis machinery through a novel motif, the F-box. *Cell* 86: 263.
62. Samach A, Klenz JE, Kohalmi SE, Risseuw E, Haughn GW, Crosby WL (2002) The UNUSUAL FLORAL ORGANS gene of *Arabidopsis thaliana* is an F-box protein required for normal patterning and growth in the floral meristem. *The Plant Journal* 20: 433-445.
63. Zhang H, Kobayashi R, Galaktionov K, Beach D (1995) p19skp1 and p45skp2 are essential elements of the cyclin A-CDK2 S phase kinase. *Cell* 82: 915-925.
64. Risseuw EP, Daskalchuk TE, Banks TW, Liu E, Cotelesage J, Hellmann H, Estelle M, Somers DE, Crosby WL (2003) Protein interaction analysis of SCF ubiquitin E3 ligase subunits from *Arabidopsis*. *The Plant Journal* 34: 753-767.
65. Zheng N, Schulman BA, Song L, Miller JJ, Jeffrey PD, Wang P, Chu C, Koepp DM, Elledge SJ, Pagano M (2002) Structure of the Cul-Rbx-Skp 1-F box Skp2 SCF ubiquitin ligase complex. *Nature* 416: 703-709.
66. Patton EE, Willems AR, Tyers M (1998) Combinatorial control in ubiquitin-dependent proteolysis: don't Skp the F-box hypothesis. *Trends in genetics: TIG* 14: 236.
67. Zhou P, Howley PM (1998) Ubiquitination and degradation of the substrate recognition subunits of SCF ubiquitin-protein ligases. *Molecular Cell* 2: 571.
68. Kipreos ET, Pagano M (2000) The F-box protein family. *Genome Biol* 1: 3002-1.
69. Jin J, Cardozo T, Lovering RC, Elledge SJ, Pagano M, Harper JW (2004) Systematic analysis and nomenclature of mammalian F-box proteins. *Genes & Development* 18: 2573-2580.
70. Tang X, Orlicky S, Lin Z, Willems A, Neculai D, Ceccarelli D, Mercurio F, Shilton BH, Sicheri F, Tyers M (2007) Suprafacial Orientation of the SCF^{Cdc4} Dimer Accommodates Multiple Geometries for Substrate Ubiquitination. *Cell* 129: 1165-1176.
71. Barbash O, Zamfirova P, Lin DI, Chen X, Yang K, Nakagawa H, Lu F, Rustgi AK, Diehl JA (2008) Mutations in *Fbx4* Inhibit Dimerization of the SCF^{Fbx4} Ligase and Contribute to Cyclin D1 Overexpression in Human Cancer. *Cancer cell* 14: 68-78.
72. Cardozo T, Pagano M (2004) The SCF ubiquitin ligase: insights into a molecular machine. *Nature reviews Molecular cell biology* 5: 739-751.

73. Hunter T (2007) The age of crosstalk: phosphorylation, ubiquitination, and beyond. *Molecular Cell* 28: 730-738.
74. Willems AR, Goh T, Taylor L, Chernushevich I, Shevchenko A, Tyers M (1999) SCF ubiquitin protein ligases and phosphorylation-dependent proteolysis. *Philosophical Transactions of the Royal Society B: Biological Sciences* 354: 1533.
75. Tsvetkov LM, Yeh KH, Lee SJ, Sun H, Zhang H (1999) p27 Kip1 ubiquitination and degradation is regulated by the SCF Skp2 complex through phosphorylated Thr187 in p27. *Current Biology* 9: 661-6S2.
76. Tedesco D, Lukas J, Reed SI (2002) The pRb-related protein p130 is regulated by phosphorylation-dependent proteolysis via the protein-specific ubiquitin ligase SCFSkp2. *Genes & Development* 16: 2946-2957.
77. Yoshida Y, Chiba T, Tokunaga F, Kawasaki H, Iwai K, Suzuki T, Ito Y, Matsuoka K, Yoshida M, Tanaka K (2002) E3 ubiquitin ligase that recognizes sugar chains. *Nature* 418: 438-442.
78. Yoshida Y, Adachi E, Fukiya K, Iwai K, Tanaka K (2005) Glycoprotein-specific ubiquitin ligases recognize N-glycans in unfolded substrates. *EMBO reports* 6: 239-244.
79. Kepinski S, Leyser O (2005) The Arabidopsis F-box protein TIR1 is an auxin receptor. *Nature* 435: 446-451.
80. Lin HK, Wang G, Chen Z, Teruya-Feldstein J, Liu Y, Chan CH, Yang WL, Erdjument-Bromage H, Nakayama KI, Nimer S (2009) Phosphorylation-dependent regulation of cytosolic localization and oncogenic function of Skp2 by Akt/PKB. *Nature cell biology* 11: 420-432.
81. Yam CH, Ng RWM, Siu WY, Lau AWS, Poon RYC (1999) Regulation of cyclin A-Cdk2 by SCF component Skp1 and F-box protein Skp2. *Molecular and cellular biology* 19: 635-645.
82. Bashir T, Dorrello NV, Amador V, Guardavaccaro D, Pagano M (2004) Control of the SCFSkp2-Cks1 ubiquitin ligase by the APC/CCdh1 ubiquitin ligase. *Nature* 428: 190-193.
83. Wei W, Ayad NG, Wan Y, Zhang GJ, Kirschner MW, Kaelin WG (2004) Degradation of the SCF component Skp2 in cell-cycle phase G1 by the anaphase-promoting complex. *Nature* 428: 194-198.
84. Rodier G, Coulombe P, Tanguay PL, Boutonnet C, Meloche S (2008) Phosphorylation of Skp2 regulated by CDK2 and Cdc14B protects it from degradation by APCdh1 in G1 phase. *The EMBO journal* 27: 679-691.

85. Huttlin EL, Jedrychowski MP, Elias JE, Goswami T, Rad R, Beausoleil SA, Villén J, Haas W, Sowa ME, Gygi SP (2010) A tissue-specific atlas of mouse protein phosphorylation and expression. *Cell* 143: 1174-1189.
86. Villén J, Beausoleil SA, Gerber SA, Gygi SP (2007) Large-scale phosphorylation analysis of mouse liver. *Proceedings of the National Academy of Sciences* 104: 1488-1493.
87. Wei N, Deng XW (2003) The COP9 signalosome. *Annual review of cell and developmental biology* 19: 261-286.
88. Saha A, Deshaies RJ (2008) Multimodal activation of the ubiquitin ligase SCF by Nedd8 conjugation. *Molecular Cell* 32: 21-31.
89. Zheng J, Yang X, Harrell JM, Ryzhikov S, Shim EH, Lykke-Andersen K, Wei N, Sun H, Kobayashi R, Zhang H (2002) CAND1 binds to unNEDDylated CUL1 and regulates the formation of SCF ubiquitin E3 ligase complex. *Molecular Cell* 10: 1519-1526.
90. Lyapina S, Cope G, Shevchenko A, Serino G, Tsuge T, Zhou C, Wolf DA, Wei N, Shevchenko A, Deshaies RJ (2001) Promotion of NEDD8-CUL1 conjugate cleavage by COP9 signalosome. *Science Signalling* 292: 1382.
91. Galan JM, Peter M (1999) Ubiquitin-dependent degradation of multiple F-box proteins by an autocatalytic mechanism. *Proceedings of the National Academy of Sciences* 96: 9124-9129.
92. Del Pozo JC, Estelle M (2000) F-box proteins and protein degradation: an emerging theme in cellular regulation. *Plant Molecular Biology* 44: 123-128.
93. Hori T, Osaka F, Chiba T, Miyamoto C, Okabayashi K, Shimbara N, Kato S, Tanaka K (1999) Covalent modification of all members of human cullin family proteins by NEDD8. *Oncogene* 18: 6829.
94. Kamitani T, Nguyen HP, Kito K, Fukuda-Kamitani T, Yeh ETH (1998) Covalent modification of PML by the sentrin family of ubiquitin-like proteins. *Journal of Biological Chemistry* 273: 3117-3120.
95. Rahighi S, Dikic I (2011) Conformational flexibility and rotation of the RING domain in activation of cullin-RING ligases. *Nature structural & molecular biology* 18: 863-865.
96. Kurz T, Chou YC, Willems AR, Meyer-Schaller N, Hecht ML, Tyers M, Peter M, Sicheri F (2008) Dcn1 functions as a scaffold-type E3 ligase for cullin NEDDylation. *Molecular Cell* 29: 23-35.

97. Chew EH, Hagen T (2007) Substrate-mediated regulation of cullin NEDDylation. *Journal of Biological Chemistry* 282: 17032-17040.
98. Cope GA, Deshaies RJ (2003) COP9 signalosome: a multifunctional regulator of SCF and other cullin-based ubiquitin ligases. *Cell* 114: 663-671.
99. Zheng J, Yang X, Harrell JM, Ryzhikov S, Shim EH, Lykke-Andersen K, Wei N, Sun H, Kobayashi R, Zhang H (2002) CAND1 binds to unneddylated CUL1 and regulates the formation of SCF ubiquitin E3 ligase complex. *Molecular Cell* 10: 1519-1526.
100. Zheng J, Yang X, Harrell JM, Ryzhikov S, Shim EH, Lykke-Andersen K, Wei N, Sun H, Kobayashi R, Zhang H (2002) CAND1 binds to unneddylated CUL1 and regulates the formation of SCF ubiquitin E3 ligase complex. *Molecular Cell* 10: 1519-1526.
101. Goldenberg SJ, Cascio TC, Shumway SD, Garbutt KC, Liu J, Xiong Y, Zheng N (2004) Structure of the Cand1-Cul1-Roc1 complex reveals regulatory mechanisms for the assembly of the multisubunit cullin-dependent ubiquitin ligases. *Cell* 119: 517-528.
102. Hotton SK, Callis J (2008) Regulation of cullin RING ligases. *Annu Rev Plant Biol* 59: 467-489.
103. Merlet J, Burger J, Gomes JE, Pintard L (2009) Regulation of cullin-RING E3 ubiquitin-ligases by NEDDylation and dimerization. *Cellular and molecular life sciences* 66: 1924-1938.
104. Hashizume R, Fukuda M, Maeda I, Nishikawa H, Oyake D, Yabuki Y, Ogata H, Ohta T (2001) The RING heterodimer BRCA1-BARD1 is a ubiquitin ligase inactivated by a breast cancer-derived mutation. *Journal of Biological Chemistry* 276: 14537-14540.
105. Tang X, Orlicky S, Lin Z, Willems A, Neculai D, Ceccarelli D, Mercurio F, Shilton BH, Sicheri F, Tyers M (2007) Suprafacial Orientation of the SCFCdc4 Dimer Accommodates Multiple Geometries for Substrate Ubiquitination. *Cell* 129: 1165-1176.
106. Suzuki H, Chiba T, Suzuki T, Fujita T, Ikenoue T, Omata M, Furuichi K, Shikama H, Tanaka K (2000) Homodimer of two F-box proteins +¹TrCP1 or BTrCP2 binds to I κ B for signal-dependent ubiquitination. *Journal of Biological Chemistry* 275: 2877-2884.
107. Kirk R, Laman H, Knowles PP, Murray-Rust J, Lomonosov M, McDonald NQ (2008) Structure of a conserved dimerization domain within the F-box protein Fbxo7 and the PI31 proteasome inhibitor. *Journal of Biological Chemistry* 283: 22325-22335.

108. Welcker M, Clurman BE (2007) Fbw7/hCDC4 dimerization regulates its substrate interactions. *Cell Div* 2.
109. McMahon M, Thomas N, Itoh K, Yamamoto M, Hayes JD (2006) Dimerization of Substrate Adaptors Can Facilitate Cullin-mediated Ubiquitylation of Proteins by a "Tethering" Mechanism. *Journal of Biological Chemistry* 281: 24756-24768.
110. Hao B, Oehlmann S, Sowa ME, Harper JW, Pavletich NP (2007) Structure of a Fbw7-Skp1-cyclin E complex: multisite-phosphorylated substrate recognition by SCF ubiquitin ligases. *Molecular Cell* 26: 131.
111. Welcker M, Clurman BE (2008) FBW7 ubiquitin ligase: a tumour suppressor at the crossroads of cell division, growth and differentiation. *Nature Reviews Cancer* 8: 83-93.
112. Vierstra RD (2003) The ubiquitin/26S proteasome pathway, the complex last chapter in the life of many plant proteins. *Trends in Plant Science* 8: 135-142. doi: 10.1016/S1360-1385(03)00014-1.
113. Vierstra RD (2009) The ubiquitin-26S proteasome system at the nexus of plant biology. *Nat Rev Mol Cell Biol* 10: 385-397. 10.1038/nrm2688.
114. Gray WM, Del Pozo JC, Walker L, Hobbie L, Risseuw E, Banks T, Crosby WL, Yang M, Ma H, Estelle M (1999) Identification of an SCF ubiquitin-ligase complex required for auxin response in *Arabidopsis thaliana*. *Genes & Development* 13: 1678-1691.
115. McGinnis KM, Thomas SG, Soule JD, Strader LC, Zale JM, Sun T, Steber CM (2003) The *Arabidopsis* SLEEPY1 gene encodes a putative F-box subunit of an SCF E3 ubiquitin ligase. *The Plant Cell Online* 15: 1120-1130.
116. Devoto A, Nieto-Rostro M, Xie D, Ellis C, Harmston R, Patrick E, Davis J, Sherratt L, Coleman M, Turner JG (2002) COI1 links jasmonate signalling and fertility to the SCF ubiquitin-ligase complex in *Arabidopsis*. *The Plant Journal* 32: 457-466.
117. Hellmann H, Hobbie L, Chapman A, Dharmasiri S, Dharmasiri N, Del Pozo C, Reinhardt D, Estelle M (2003) *Arabidopsis* AXR6 encodes CUL1 implicating SCF E3 ligases in auxin regulation of embryogenesis. *The EMBO journal* 22: 3314-3325.
118. Dezfulian MH, Soulliere DM, Dhaliwal RK, Sareen M, Crosby WL (2012) The SKP1-Like Gene Family of *Arabidopsis* Exhibits a High Degree of Differential Gene Expression and Gene Product Interaction during Development. *PloS one* 7: e50984.

119. Moon J, Zhao Y, Dai X, Zhang W, Gray WM, Huq E, Estelle M (2007) A new CULLIN 1 mutant has altered responses to hormones and light in Arabidopsis. *Plant Physiology* 143: 684-696.
120. Hellmann H, Hobbie L, Chapman A, Dharmasiri S, Dharmasiri N, Del Pozo C, Reinhardt D, Estelle M (2003) Arabidopsis AXR6 encodes CUL1 implicating SCF E3 ligases in auxin regulation of embryogenesis. *The EMBO journal* 22: 3314-3325.
121. Liu F, Ni W, Griffith ME, Huang Z, Chang C, Peng W, Ma H, Xie D (2004) The ASK1 and ASK2 Genes Are Essential for Arabidopsis Early Development. *Plant Cell* 16: 5-20.
122. Gray WM, Hellmann H, Dharmasiri S, Estelle M (2002) Role of the Arabidopsis RING-H2 protein RBX1 in RUB modification and SCF function. *The Plant Cell Online* 14: 2137-2144.
123. Davies PJ (2010) The plant hormones: their nature, occurrence, and functions. *Plant hormones* 1-15.
124. Santner A, Calderon-Villalobos LIA, Estelle M (2009) Plant hormones are versatile chemical regulators of plant growth. *Nature chemical biology* 5: 301-307.
125. Santner A, Estelle M (2009) Recent advances and emerging trends in plant hormone signalling. *Nature* 459: 1071-1078.
126. Dharmasiri N, Estelle M (2004) Auxin signaling and regulated protein degradation. *Trends in Plant Science* 9: 302-308.
127. Dharmasiri N, Dharmasiri S, Weijers D, Lechner E, Yamada M, Hobbie L, Ehrismann JS, Jürgens G, Estelle M (2005) Plant development is regulated by a family of auxin receptor F box proteins. *Developmental cell* 9: 109-119.
128. Mockaitis K, Estelle M (2008) Auxin receptors and plant development: a new signaling paradigm. *Annual review of cell and developmental biology* 24: 55-80.
129. Villalobos LIAC, Lee S, De Oliveira C, Ivetac A, Brandt W, Armitage L, Sheard LB, Tan X, Parry G, Mao H (2012) A combinatorial TIR1/AFB-Aux/IAA co-receptor system for differential sensing of auxin. *Nature chemical biology* 8: 477-485.
130. Sheard LB, Tan X, Mao H, Withers J, Ben-Nissan G, Hinds TR, Kobayashi Y, Hsu FF, Sharon M, Browse J, He SY, Rizo J, Howe GA, Zheng N (2010) Jasmonate perception by inositol-phosphate-potentiated COI1-JAZ co-receptor. *Nature* 468: 400-405. 10.1038/nature09430.

131. Thines B, Katsir L, Melotto M, Niu Y, Mandaokar A, Liu G, Nomura K, He SY, Howe GA, Browse J (2007) JAZ repressor proteins are targets of the SCFCO11 complex during jasmonate signalling. *Nature* 448: 661-665. [10.1038/nature05960](https://doi.org/10.1038/nature05960).
132. Hauvermale AL, Ariizumi T, Steber CM (2012) Gibberellin Signaling: A Theme and Variations on DELLA Repression. *Plant Physiology* 160: 83-92.
133. Bartek J, Lukas J (2001) p27 destruction: Cks1 pulls the trigger. *Nature cell biology* 3: 95.
134. Bartel B, Citovsky V (2012) Focus on Ubiquitin in Plant Biology. *Plant Physiology* 160: 1.
135. Chae E, Tan QKG, Hill TA, Irish VF (2008) An Arabidopsis F-box protein acts as a transcriptional co-factor to regulate floral development. *Development* 135: 1235-1245.
136. Gusti A, Baumberger N, Nowack M, Pusch S, Eisler H, Potuschak T, De Veylder L, Schnittger A, Genschik P (2009) The Arabidopsis thaliana F-box protein FBL17 is essential for progression through the second mitosis during pollen development. *PloS one* 4: e4780.
137. Mès P, Kim WY, Somers DE, Kay SA (2003) Targeted degradation of TOC1 by ZTL modulates circadian function in Arabidopsis thaliana. *Nature* 426: 567-570.
138. Cardozo T, Pagano M (2004) The SCF ubiquitin ligase: insights into a molecular machine. *Nature reviews Molecular cell biology* 5: 739-751.
139. Yen HCS, Elledge SJ (2008) Identification of SCF ubiquitin ligase substrates by global protein stability profiling. *Science Signalling* 322: 923.
140. Kelley DR, Estelle M (2012) Ubiquitin-mediated control of plant hormone signaling. *Plant Physiology* 160: 47-55.
141. Peng J, Schwartz D, Elias JE, Thoreen CC, Cheng D, Marsischky G, Roelofs J, Finley D, Gygi SP (2003) A proteomics approach to understanding protein ubiquitination. *Nature biotechnology* 21: 921-926.
142. Kirkpatrick DS, Weldon SF, Tsaprailis G, Liebler DC, Gandolfi AJ (2005) Proteomic identification of ubiquitinated proteins from human cells expressing His-tagged ubiquitin. *Proteomics* 5: 2104-2111.
143. Saracco SA, Hansson M, Scalf M, Walker JM, Smith LM, Vierstra RD (2009) Tandem affinity purification and mass spectrometric analysis of ubiquitylated proteins in Arabidopsis. *The Plant Journal* 59: 344-358.

144. Tagwerker C, Flick K, Cui M, Guerrero C, Dou Y, Auer B, Baldi P, Huang L, Kaiser P (2006) A Tandem Affinity Tag for Two-step Purification under Fully Denaturing Conditions Application in Ubiquitin Profiling and Protein Complex Identification Combined with in vivo Cross-Linking. *Molecular & Cellular Proteomics* 5: 737-748.
145. Maor R, Jones A, Nhs TS, Studholme DJ, Peck SC, Shirasu K (2007) Multidimensional protein identification technology (MudPIT) analysis of ubiquitinated proteins in plants. *Molecular & Cellular Proteomics* 6: 601-610.
146. Mayor T, Deshaies RJ (2005) Two Step Affinity Purification of Multiubiquitylated Proteins from *Saccharomyces cerevisiae*. *Methods in enzymology* 399: 385-392.
147. Hicke L, Schubert HL, Hill CP (2005) Ubiquitin-binding domains. *Nature reviews Molecular cell biology* 6: 610-621.
148. Tomlinson E, Palaniyappan N, Tooth D, Layfield R (2007) Methods for the purification of ubiquitinated proteins. *Proteomics* 7: 1016-1022.
149. Manzano C, Abraham Z, Lopez-Torres G, Del Pozo JC (2008) Identification of ubiquitinated proteins in Arabidopsis. *Plant Molecular Biology* 68: 145-158.
150. Xu G, Paige JS, Jaffrey SR (2010) Global analysis of lysine ubiquitination by ubiquitin remnant immunoaffinity profiling. *Nature biotechnology* 28: 868-873.
151. Newton K, Matsumoto ML, Wertz IE, Kirkpatrick DS, Lill JR, Tan J, Dugger D, Gordon N, Sidhu SS, Fellouse FA (2008) Ubiquitin chain editing revealed by polyubiquitin linkage-specific antibodies. *Cell* 134: 668-678.
152. Yen HCS, Xu Q, Chou DM, Zhao Z, Elledge SJ (2008) Global protein stability profiling in mammalian cells. *Science Signalling* 322: 918.
153. Gupta R, Kus B, Fladd C, Wasmuth J, Tonikian R, Sidhu S, Krogan NJ, Parkinson J, Rotin D (2007) Ubiquitination screen using protein microarrays for comprehensive identification of Rsp5 substrates in yeast. *Molecular systems biology* 3.

CHAPTER 2

The *SKP1-like* Gene Family of Arabidopsis Exhibits a High Degree of Differential Gene Expression and Gene Product Interaction During Development¹

¹ This chapter is the outcome of joint research.

INTRODUCTION

Genetic and molecular studies in the model plant species *Arabidopsis thaliana* have emphasized the importance of ubiquitin-mediated targeted protein degradation for the regulation of diverse plant-specific processes [1–3]. Genetic surveys for the identification of loci that regulate patterning and development have revealed numerous genes that encode known or predicted subunit components of both RING and HECT classes of E3-ubiquitin ligases (E3-Ub). Functional analysis of mutants at many of these loci suggests a central role for post-translational protein degradation in such plant-specific functions as auxin response [4,5], response to jasmonate [6], maintenance of circadian rhythm [7,8], photomorphogenesis [9] and floral development [10], to name but a few.

Arabidopsis is an attractive model system in which to study the role of post-translational protein modification in the regulation of development, in part due to its many technical advantages coupled with a wealth of genetic resources and genomic data sets that facilitate hypothesis generation and functional analysis. Although *Arabidopsis* possesses one of the smallest known angiosperm genomes studied to date, with 147Mbp encoding approximately 27,000 protein coding genes, it has nevertheless been annotated to contain over 1,500 genes that are known or predicted to encode subunits of ubiquitin ligase complexes (nearly 6% of the coding capacity) including more than 700 F-box proteins comprising about 3% of the *Arabidopsis* genome coding capacity [1]. This genetic complexity and allocation of gene coding capacity to SCF-ligase complexes involved in post-translational protein turnover-related processes is prominent in plants, and can be compared with that of *Homo sapiens* where only 69 F-box genes have been identified [11].

The quaternary subunit composition of the SCF-class of E3-Ub complexes have been studied in numerous model systems [5,12–15], and are minimally comprised of one each of the F-box, Skp1-like, Rbx1 and Cull1 class of polypeptide subunits [15,16]. For the most part, the subunit stoichiometry of individual functional complexes has yet to be experimentally determined, although crystal structures for select SCF-class E3-ubiquitin ligases have been described for yeast, human and Arabidopsis protein complexes [5,13,15,17]. Recent evidence suggests that assembly of SCF-class E3-Ub ligase complexes may result in protein interactions involving multiple F-box subunits [16,18–20]. The characterization of subunit interaction potential and stoichiometry for select SCF-class of E3-Ub complexes will likely prove important for understanding the combinatorial diversity of complexes that may form across developmental time and space, together with a determination of their associated biological function [21]. Given the relatively large number of genes that are known or predicted to function in post-translational ubiquitination of proteins in Arabidopsis, together with the close primary structural similarity of the genes within the *ASK* gene family, a significant degree of functional redundancy might be expected. Knock down-based functional assessment of potentially redundant genes is commonly conducted on the basis of deduced amino acid sequence similarity, often ignoring functional aspects of genetic redundancy such as expression, localization and gene-product interaction. Since amino acid sequence similarity is not the only factor contributing to gene redundancy, such studies often result in a lack of observable phenotype. Therefore, a more insightful assessment of gene redundancy potential within the *ASK* gene family should include multiple aspects of gene

function as a foundation upon which any hypothesis driven functional assessment might be derived.

Among the four canonical subunit classes that are known to participate in the formation of the SCF-class of E3-Ub complexes, relatively little is known about the functional role of the individual Arabidopsis Skp1-like family of polypeptides (ASK proteins). The gene family encoding ASK polypeptides in Arabidopsis is complex, with 21 known expressed genes compared to a single Skp1-like gene in yeast and *H. sapiens* [22–24]. Phylogenetic analysis of the *ASK* gene family based upon the deduced amino acid sequence has been used to define clades that are suggested to predict functional redundancy among individual *ASK* genes [24]. Indeed, studies involving loss of function alleles in the closely related genes *ASK1* and *ASK2* indicate these two genes perform strongly overlapping functions that are essential for early patterning and development [24]. These studies are complemented by the finding that the ASK1 and ASK2 proteins interact broadly with F-box proteins, suggesting correspondingly diverse roles in the formation of functional SCF complexes in Arabidopsis [21]. The function of the remaining 19 members of the *ASK* gene family remains largely uncharacterized.

Expression studies involving *ASK* genes in Arabidopsis have generally involved reporter-gene fusion and non-quantitative RT-PCR approaches, where such studies indicate that certain members of the *ASK* gene family are preferentially expressed in a subset of organs and tissues at different times during development [23,25]. Quantitative studies provide the desired precision needed for higher-resolution comparison of *ASK* gene expression and clustering on the basis of expression – an aspect that has been largely neglected from previous studies to date. This type of information can also be

important for defining the extent of expression overlap among SCF subunits, and for elucidating their potential to participate in the formation of SCF complexes.

In this report we analyze functional redundancy within the *ASK* gene family by evaluating three aspects of ASK protein and cognate gene redundancy; a quantitative analysis of *ASK* transcript abundance in select organs during development; the sub-cellular compartmentation of expressed tagged ASK proteins; and an *in situ* analysis using bimolecular fluorescence complementation (BiFC)-based approaches to assess protein-protein interactions involving ASK polypeptides. Taken together, the study concludes that phylogenetic relatedness based upon primary amino acid sequence similarity is a poor predictor of redundancy defined by steady-state transcript abundance, sub-cellular localization and gene product interactions exhibited by products of the *ASK* gene family. The results are discussed in the context of the potential for combinatorial complexity of SCF complex formation by products of the *ASK* gene family.

MATERIALS AND METHODS

Plant Material and Growth Conditions

Arabidopsis ecotype Columbia (Col-0) was used throughout the study (ABRC stock No. CS7000). Seeds were sterilized by brief sequential washes in 50% ethanol and 50% Bleach/SDS prior to plating on 0.5X MS medium [26] containing 1% sucrose, and 0.8% agar. Seeds from treated plants were harvested, sterilized and stratified at 4°C for 2-3 days prior to plating and germination on solid 0.5X MS medium containing 50 µM D,L-phosphinothricin (a gift from Bayer Crop Science Canada) using the rapid procedure as described [27]. Two to three independent transgenic plants were subsequently selected for each analysis.

Plasmid Construction

For all expression constructs, a summary of standard gene nomenclature and molecular constructs are summarized in **Table 2.1**. For *35S-YFP-ASK(s)* plasmid assembly, Gateway™-compatible cDNA clones were obtained from the ABRC stock center (Columbus, OH; see **Table 2.2**) and were cloned into pEarleyGate104 [28] using the commercial Gateway™ recombination system (Invitrogen). To assemble *35S-ASK1-CFP*, *35S-TIR1-CFP* and *35S-CUL1-CFP* constructs, termination codons were first removed from the cDNA clones by PCR amplification of the coding region using the indicated primers (**Table 2.2**). Amplified PCR products were subsequently cloned into pDONR221 using the Gateway™ recombination system prior to recombination into pEarleyGate102 [28]. All recombinants were sequenced to verify the integrity of expression constructs.

Gene Name	TAIR Locus identifier	ABRC cDNA stock Number
<i>ASK1</i>	<i>At1g75950</i>	G10618
<i>ASK2</i>	<i>At5g42190</i>	N/A
<i>ASK3</i>	<i>At2g25700</i>	G13779
<i>ASK4</i>	<i>At1g20140</i>	G14059
<i>ASK5</i>	<i>At3g60020</i>	PENTR221-AT3G60020
<i>ASK6</i>	<i>At3g53060</i>	PENTR221-AT3G53060
<i>ASK7</i>	<i>At3g21840</i>	N/A
<i>ASK8</i>	<i>At3g21830</i>	PENTR221-AT3G21830
<i>ASK9</i>	<i>At3g21850</i>	PENTR221-AT3G21850
<i>ASK10</i>	<i>At3g21860</i>	PENTR221-AT3G21860
<i>ASK11</i>	<i>At4g34210</i>	PENTR221-AT4G34210
<i>ASK12</i>	<i>At4g34470</i>	N/A
<i>ASK13</i>	<i>At3g60010</i>	N/A
<i>ASK14</i>	<i>At2g03170</i>	PENTR221-AT2G03170
<i>ASK15</i>	<i>At3g25650</i>	PENTR221-AT3G25650
<i>ASK16</i>	<i>At2g03190</i>	N/A
<i>ASK17</i>	<i>At2g20160</i>	N/A
<i>ASK18</i>	<i>At1g10230</i>	N/A
<i>ASK19</i>	<i>At2g03160</i>	PENTR221-AT2G03160
<i>ASK20</i>	<i>At2g45950</i>	N/A
<i>ASK21</i>	<i>At3g61415</i>	N/A
<i>CUL1</i>	<i>At4g02570</i>	G09998
<i>TIR1</i>	<i>At3g62980</i>	GC105370
<i>AFR</i>	<i>At2g24540</i>	G21324
<i>COII</i>	<i>At2g39940</i>	G12955
<i>EIDI</i>	<i>At4g02440</i>	G15754
<i>SKP2A</i>	<i>At1g21410</i>	G14226
<i>SLY1</i>	<i>At4g24210</i>	G50138
<i>UFO</i>	<i>At1g30950</i>	PENTR221-AT1G30950

Table 2.1. Gene names and locus identifiers for genes used in this study.

attB1-AtCUL1	GGG GACAAGTTTGTACAAAAAAGCAGGCTT AAT GCCAACTTTGTACAAAAAAG
attB2-AtCUL1-stop	GGGGACCACTTTGTACAAGAAAGCTGGGTA AGCCAAGTACCTAAACATGTTA
attB1-AtTIR1	GGGGACAAGTTTGTACAAAAAAGCAGGCTTAATG CCAACCTTTGTACAAAAAAG
attB2-AtTIR1-stop	GGGGACCACTTTGTACAAGAAAGCTGGGTATAAT CCGTTAGTAGTAATGATT
attB1-AtASK1	GGGGACAAGTTTGTACAAAAAAGCAGGCTTAATG TCTGCGAAGAAGATTGTGT
attB2-AtASK1-stop	GGGGACCACTTTGTACAAGAAAGCTGGGTATTCA AAAGCCCATTGGTTCTCT

Table 2.2. Primers used for stop codon removal in Gateway® vectors.

All primers are indicated in the 5'-3' orientation.

To assemble the described BiFC constructs, cDNA domains coding for the indicated ASK and F-box proteins were fused to the N- or C-terminal domains of EYFP (nEYFP or cEYFP). The *ASK* Gateway™-based cDNA clones (listed in **Table 2.3**) were subsequently cloned into BiFP2 [29] vectors using the Gateway™ recombination system, resulting in an experimental set of *35S-cEYFP-ASK* constructs. Similarly, F-box protein-encoding cDNA clones were cloned into BiFP3 [29], resulting in the *35S-nEYFP-F-box* set of constructs. A complete list of the vectors used is summarized in Table S4. In those instances where the entry clone and destination plasmid backbone carried the same selection marker, for cloning purposes 1 µg of the pEntry plasmid was initially digested and counter-selected by restriction digestion with MluI prior to input to the LR clonase reaction. Correct expression of the desired BiFC fusion products was independently evaluated in *N. benthamiana* leaves by construction, transformation and expression of select ASK and F-box fusions in the pE-SPYNE-GW and pE-SPYCE-GW gateway compatible BiFC vectors harboring Myc and HA tags at the N-terminus of the split YFP domain, respectively [30].

Generation of Transgenic Plants

The *35S-YFP-ASK* constructs were transformed into *Agrobacterium tumefaciens* strain AGL1 by electroporation, and the presence of transgenes were confirmed by *in situ* PCR. Plant transformations were performed using the floral dip method [31]. Seeds from treated plants were harvested, sterilized and stratified at 4°C for 2-3 days prior to plating and germination on solid 0.5X MS medium containing 50 µM D,L-phosphinothricin (a gift from Bayer Crop Science Canada) using a rapid procedure previously described [27]. Two to three independent transgenic plants were subsequently selected for each analysis.

pENTR	pDestination	pExpression
<i>ASK1</i>	pEarlygate104(35S-YFP-attR)	35S-YFP-ASK1
<i>ASK3</i>	pEarlygate104(35S-YFP-attR)	35S-YFP-ASK3
<i>ASK4</i>	pEarlygate104(35S-YFP-attR)	35S-YFP-ASK4
<i>ASK5</i>	pEarlygate104(35S-YFP-attR)	35S-YFP-ASK5
<i>ASK6</i>	pEarlygate104(35S-YFP-attR)	35S-YFP-ASK6
<i>ASK8</i>	pEarlygate104(35S-YFP-attR)	35S-YFP-ASK8
<i>ASK9</i>	pEarlygate104(35S-YFP-attR)	35S-YFP-ASK9
<i>ASK10</i>	pEarlygate104(35S-YFP-attR)	35S-YFP-ASK10
<i>ASK1</i>	pEarlygate102(35S-attR-CFP)	35S-ASK1-CFP
<i>TIR1</i>	pEarlygate102(35S-attR-CFP)	35S-TIR1-CFP
<i>CUL1</i>	pEarlygate102(35S-attR-CFP)	35S-CUL1-CFP
<i>ASK1</i>	BiFP3(35S-cYFP-attR)	35S-cYFP-ASK1
<i>ASK3</i>	BiFP3(35S-cYFP-attR)	35S-cYFP-ASK3
<i>ASK4</i>	BiFP3(35S-cYFP-attR)	35S-cYFP-ASK4
<i>ASK5</i>	BiFP3(35S-cYFP-attR)	35S-cYFP-ASK5
<i>ASK6</i>	BiFP3(35S-cYFP-attR)	35S-cYFP-ASK6
<i>ASK8</i>	BiFP3(35S-cYFP-attR)	35S-cYFP-ASK8
<i>ASK9</i>	BiFP3(35S-cYFP-attR)	35S-cYFP-ASK9
<i>ASK10</i>	BiFP3(35S-cYFP-attR)	35S-cYFP-ASK10
<i>UFO</i>	BiFP2(35S-nYFP-attR)	35S-nYFP-UFO
<i>TIR1</i>	BiFP2(35S-nYFP-attR)	35S-nYFP-TIR1
<i>COI1</i>	BiFP2(35S-nYFP-attR)	35S-nYFP-COI1
<i>EID1</i>	BiFP2(35S-nYFP-attR)	35S-nYFP-EID1
<i>AFR</i>	BiFP2(35S-nYFP-attR)	35S-nYFP-AFR
<i>SLY1</i>	BiFP2(35S-nYFP-attR)	35S-nYFP-SLY1
<i>SKP2A</i>	BiFP2(35S-nYFP-attR)	35S-nYFP-SKP2

Table 2.3. Plasmid constructs generated in this study.

Western Blotting

Protein was extracted following fusion construct expression in a *N. benthamiana* transient expression system. 100 mg of leaves, infiltrated with the indicated expression constructs were ground in liquid nitrogen and mixed with 100 µl of extraction buffer [100 mM Tris·HCl (pH 7.5), 150 mM NaCl, 5 mM EDTA, 10 mM 2-mercaptoethanol, 10% glycerol, 0.1% Triton X-100, 1× EDTA free Complete protease inhibitors (Roche Applied Science)] [32]. Extracts were centrifuged at 14,000 *g* for 15 min and the supernatant was collected. Proteins were resolved by 12% SDS-PAGE and transferred to a PVDF membrane using a TransblotSD™ Semi Dry Transfer (Biorad) in Bjerrum and Schaefer-Nielsen buffer (48 mM TRIS, 39 mM glycine, 20% methanol). The blots were incubated with either anti-HA (Y-11) or anti-*c-myc* (9E10) antibodies (Santa Cruz Biotechnology) at a 1:1,000 dilution in 1% skim milk powder in TBST overnight at 4°C. Blots were washed 3 times with TBST for 10 min and incubated with secondary antibody at a 1:10,000 dilution in 2% skim milk/TBST for 1 h at room temperature. Blots were subsequently washed and exposed using Pico West Reagent™ (Fisher Scientific) and imaged using an AlphaImager device (Alpha Innotech Corp., San Leandro, CA).

Transient Expression in *N. benthamiana*

All BiFC vectors were transformed into *Agrobacterium tumefaciens* strain AGL1 by electroporation, and the presence of transgenes was confirmed by *in situ* PCR. Mixed *Agrobacterium* cultures were co-infiltrated to the abaxial surface of 3-4 week-old *N. benthamiana* plants as described [33]. The p19 protein of tomato bushy stunt virus was co-expressed with all binary BiFC expression constructs in order to suppress gene

silencing [33]. Fluorescence signals were visualized in epidermal cell layers of the leaves after 3 days of infiltration using confocal microscopy.

Confocal Imaging

Imaging of BiFC signals *in planta* was done using an Olympus Model FV1000 point-scanning/point-detection laser scanning confocal microscope. Cyan fluorescent protein (CFP), yellow fluorescent protein (YFP) and propidium iodide (PI) were excited by using 440, 512 and 543 nm laser lines, respectively. When using multiple fluorophores simultaneously, images were acquired sequentially in order to reduce excitation and emission overlaps. Olympus water immersion PLAPO60XWLSM (NA 1.0) and UPLSAPO 20x (NA 0.75) objectives were employed. Image acquisition was conducted at a resolution of 512 x 512 pixels, with a scan rate of 10 ms per pixel. Olympus FLUOVIEW v1.5 software was used for image acquisition and the export of TIFF files. Figures were assembled using GIMP 2.0 (<http://www.gimp.org/>).

Quantitative Real-Time PCR

Total RNA was isolated using a commercial mini-preparation kit (RNeasy™, Qiagen) and contaminating DNA was removed using an immobilized DNase column (RNase-Free DNase Set™, Qiagen). Two micrograms of total RNA was used as template for first strand cDNA synthesis in a 20-μL reaction using the RevertAid™ synthesis kit (Fermentas). The resulting cDNA was diluted 1:20 and 1.5 μL of cDNA was used in a standard 20-μL PCR reaction. Analysis of gene expression used the Maxima™ Sybr-green qPCR master mix (Fermentas) in an Applied Biosystems 7300 RT-PCR System, following the manufacturer's instructions. The primers used in the qRT-PCR analyses are listed in **Table 2.4**.

Name	Sequence (5'-3')
CUL1_Sense	ACAGCAGCCTGGTAAGTAGA
CUL1_Antisense	CAAGTGTGTTGAAGTCTTCA
ASK1_Sense	CAGCCAGAATGAGTTCAAAG
ASK1_Antisense	GAGTATTGCAAGAGGCACGT
ASK2_Sense	CAGCCAGGATAAGATCGAAG
ASK2_Antisense	GCTGAGAAATCCGAAACCAC
ASK3_Sense	AAATAGTTGGCAGCCCGAAG
ASK3_Antisense	CTGGTGGAGACAAGGATTTC
ASK4_Sense	TAGTTCGCAGCCAAGATGAG
ASK4_Antisense	GAGTATTGCAAGAAGCACGT
ASK11-12_Sense	GGTGGAAGAAGCGGTAGCAA
ASK11-12_Antisense	GAGGGATTCCATCAGCAACG
ASK7_Sense	CTCCCCACAAAGAAAACAA
ASK7_Antisense	CGTACATTCGGCTTCAATCA
ASK20_Sense	GGCTCTGTGAGTTGACCTCT
ASK20_Antisense	CCTCCTCAGTAAGGTCATCA
Actin2_Sense	TCCCTCAGCACATTCCAGCAGAT
Actin2_Antisense	AACGATTCTGGACCTGCCTCATC
Ubiquitin10_Sense	CACACTCCACTTGGTCTTGCGT
Ubiquitin10_Antisense	TGGTCTTTCCGGTGAGAGTCTTCA
β -6-tubulin_Sense	ACCACTCCTAGCTTTGGTGATCTG
β -6-tubulin_Antisense	AGGTTCACTGCGAGCTTCTCTCA
ASK5_Sense	GACGGCTGCGCCACTGATGT
ASK5_Antisense	TTTGCTCTTGACGTGCTTCTCGCA
ASK8_Sense	ACGATCTTTGCTCTCACCAATGCTGC
ASK8_Antisense	AAGAATTCGCGCATCTGCTTCGGA
ASK9_Sense	GCCGCACGCCAATGCCAGATTA
ASK9_Antisense	GCGGCATCGACGTGGTGCTT
ASK10_Sense	GCATGCCAAACCGTCGCGGA
ASK10_Antisense	GTTGAAGAATTTGCGAGTGTGCTCCAC
ASK15_Sense	AGAAGAAGCCCGATGATGAGGCGAA
ASK15_Sense	TCGACGTTGAGATAGTTAGCAGCGAGA
ASK14_Sense	CGTCGTTGACGAAGAAAGCGACGA
ASK14_Antisense	CAGCGAGCAAGAGTTGGAAGACCG
TIR1_Sense	GCGCCTCTGGGTGCTTGA
TIR1_Antisense	GCCCCTGTTCCGTCAATGCCA
ASK6_Sense	AAGGGTATGGCAGAAGACGA
ASK6_Antisense	TCTTTGCTCTCAACGACGTG

Table 2.4. Oligonucleotide primers used for qRT-PCR analyses.

To identify the optimal internal reference control *β6-tubulin*, *ACTIN2* and *UBQ10* expression was assessed across all organs. *ACTIN2* (At3g18780) transcript expression showed the least amount of variation across all tissues examined and was used as the internal standard in order to normalize the qRT-PCR data. Real time PCR results were analyzed using Q-Gene software that expresses data as Mean Normalized Expression (MNE) [34] which is directly proportional to the amount of mRNA of the target genes relative to the amount of mRNA of the *ACTIN2* internal reference standard. In brief, to calculate MNE, the PCR efficiency (E), mean cycle threshold (Ct) and related standard errors (SEs) were used to calculate ECt for both the reference and target genes. MNE was subsequently calculated by dividing the ECt of the reference gene by the ECt of the target gene. Gene expression is depicted in MNE units after *ACTIN2* normalization (Table S5). Two biological and 3 sample replicates were performed for each tissue/organ studied while taking into consideration the efficiency of the reaction for each primer combination [34]. Data is depicted as the mean of two independent biological repetitions ± SE. To calculate the relative fold-change expression among *ASK* genes, the ‘Relative Expression Software Tool-Multiple Condition Solver’ (REST-MCS) was used [35,36]. Pearson-based hierarchical clustering of *ASK* gene expression data was done using the online version of Expression Profiler found at EBI (<http://www.ebi.ac.uk/expressionprofiler/>) [37].

Phylogenetic Analysis

ASK protein sequences were retrieved from the TAIR10 genome annotation data set (<http://www.arabidopsis.org/>). Multiple alignments were carried out using the CLUSTAL algorithm found within the MEGA 4 software suite [38] using a BLOSUM 30 matrix with

a gap penalty of 10, an extended gap penalty of 0.2 and a gap distance of 5. The tree was constructed using the Neighbor Joining (NJ) method utilizing the p-distance substitution method in MEGA 4 and node reliability was calculated using 1,000 Bootstrap replicas [38]. In order to evaluate different clustering methods for their possible effect on tree construction, we compared three different methods: NJ Maximum Parsimony, Un-weighted Pair Group and Arithmetic Mean (UPGMA) using MEGA 4. This comparison revealed slight differences in the clustering pattern. Clustering using UPGMA resulted in the grouping of ASK13 with ASK11 and ASK12 but not with ASK5 and ASK6. However, based on the chromosomal location and supporting literature [39] we believe that *ASK13* is a result of tandem duplication of *ASK5*, thus NJ clustering was used for this study.

RESULTS

A phylogenetic analysis of relatedness within the *ASK* gene family of Arabidopsis reveals that the 21 members of this gene family fall into 7 distinct clades when clustered on the basis of primary deduced amino acid sequence, as summarized in **Figure 2.1**. This clustering of the predicted ASK proteins is consistent with published results, where *ASK1* and *ASK2* are grouped within a clade and were found to overlap functionally and are known to be essential for early development in Arabidopsis [40]. We used this phylogenetic tree as a basis to assess the functional relatedness among *ASK* paralogs as measured by three functional criteria: tissue/organ-specific transcript abundance, sub-cellular localization of YFP-tagged ASK proteins, and the protein-protein interaction profiles of ASK proteins in conjunction with selected F-box proteins expressed as BiFC fusion constructs.

qRT-PCR Analysis of *ASK* Gene Transcript Abundance

A qRT-PCR analysis of transcript abundance was undertaken for members of the *ASK* gene family which reside in common phylogenetic clades based on their primary deduced amino acid sequence (*ASK1,2,3,4,5,6,7,8,9,10,11/12,13,14,15,16,17,18,19,20,21*). Included were two genes known to be associated with SCF type E3-Ub function (*CUL1, TIR1*) as well as β -tubulin, *Actin2* and *UBQ10* as internal reference controls. We were unable to design unique qRT-PCR primers capable of distinguishing *ASK11* from *ASK12* transcripts, due to the high DNA sequence similarity (99.3%) between these two genes. Thus, for purposes of this study, a single primer pair for *ASK11/ASK12* was used. Transcript-specific primers and their associated genomic identifiers are listed in **Tables 2.1** and **2.2**.

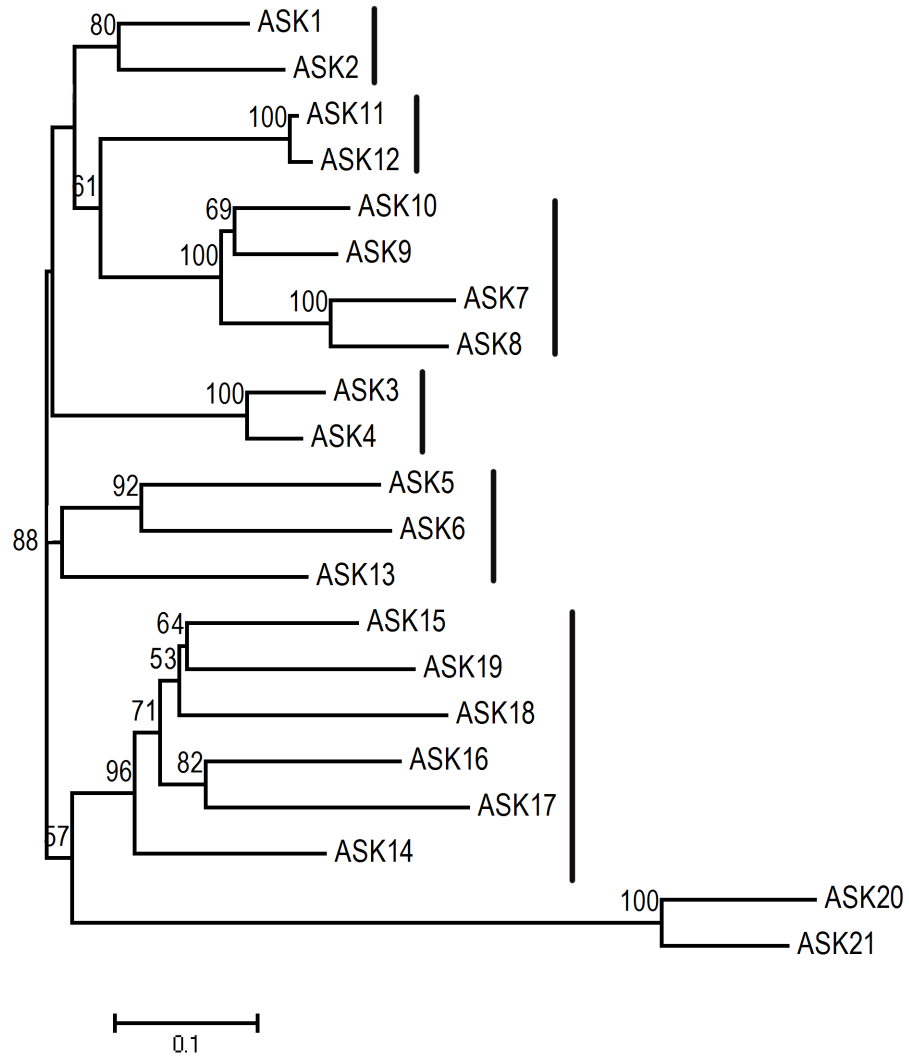


Figure 2.1. Relationship of the *ASK* gene family in Arabidopsis.

The phylogenetic grouping of *ASK* genes based on their deduced primary amino acid sequence was calculated using the NJ method described. The genes are grouped into seven distinct clades as denoted by the vertical lines. Numbers at the branches represents percentage bootstrap support calculated for 1000 replicates. All tree branches are scaled to the number of amino acid substitutions per site.

Transcript abundance was quantified in cDNA preparations constructed from total RNA fractions prepared from rosette leaves of plants prior to stage 5.2, roots of 7-day-old seedlings, green stems (1st and 2nd internodes of bolted plants), green siliques with seeds (late heart to mid torpedo embryo), whole 5-day-old seedlings, old stage 9 whole flowers (petal primordia stalked at base) from 19-23-day-old plants and stage 15 whole flowers (stigma extends above long anther) from 21-23-day-old plants [41]. Quantitative RT-PCR analysis and cDNA measurements were the result of 3 independent experiments involving 2 biological replicate samples for each as summarized in **Figure 2.2**, where data for each gene/organ combination are shown and clustered on the basis of their relative expression abundance across all biological samples analyzed (**Figure 2.3**).

From this analysis, and in agreement with previously published studies, the relative abundance of mRNAs for *ASK1* and *ASK2* were found to be elevated and constant in comparison to other *ASK* genes across all biological organs examined [23,42]. However for the common clade comprised of *ASK3* and *ASK4*, the transcripts for these two genes were found to be expressed at markedly different steady state levels, where the abundance of *ASK4* mRNA was consistently an order of magnitude higher in all organs examined except siliques. Moreover, the relative expression of *ASK3* was elevated in reproductive organs in comparison to other organs, whereas *ASK4* mRNA abundance was relatively constant across all organs examined. When expressed as the ratio relative to whole seedling organs, *ASK3* mRNA was found to be 500-fold more abundant in green siliques (**Figure 2.4C**) and was elevated in stage 9 and stage 15 flowers excised from 21-25-day-old plants (**Figure 2.4A,B**).

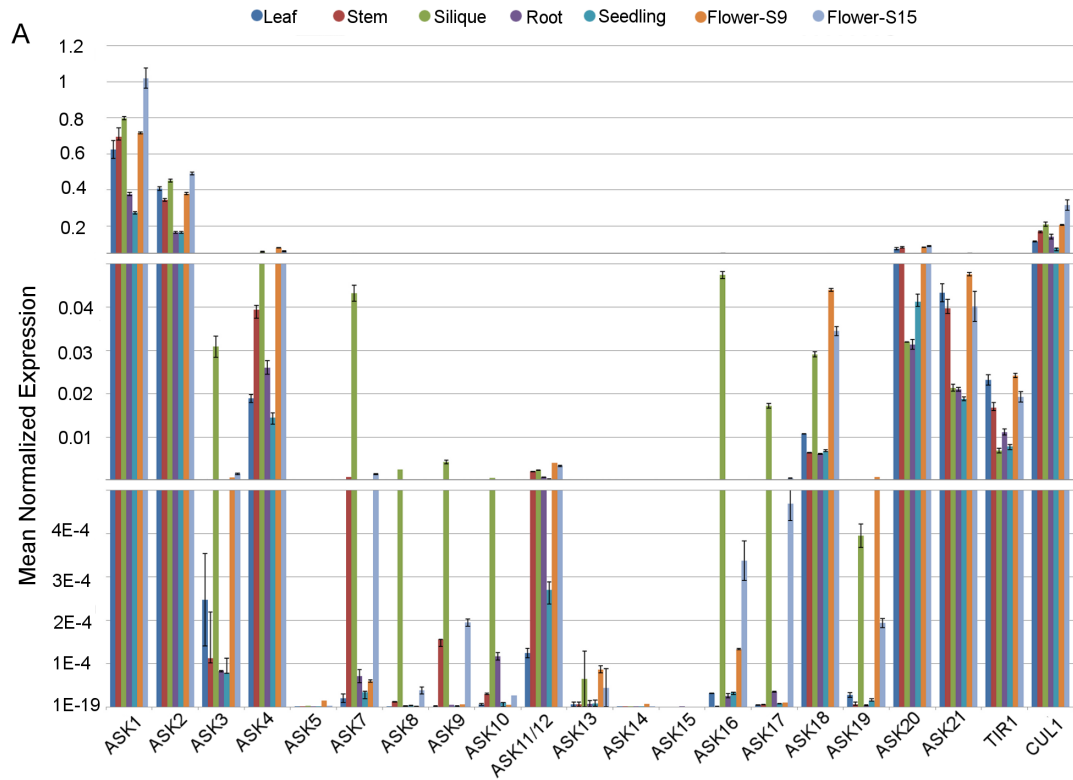


Figure 2.2. Real-time expression analysis of the Arabidopsis *ASK* gene family.

RNA from the indicated organs was isolated and used to assess *ASK* gene expression as described in the methods. Organs examined were 4-5-day-old seedlings, stage 5 leaves, green stem, green siliques, stage 9 flowers, and stage 15 flowers. Gene expression is depicted in MNE units \pm SE after *ACTIN2* normalization. Data are means of two independent biological repetitions \pm SE.

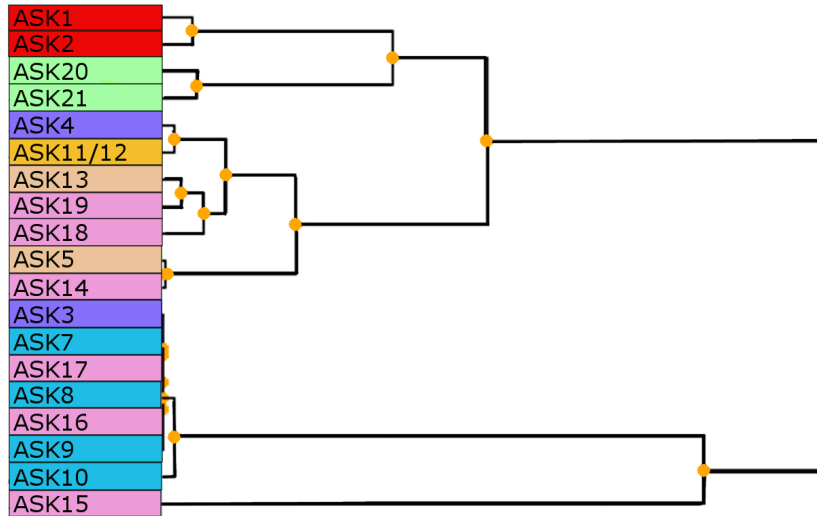


Figure 2.3. Pearson-based hierarchical clustering of *ASK* gene expression.

Cluster summary of the Pearson-based hierarchical clustering of *ASK* gene expression among select organs. The colors represent genes within the different phylogenetic clades as defined within **Figure 2.1**.

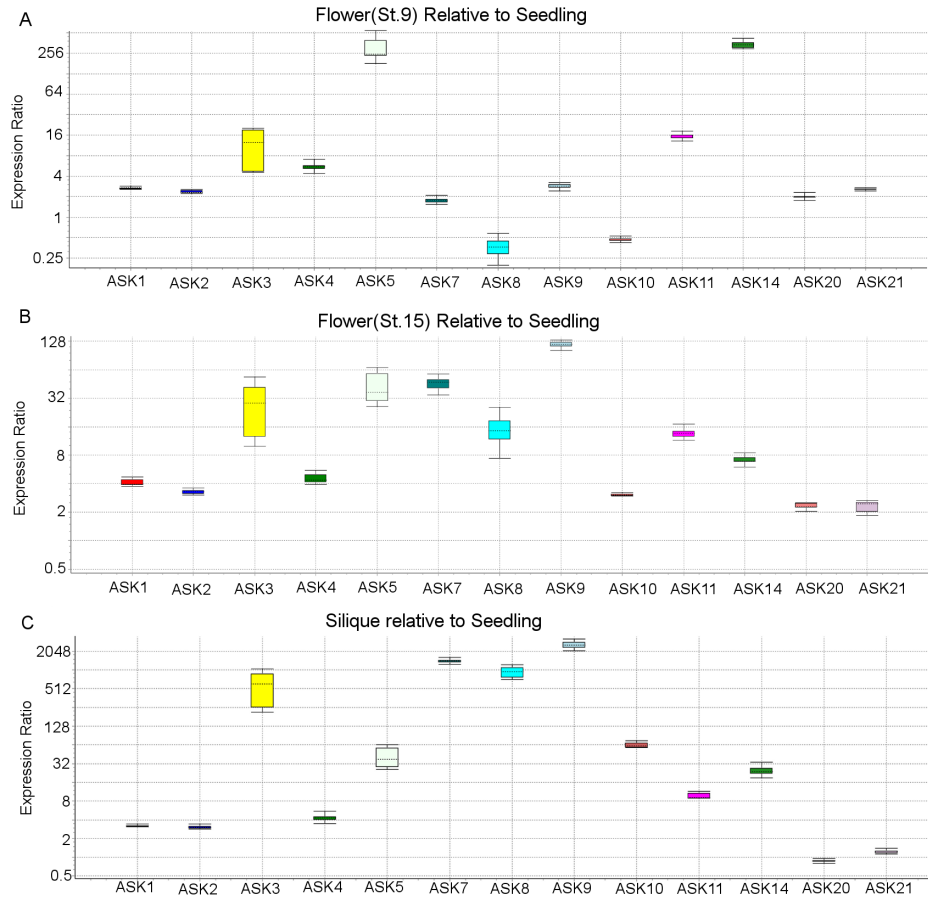


Figure 2.4. Relative organ-specific abundance of cDNAs for select *ASK* genes. All gene expression was normalized relative to *ACTIN2* expression. **A**; Relative abundance of *ASK* gene cDNAs in flowers from stage 9 plants relative to seedlings. **B**; Relative abundance of *ASK* cDNAs in stage 15 flowers relative to seedlings. **C**; Relative expression of *ASK* genes in siliques relative to seedlings.

In contrast, the expression ratio for *ASK4* mRNA was only modestly elevated (about 3-4-fold) in these same organs.

A distinct expression pattern was observed within the clade comprised of *ASK5/6/13* where *ASK13* transcripts were found to have a relatively higher abundance in foliar tissues and the silique. *ASK6* transcripts were not detectable in the organs examined (data not shown), whereas its close paralog *ASK5* albeit lower than *ASK13*, expressed measurable transcripts in all organs examined (**Figure 2.2**). Although *ASK6* has been suggested in the literature to be a pseudogene [43] we think this is unlikely since *ASK6* cDNA has been enriched from a low-abundance RNA library and the corresponding clone is available from the ABRC stock center (stock number PENTR221-AT3G53060).

Within the phylogenetic clade defined by *ASK7,8,9,10*, all four gene transcripts were found to be relatively abundant in tissues from later-stage flowers (stage 15) and siliques, whereas their abundance was relatively low in earlier (stage 9) flowers compared to seedlings (**Figure 2.4**). The *ASK10* gene expression pattern was unique among genes defining the *ASK7,8,9,10* clade in that it exhibited a conspicuously lower relative transcript level compared to the other 3 genes in the clade.

For the clade defined by *ASK20* and *ASK21*, transcripts were expressed at a relatively low and constant level, with a modest increase in abundance (2- to 4-fold) in stage 9 and stage 15 flowers (**Figure 2.4**). Interestingly, the expression pattern of *ASK20* and *ASK21* most closely resembled that of *ASK1* and *ASK2* in light of their constant level of expression throughout development of Arabidopsis. The lowest transcript level in comparison to all other *ASK* genes studied was observed for *ASK14,15*, which co-reside within the clade comprising *ASK14,15,16,17,18,19*. However, transcripts for these two

genes showed a distinct expression pattern between them in that *ASK15* was expressed only in roots and siliques (**Figure 2.2**) whereas *ASK14*, similar to *ASK5*, was expressed preferentially in early stages of flower development (stage 9) followed by a decline in transcript abundance at later stages of flower maturation (stage15) and silique development.

The data underlying the observed pattern of relative abundance of mRNAs for each *ASK* gene, across all organ sources examined, was submitted to clustering analysis with the resulting grouping presented in **Figure 2.3**. The data indicate that *ASK4* and *ASK11/12* are similar with respect to the relative abundance of their respective transcripts and their pattern of expression across the organs examined. In this analysis, *ASK3* mRNA abundance in the organ samples assessed was distinct from *ASK4* as its closest primary sequence paralog in Arabidopsis.

It should be noted that several deviations were observed between the expression data here versus the microarray data available through several databases such as Bio-Array [44,45] and GeneInvestigator™ [46]. In those instances where deviations were observed, such variations could be attributed to the probes used in the microarray construction. For instance, and in contrast to our findings, closely related genes such as *ASK3* and *ASK4* as well as *ASK20* and *ASK21* exhibit identical expression behaviour when measured using microarray approaches (**Figure 2.5**), where the results can be explained by the use of probes that did not distinguish between the mRNAs encoded by these two genes.

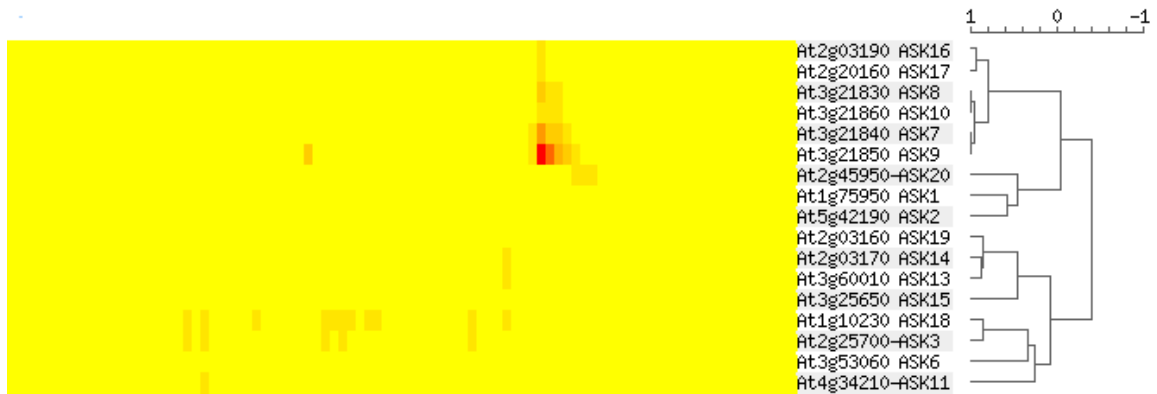


Figure 2.5. Hierarchical clustering of *ASK* gene expression.

Hierarchical clustering of publically available microarray expression data for *ASK* genes across different Arabidopsis tissues, using the Expression Browser tool found online at <http://bar.utoronto.ca>. The difference observed between this clustering and that generated by the present study can be attributed principally to the non-uniqueness of the probes used in construction of the microarrays, coupled with the higher resolution of the qRT-PCR data.

Sub-cellular Localization of YFP:ASK Fusion Proteins in Arabidopsis

One explanation for the presence of the large number of ASK proteins in Arabidopsis could be a corresponding diversity of sub-cellular localization for some of the ASK proteins. A study was therefore undertaken to evaluate the sub-cellular localization profile of 9 selected ASK proteins expressed as functional fusions with the YFP auto-fluorescent protein in transgenic Arabidopsis. The YFP:ASK fusion proteins were expressed from CaMV 35S promoter constructs assembled and transformed into Arabidopsis as described, and the results are summarized in **Figure 2.6**. Propidium iodide (PI) staining was used to visualize cell walls and general morphology in whole mounts of roots and 5-day-old seedling leaf epidermal cells including guard cells (**Figure 2.6A,C**). The signal arising from chlorophyll auto-fluorescence is shown in **Figure 2.6B**. In parallel, cellular expression and sub-cellular localization of the YFP:ASK3 fusion protein is shown in **Figure 2.6D-F**, and the composite PI-YFP images is shown in **Figure 2.6G-I**. Taken together, and in agreement with previous studies described for *ASK1* [47,48], YFP:ASK3 proteins accumulate in both the nucleus and the cytoplasm in epidermal leaf cells of Arabidopsis. We observed no overlap between the YFP and chlorophyll auto-fluorescence signals, suggesting that the extra-nuclear YFP:ASK3 fusion protein does not detectably localize to the chloroplast and largely accumulates in the cytoplasm.

This same pattern of YFP fusion protein accumulation in the nucleus and cytoplasm, with no significant localization to chloroplasts was reiterated across all other YFP:ASK gene fusions assessed (*ASK1,2,3,4,5,6,8, 9,10*) with the exception of *ASK8* (see **Figure 2.7**). The YFP:ASK8 protein fusion, when expressed in transgenic Arabidopsis was found to apparently aggregate predominantly in the nuclei of epidermal

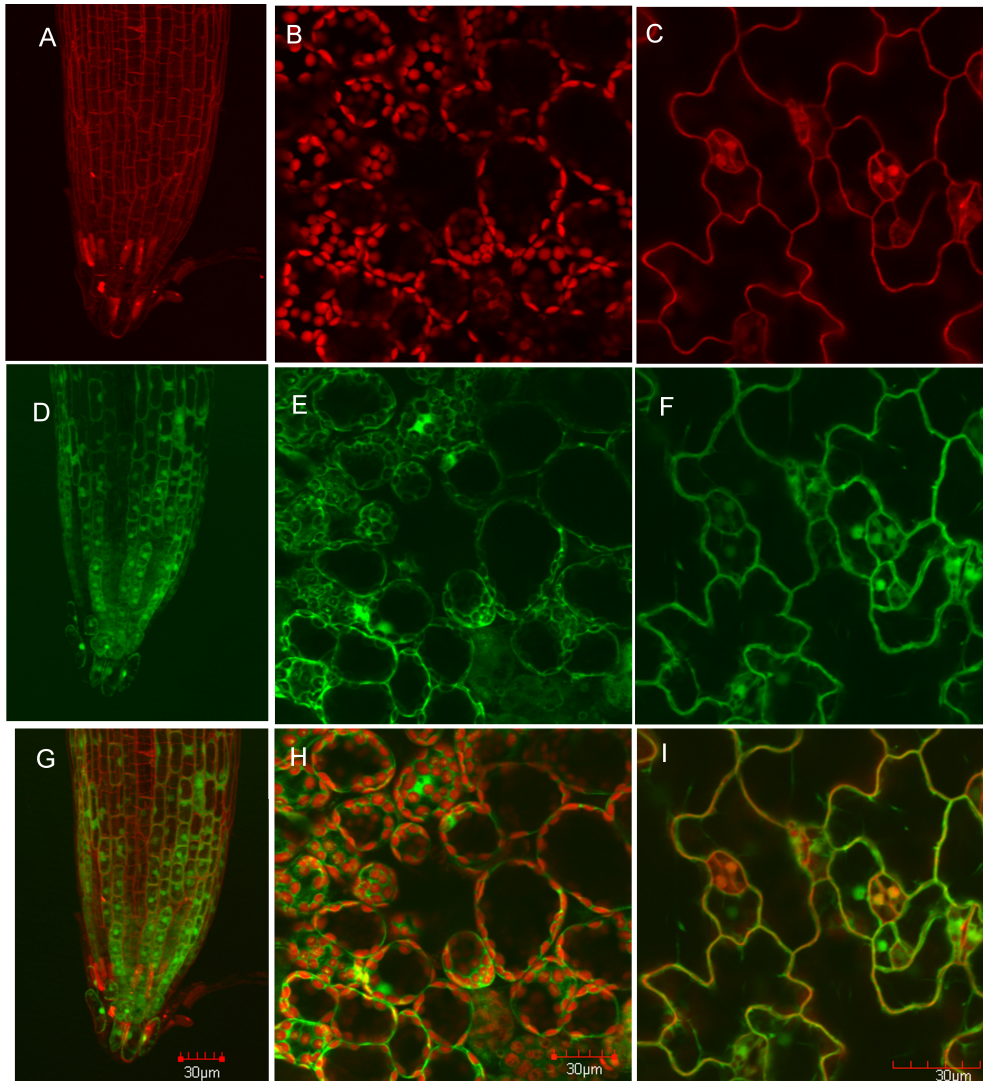


Figure 2.6. Confocal imaging and sub-cellular localization of ASK proteins in transgenic Arabidopsis.

A&C; Propidium iodide-stained epidermal root cell walls or leaf epidermal cell walls and guard cell nuclei. **B;** Chlorophyll auto-fluorescence from the leaf mesophyll cell layer. **D-F;** stable expression of N-terminal YFP-tagged ASK3 protein in transgenic Arabidopsis.

G- I; merged channels corresponding to panels (**A-C**) and (**D-F**).

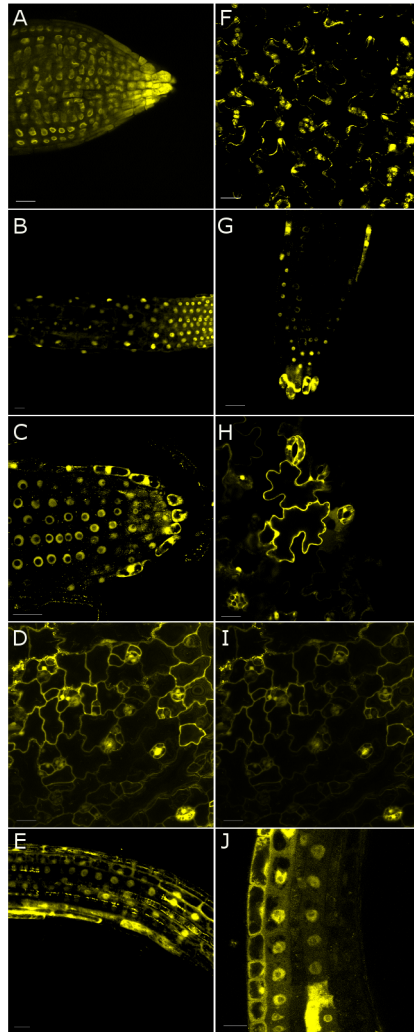


Figure 2.7. Confocal imaging and sub-cellular localization of YFP:ASK protein fusions in transgenic Arabidopsis.

Fusion protein visualization in stable transgenic lines was carried out as described in the methods. **A,B,C,E,G, J**; sub-cellular localization of YFP:ASK1, YFP:ASK2, YFP:ASK4, YFP:ASK8 and YFP:ASK10 in root tissues, respectively. **D,F,H,I**; localization of YFP:ASK5, YFP:ASK8, YFP:ASK9 and YFP:ASK10 in leaf tissues, respectively. Scale bars = 30 μm .

leaf cells, resulting in highly localized and intense YFP signals. Notably, these aggregates were not observed in root tissues of the same transgenic lines (**Figure 2.8A**). In order to investigate whether the apparent aggregation of ASK8 was the result of YFP:ASK8 over-expression, the expression of this fusion was compared to that of the YFP:ASK1 protein using Western blot analysis. As shown in **Figure 2.8B**, the level of YFP:ASK8 expression in three independent lines was qualitatively lower than that of the YFP:ASK1 fusion protein. Although ASK sub-cellular localization resembles that of GFP sub-cellular localization, the lack of available ASK protein-specific antibodies precludes the possibility of taking immunohistochemical approaches to localizing nascent ASK proteins *in situ*. However, we noted that the majority of reported SCF substrates in Arabidopsis are known transcription factors [5,49], which is consistent with our observation of a general nuclear localization of YFP-ASK fusion proteins. To investigate whether N-terminal fusions could mask nascent localization signals, C-terminal CFP fusion constructs using the *ASK1* coding region were generated, and a similar localization pattern was observed following transient expression in *N. benthamiana* leaves (**Figure 2.9C**). In addition, we asked whether other known SCF ligase subunits exhibited a similar localization pattern to ASK proteins, suggesting the potential for co-localization and participation in SCF complex assembly. Upon assessing the localization pattern of TIR1 and CUL1 as C-terminal CFP fusions, we found that a similar localization was observed relative to the YFP:ASK protein studies described above (**Figure 2.9A,B**).

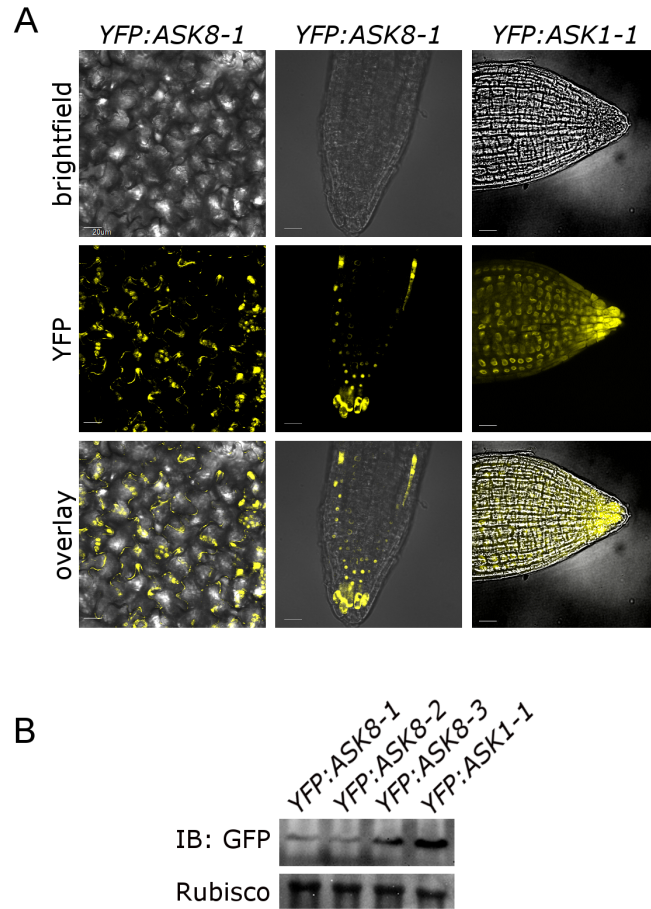


Figure 2.8. Expression and localization of YFP:ASK8 fusion protein in transgenic Arabidopsis.

A; Localization of YFP:ASK8 in leaves and roots of transgenic plants. The YFP:ASK8 fusion protein was found to aggregate exclusively in the leaves of transgenic plants, but exhibited a similar pattern to that of other YFP:ASK fusion proteins in the roots of the same transgenic plants. **B;** Comparison of YFP:ASK8 and YFP:ASK1 protein expression in three different transgenic Arabidopsis lines, where YFP:ASK1 expression showed no sign of aggregation. The results indicate that the observed signal aggregation in the ASK8:YFP transgenic backgrounds were not due to over-expression of the fusion protein. Scale bars = 30 μ m.

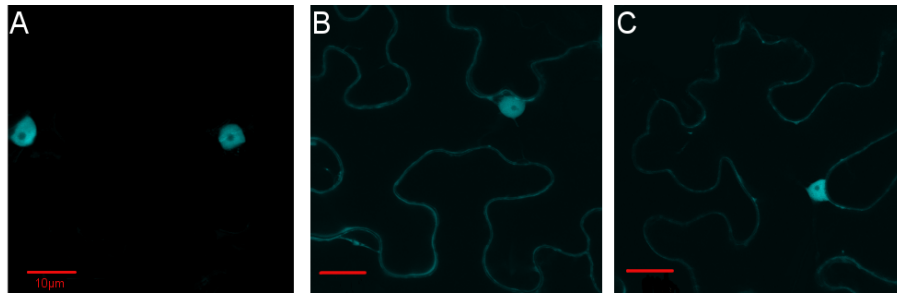


Figure 2.9. Confocal imaging and sub-cellular localization of CFP fusion proteins in *N. benthamiana*

C-terminal CFP fusion proteins were transiently expressed in *N. benthamiana* leaf epidermal cells and visualized using confocal microscopy. **A**; TIR:CFP fusion protein. **B,C**; CUL1:CFP and ASK1:CFP fusion protein. The sub-cellular localization of ASK1:CFP in *N. benthamiana* leaves parallels that of YFP:ASK1 in transgenic Arabidopsis lines, and confirms the fidelity of the *N. benthamiana* transient expression assay. Scale bars = 30 μm .

ASK-F-box Protein Interaction Profiling *In Vivo*

Previous studies have shown that individual protein products of the *ASK* gene family exhibit both general as well as specific protein-protein interactions involving select F-box proteins, when assessed in the heterologous yeast 2-hybrid system [21,50]. This property of generalized versus specific F-box protein interaction capability is of importance for determining which specific ASK polypeptides are capable of interacting with specific F-box proteins, with implications for the combinatorial diversity of SCF E3-Ub complexes that could form *in vivo* involving subunit polypeptides of either class. Accordingly, we undertook to analyze the *in situ* interaction of polypeptides encoded by *ASK1,2,3,4,5,6,8,9* and *ASK10* in combination with a selected panel of 7 F-box proteins (TIR1, SLY1, COI1, EID1, SKP2A, AFR and UFO) known to participate in SCF complex assembly. These proteins are involved in the regulation of diverse aspects of plant development such as auxin sensing, circadian rhythm maintenance, ethylene sensing, patterning and development [4,10,51–59]. Protein interactions were assessed as the reconstitution of fluorescence signal upon co-expression of all 56 pair-wise combinations of split-YFP fusion expression constructs assembled as described in the methods, and subsequently expressed through co-infection of *Agrobacterium*-containing constructs in the high-fidelity *N. benthamiana* transient expression system [33]. The data for a subset of 16 pair-wise combinations of ASK-F-box interactions are summarized in **Figure 2.10** with the exception of ASK2, which is shown in **Figure 2.11**. An interaction profile map is depicted in **Figure 2.12**.

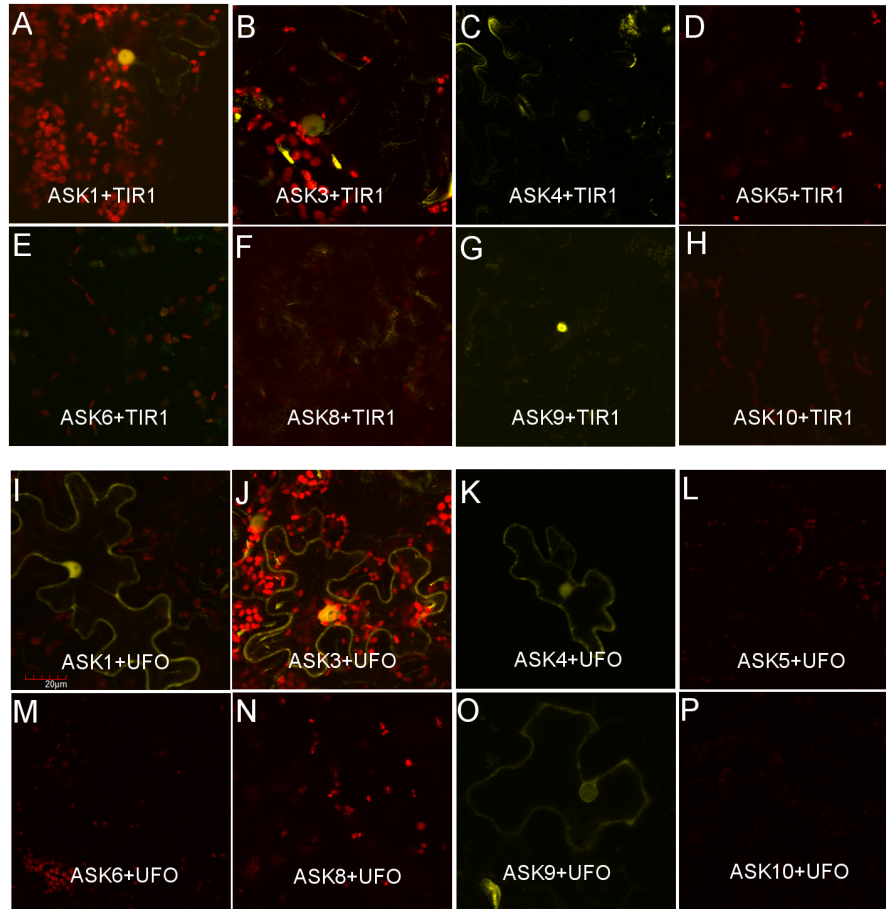


Figure 2.10. Interaction profile of select ASK and F-box proteins as assessed using BiFC.

Visualization of BiFC-based sub-cellular protein interactions between select ASK and F-box proteins (TIR1 or UFO) in *N. benthamiana* epidermal leaf cells: YFP signal indicates a positive interaction; chlorophyll auto-fluorescence is shown in red. **A-H**; protein interactions between TIR1 and the ASK1,3,4,9 proteins expressed as BiFC fusion expression constructs. **I-P**; protein interactions between UFO and ASK1,3,4,9 proteins expressed as BiFC fusion expression constructs. Scale bars = 30 μ m.

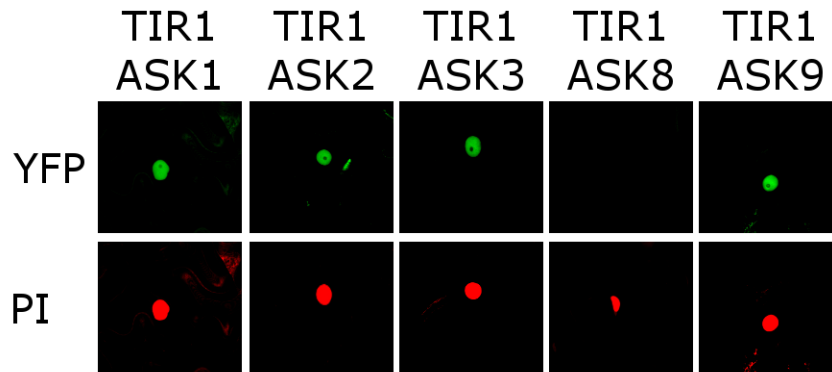


Figure 2.11. Sub-cellular localization of BiFC signals.

The sub-cellular localization of BiFC signals were assessed by determining co-localization of select BiFC signals with the nuclear-specific prodium iodide (PI) signal, as described. **A,B,C,D,E**; the YFP fluorescent signal from the BiFC assays. **F,G,H,I,J**; fluorescent signal from the PI-stained nuclei.

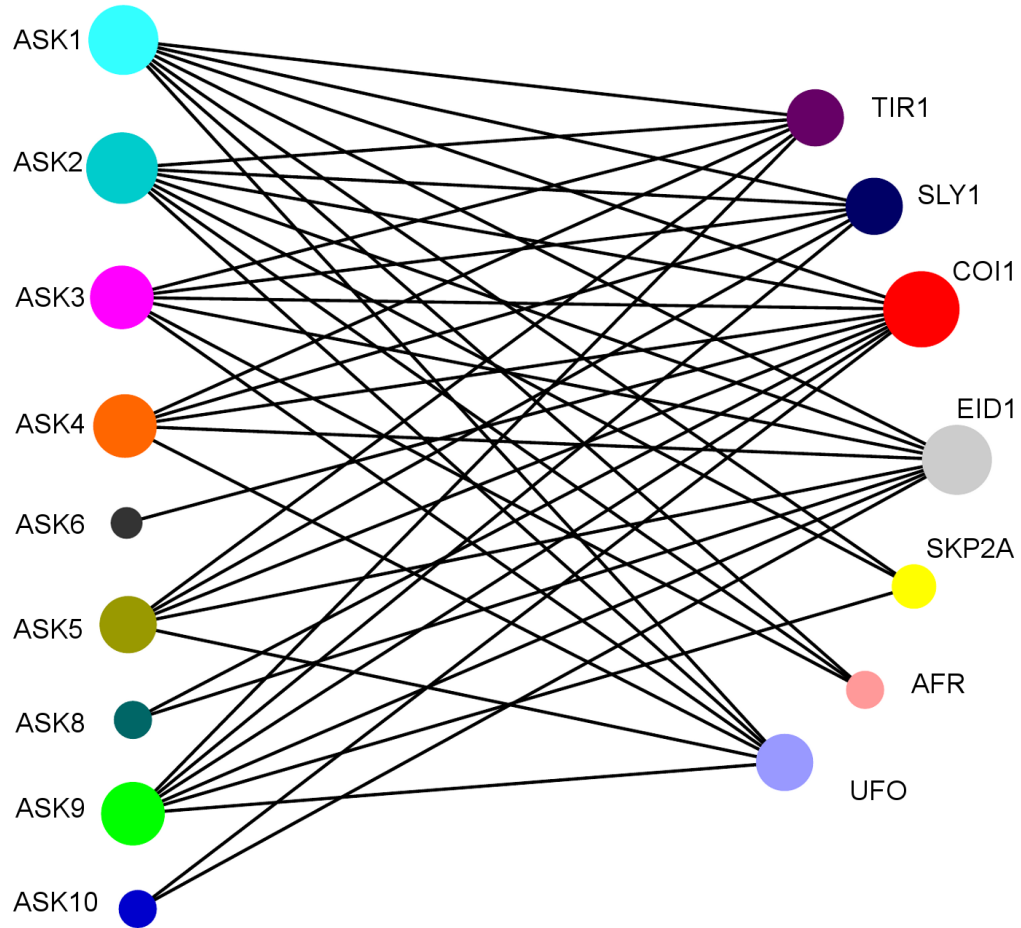


Figure 2.12. Interaction profile map of select ASK and F-box proteins.

The indicated interaction map was developed as described in the methods, and summarizes the results obtained following transient expression of BiFC constructs in *N. benthamiana* leaf epidermal cells. Edge lines joining nodes represent a positive interaction.

With respect to protein interactions involving TIR1, five ASK polypeptides (ASK1,2,3,4 and ASK9) were found to interact with TIR1 *in vivo*. Interestingly, the interaction signal observed was predominantly localized to the nucleus in leaf epidermal cells (**Figure 2.10A-D**). Similarly, expression fusion products involving ASK1,2,3,4 and 9 were found to interact with UFO in a pattern that was analogous to TIR1. Although closely related at the primary amino acid sequence level with ASK9, split-YFP expression constructs involving ASK10 did not detectably interact *in vivo* with TIR1 or UFO.

The results summarizing binary protein interactions involving the remaining 40 F-box-ASK combinations are depicted in the interaction map shown in **Figure 2.10Q**. For all protein interactions involving COI and TIR1, the YFP signal was restricted to the nucleus, whereas all other F-box-ASK protein combinations were observed in both the cytoplasm and the nucleus. Also noteworthy was the finding that SKP2a interacted with ASK3 in the split-YFP system but not with ASK4, notwithstanding the high degree of deduced primary amino acid sequence similarity between these two ASK polypeptides (94.5%).

Considering that all ASK and F-box proteins tested were found to interact with at least one other binding partner, we concluded that the observed negative interacting protein combinations were biologically significant and were not due to low levels of protein expression. To confirm that protein expression among the observed negative interacting combinations was comparable to that of positive interacting proteins, we cloned select F-box and ASK coding domains into a second set of BIFC vectors where the split-YFP coding region incorporated c-Myc- and HA-tag domains, thus facilitating

comparative protein expression studies via Western Blot analysis [30]. As shown in **Figure 2.13**, from the select proteins investigated all were expressed to levels qualitatively comparable to that of the positive interacting proteins, indicating that the observed negative interactions were not due to the lack of protein expression.

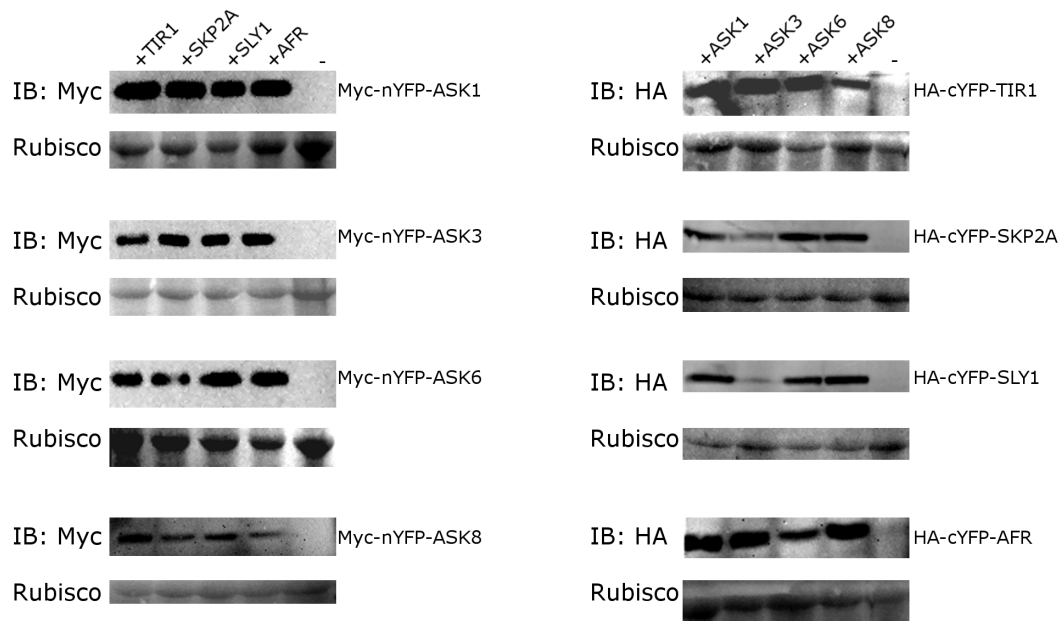


Figure 2.13. Protein expression verification of the split-YFP fragments in the BiFC assay.

Following visualization of the BIFC signal, injected *N. benthamiana* leaves were subjected to protein extraction and immunoblotting (IB), the expression of ASK1, ASK3, ASK6 and ASK8 in combination with TIR1, SKP2A, SLY1 and AFR was examined. The ASK genes were cloned into a Myc-tag BiFC vector and the F-box proteins in an HA-tagged BiFC vector. Protein immunoblots decorated with anti-Myc (left panel) and anti-HA (right panel) antibodies were used for detection of the nEYFP:ASK, and cEYFP:F-box fusion proteins, respectively.

DISCUSSION

In evolutionary terms, and when compared with other well-characterized multi-cellular model systems, plants exhibit a relatively complex complement of genes that are known or predicted to encode subunit components of the SCF-class of E3-Ub ligase complexes [1,60]. Despite having one of the smallest known genomes among angiosperm plants [61], *Arabidopsis* harbours a Skp1-like protein subunit-encoding gene family that is several-fold to orders-of-magnitude greater in complexity than the single gene found in mammals or yeast [39,62,63], with variable degrees of complexity found in other model systems such as *Caenorhabditis elegans* (21 genes) or *Drosophila melanogaster* (6 genes) [64,65]. The apparent high degree of gene duplication of *SKP1* genes is a feature of plants in general (e.g., the 28 *Skp1*-like genes in rice; [39]). Furthermore, the average rate of gene duplication of the *ASK* gene family in comparison to other gene families in *Arabidopsis* is roughly ten times higher [39]. This feature of plant SCF-E3 ligase subunit-encoding complexity can be traced to their earliest evolutionary origin in pre-vascular plants, as revealed by the predicted proteome containing 4 *Skp1*-like genes in the moss, *Physcomitrella patens* [66].

Given the complexity of gene families that are known or predicted to encode subunits of SCF complexes in *Arabidopsis*, studies ascribing function to individual genes will minimally involve an assessment of subunit functional redundancy, together with an evaluation of the specific SCF complexes that may assemble across developmental time and space. Notions of functional redundancy can be approached from several perspectives, including genetic approaches where loss-of-function alleles in genetic backgrounds carrying single or combinations of mutant loci can be examined for aberrant

phenotypes. Single and multiple mutant lines are also valuable for complementation studies from which insight into structure-function relationships involving specific proteins can be derived. Where large gene families are involved, genetic approaches to defining redundancy are commonly guided by phylogeny and clustering of gene products based on their deduced primary amino sequence [67].

Functional redundancy among gene paralogs has been recently extended to include multiple independent biological criteria including quantitative assessment of gene expression, protein-interaction networks involving specific gene products, as well as sub-cellular compartmentation of individual gene products in recognition of the potential complexity of regulatory interactions and functional divergence among genes duplicated in the course of evolution [68]. The analysis presented here embraces this approach, and highlights variations in key functional properties among the Arabidopsis *ASK* gene family.

Clade analysis reveals that clade 1 is comprised of two *ASK* genes, *ASK1* and *ASK2* with an overall similarity of greater than 83% between these two genes. These two genes are also representative of the four *ASK* genes (*ASK1*, 2, 3 and 4) bearing an intron. *ASK1* and *ASK2* are thought to be the evolutionary result of a segmental duplication and subsequent slow evolution of a highly conserved function in plants [39,43]. Although *ASK1* exhibits a higher transcript level than *ASK2*, the expression pattern of these two genes shows a high degree of co-regulation in terms of transcript abundance. The BiFC-based protein interaction profile described here for *ASK1* and *ASK2* confirms earlier findings arising from yeast 2-hybrid and co-enrichment experiments that highlight the broad F-box protein interaction potential of both *ASK1* and *ASK2* proteins [21]. This

pattern of broad interaction potential suggests that both *ASK1* and *ASK2* participate in a combinatorially diverse array of SCF complexes, which is consistent with the findings from genetic studies that these two proteins exhibit significant functional overlap and are essential for growth early in development [40]. The high degree of similarity in terms of interaction and expression profile is reminiscent of the phylogenetic clades defined by primary deduced amino acid sequence similarity, which could be in part explained by the high level of conservation of these two genes during the course of *Arabidopsis* evolution.

The second clade is defined by *ASK3* and *ASK4* as two members of the *ASK* gene family whose products are predicted to be highly similar (94.5% at the deduced protein level) and where both genes possess an intron. The high degree of similarity of the deduced protein products of these genes might suggest a similar interaction profile by the two proteins, in a manner reminiscent of *ASK1* and *ASK2*. However, we describe here the finding that *ASK3* was able to interact with the SKP2a F-box protein whereas *ASK4* could not in the split-YFP system. Furthermore, the *ASK3* and *ASK4* transcripts exhibited markedly different steady-state abundance where *ASK4* levels were consistently ten-fold higher than *ASK3* in most organ samples. The exceptions were flowers (both stages 9 and 15) and green siliques, where an inverse abundance relationship was observed, characterized by a much-elevated relative abundance of *ASK3* transcripts over those of *ASK4*. The relative high level of expression of *ASK4* might in part be explained by the suggestion that *ASK4* is hypothesized to have arisen as the result of large-scale segmental duplication of the highly expressed *ASK1* [39]. While our studies have not yet been extended to include a corresponding analysis of *ASK3* versus *ASK4* protein abundance, the available data suggests a significant disparity in gene expression levels between these

two close paralogs thus providing a possible explanation for the evolutionary retention of these two genes. In light of our previous finding that ASK3 and ASK4 exhibited similar F-box interaction profiles in the yeast 2-hybrid system [21], coupled with the finding that both share a common cytoplasmic/nuclear sub-cellular localization in the transient *Nicotiana* expression system, the data suggest that SCF complexes incorporating ASK4 subunits will be relatively abundant in most foliar organs, roots and whole seedlings, with the exception of late-stage flowers and green siliques where ASK3-containing complexes may preferentially form.

Clade three is comprised of *ASK5* and *ASK6* as two genes that are rapidly evolving and seem to be less conserved throughout plant evolution [39]. This clade includes a controversial member of the *ASK* gene family, *ASK6*, which has been suggested to be a pseudogene due to the extreme low abundance of its transcript in *Arabidopsis*, coupled with an apparent C-terminal truncation of its deduced polypeptide sequence. Although we likewise could not detect transcripts for *ASK6* in the organs examined, others have nevertheless managed to clone a full-length *ASK6* cDNA as part of the high-throughput cDNA cloning of low-expressing genes (C. Town, J. Craig Venter Institute, personal communication). As described here, the *ASK6* protein containing an extended coding region was found to interact exclusively with COI1, suggesting a role for *ASK6* in some aspect of jasmonate signal generation or perception. We conclude that *ASK6* is both expressed and is functional at the polypeptide level. The data presented in this study show that both *ASK5* and *ASK6* have divergent expression profiles and their corresponding proteins exhibit different interaction profiles despite their high degree of similarity at the deduced protein level (~70%). As described here, the *ASK5* transcript

abundance more closely parallels that of *ASK14* in various organ samples in a way that was not predicted by sequence-based phylogeny.

The *ASK7,8,9,10* clade is defined by a group of closely related genes that are also tightly clustered within a 10 Kbp span of chromosome 3 (**Figure 2.14**), suggesting a recent localized tandem duplication event and a possible conserved expression profile for these genes. Indeed hierarchical clustering of transcript expression resulted in a relatively tight clustering of these genes reminiscent of their phylogenetic clade. Strikingly, a distinct protein interaction profile was observed among the genes within this cluster, where *ASK8* and *ASK10* interacted solely with *COI1* and *EID1*, whereas *ASK9* interacted more generally with 6 out of the 7 F-box proteins tested with the exception of *AFR*. Taken together, the results suggest a strong sub-functionalization and a possible basis for evolutionary retention of the four genes within this clade.

The clade defined by *ASK14,15,16,17,18,19* appears to have diverged from *ASK3* and *ASK4* as a result of an initial retrotransposition event followed by two recent tandem duplications within the clade, giving rise to the 5 clade members [39]. Given the probable recent evolution of the clade, one might anticipate similar expression and protein interaction profiles among its members. Although we did not investigate the sub-cellular localization or protein interaction properties of genes in this clade, the expression profile of the genes was found to exhibit a semi-divergent expression profile where *ASK14* and *ASK16* exhibited an expression profile distinct from the other genes in this clade, but highly similar to that of *ASK5* and *ASK13*, respectively.

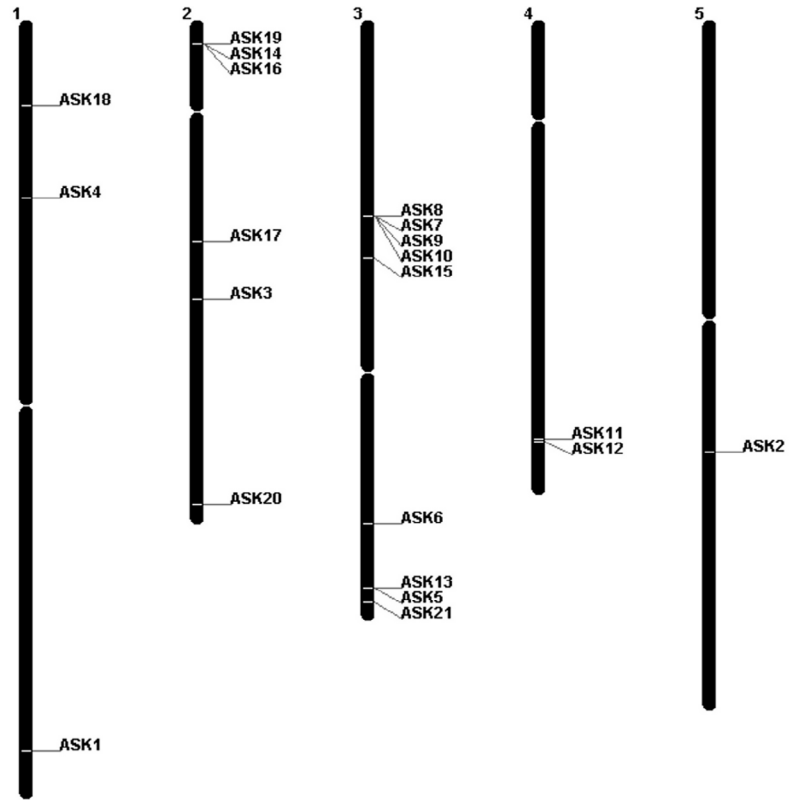


Figure 2.14. *ASK* gene chromosomal location.

Chromosomal location of the *ASK* gene family in the genome of Arabidopsis.

Interestingly *ASK16* and *ASK17*, with close to 62% protein sequence similarity, also have a high similarity expression profile, with a minor difference in stage 9 flowers where *ASK16* transcripts were expressed with no detectable expression of *ASK17*.

Defining nodes of *ASK* gene expression and ASK protein interaction at a higher resolution across different spatial and temporal dimensions at the organ, cellular and sub-cellular level, may contribute to an improved understanding of potential function, or at least lead to the advancement of predictive hypotheses for the formation of specific SCF complexes with an inferred biological function. An illustrative example arises from the selective interaction of *ASK6* with *COI*, where a role for jasmonate signalling is inferred among other possible functional roles for this member of the ASK protein family.

Similarly, the interaction of *ASK10* with *EID1* may suggest that this member of the ASK protein family engages in the formation of a subset of SCF complexes that play a role in ethylene signal perception in *Arabidopsis*. Recent findings have shown that *FBL17*, an F-box protein which is known to be involved in cell cycle regulation during male gametogenesis, is able to interact with *ASK11* in yeast 2-hybrid and BiFC-based studies [69], which is in full accord with our observation of a flower-specific expression pattern for *ASK11*.

The study presented here serves to highlight the importance of defining functional equivalence or redundancy from multiple biological perspectives, here including quantitative gene expression profiling, sub-cellular localization and *in vivo* analysis of protein interaction potential. A third perspective arises from the phenotypic analysis of individual loss-of-function alleles, both alone and in combination. A genetic perspective of redundancy within the *ASK* gene family is complicated by the fact that genes in this

family are generally small and are therefore significantly under-represented for null alleles within reverse-genetic resources such as the T-DNA insertion mutagenesis population organized as the SIGnAL resource [22]. Future work to define genetic interactions within the *ASK* gene family would logically involve transgenic miRNA expression interdiction approaches [70], the development of alternative reverse genetic resources [71], or perhaps targeted deletion strategies directed to the disruption of *ASK* gene function [72].

In the present study, we have characterized the steady-state transcript levels, sub-cellular distribution profiles, together with the analysis of a restricted set of protein-protein interactions within the confines of a set of ‘standard’ laboratory propagation and environmental interaction conditions. It remains to be seen whether the observed expression, localization and gene product interaction profiles described here might further diversify in the face of changing environmental conditions, or treatment with different plant growth regulatory compounds with which several of the proteins involved are directly implicated. Indeed, related studies suggest that sub-cellular localization of select *ASK*-F-box protein interactions with a known role in hormone signal perception are altered in the presence of the relevant signalling compounds, thus presenting an additional dimension for our understanding of the molecular basis of their function (Dezfulian *et al.*, manuscript in preparation).

Notwithstanding its relatively small genome size and genetic complexity, *Arabidopsis* has nevertheless retained a complex family of closely related genes encoding Skp1-like proteins. This observation, which can be extrapolated more generally to other model plant species for which significant genome content information is available, is a

general feature of plants and may relate to their unique adaptive strategy as sessile organisms in dynamic interaction with their environment. In basic terms, the large number of structurally related genes raises questions surrounding the issue of functional redundancy versus evolutionary retention within the gene family. In this study, we provide some novel perspectives on the issue of redundancy, which may help to explain the retention of these genes during Arabidopsis genome evolution. Although we cannot currently rule out the possibility that the other *ASK* genes not investigated as part of this study show unique sub-cellular localization, the similar localization pattern observed for all the *ASK* proteins studied suggests that there has been no evolutionary pressure for retention arising from specialized sub-cellular localization among *ASK* gene products. Our finding that structurally closely-related genes are nonetheless distinguished on the basis of expression and/or protein interaction profiles offers an alternative explanation for their retention based on functional diversification. Indeed, virtually every clade defining the phylogeny of the *ASK* protein family was found to contain one or more members that have diverged at the level of expression and/or protein interaction profile, thus defining a potential molecular basis for an expanded functional repertoire. Only through an expanded study that includes additional facets of redundancy will a reliable picture of functional redundancy within the *ASK* gene family emerge, with implications for future studies into their shared versus divergent molecular functions.

BIBLIOGRAPHY

1. Vierstra RD (2009) The ubiquitin-26S proteasome system at the nexus of plant biology. *Nat Rev Mol Cell Biol* 10: 385-397.
2. Lechner E, Achard P, Vansiri A, Potuschak T, Genschik P (2006) F-box proteins everywhere. *Curr Opin Plant Biol* 9: 631-638.
3. Vierstra RD (2003) The ubiquitin/26S proteasome pathway, the complex last chapter in the life of many plant proteins. *Trends Plant Sci* 8: 135-142.
4. Dharmasiri N, Dharmasiri S, Estelle M (2005) The F-box protein TIR1 is an auxin receptor. *Nature* 435: 441-445.
5. Tan X, Calderon-Villalobos LI, Sharon M, Zheng C, Robinson CV, et al. (2007) Mechanism of auxin perception by the TIR1 ubiquitin ligase. *Nature* 446: 640-645.
6. Thines B, Katsir L, Melotto M, Niu Y, Mandaokar A, et al. (2007) JAZ repressor proteins are targets of the SCF(COI1) complex during jasmonate signalling. *Nature* 448: 661-665.
7. Imaizumi T, Tran HG, Swartz TE, Briggs WR, Kay SA (2003) *FKF1* is essential for photoperiodic-specific light signalling in Arabidopsis. *Nature* 426: 302-306.
8. Kim WY, Fujiwara S, Suh SS, Kim J, Kim Y, et al. (2007) *ZEITLUPE* is a circadian photoreceptor stabilized by *GIGANTEA* in blue light. *Nature* 449: 356-360.
9. Moon J, Zhao Y, Dai X, Zhang W, Gray WM, et al. (2006) A New CUL1 Mutant has Altered Responses to Hormones and Light in Arabidopsis. *Plant Physiol* ..
10. Chae E, Tan QK, Hill TA, Irish VF (2008) An Arabidopsis F-box protein acts as a transcriptional co-factor to regulate floral development. *Development* 135: 1235-1245.
11. Jin J, Cardozo T, Lovering RC, Elledge SJ, Pagano M, et al. (2004) Systematic analysis and nomenclature of mammalian F-box proteins. *Genes & Development* 18: 2573-2580.
12. Schulman BA, Carrano AC, Jeffrey PD, Bowen Z, Kinnucan ER, et al. (2000) Insights into SCF ubiquitin ligases from the structure of the Skp1-Skp2 complex. *Nature* 408: 381-386.

13. Sheard LB, Tan X, Mao H, Withers J, Ben-Nissan G, et al. (2010) Jasmonate perception by inositol-phosphate-potentiated COI1-JAZ co-receptor. *Nature* 468: 400-405.
14. Wu G, Xu G, Schulman BA, Jeffrey PD, Harper JW, et al. (2003) Structure of a beta-TrCP1-Skp1-beta-catenin complex: destruction motif binding and lysine specificity of the SCF(beta-TrCP1) ubiquitin ligase. *Mol Cell* 11: 1445-1456.
15. Zheng N, Schulman BA, Song L, Miller JJ, Jeffrey PD, et al. (2002) Structure of the Cul1-Rbx1-Skp1-F boxSkp2 SCF ubiquitin ligase complex. *Nature* 416: 703-709.
16. Tang X, Orlicky S, Lin Z, Willems A, Neculai D, et al. (2007) Suprafacial orientation of the SCFCdc4 dimer accommodates multiple geometries for substrate ubiquitination. *Cell* 129: 1165-1176.
17. Cardozo T, Pagano M (2004) The SCF ubiquitin ligase: insights into a molecular machine. *Nat Rev Mol Cell Biol* 5: 739-751.
18. Barbash O, Diehl JA (2008) SCF(Fbx4/alphaB-crystallin) E3 ligase: when one is not enough. *Cell Cycle* 7: 2983-2986.
19. Barbash O, Zamfirova P, Lin DI, Chen X, Yang K, et al. (2008) Mutations in Fbx4 inhibit dimerization of the SCF(Fbx4) ligase and contribute to cyclin D1 overexpression in human cancer. *Cancer Cell* 14: 68-78.
20. Li Y, Hao B (2010) Structural basis of dimerization-dependent ubiquitination by the SCF(Fbx4) ubiquitin ligase. *J Biol Chem* 285: 13896-13906.
21. Risseuw EP, Daskalchuk TE, Banks TW, Liu E, Cotelesage J, et al. (2003) Protein interaction analysis of SCF ubiquitin E3 ligase subunits from *Arabidopsis*. *Plant J* 34: 753-767.
22. Alonso JM, Stepanova AN, Leisse TJ, Kim CJ, Chen H, et al. (2003) Genome-Wide Insertional Mutagenesis of *Arabidopsis thaliana*. *Science* 301: 653-657.
23. Zhao D, Ni W, Feng B, Han T, Petrasek MG, et al. (2003) Members of the *Arabidopsis*-SKP1-like gene family exhibit a variety of expression patterns and may play diverse roles in *Arabidopsis*. *Plant Physiol* 133: 203-217.
24. Zhao D, Han T, Risseuw E, Crosby WL, Ma H (2003) Conservation and divergence of ASK1 and ASK2 gene functions during male meiosis in *Arabidopsis thaliana*. *Plant Mol Biol* 53: 163-173.

25. Marrocco K, Lecureuil A, Nicolas P, Guerche P (2003) The Arabidopsis SKP1-like genes present a spectrum of expression profiles. *Plant Mol Biol* 52: 715-727.
26. Murashige T, Skoog F (1962) A revised medium for rapid growth and bioassays with tobacco tissue cultures. *Physiol Plant* 15: 473-479.
27. Harrison S, Mott E, Parsley K, Aspinall S, Gray J, et al. (2006) A rapid and robust method of identifying transformed Arabidopsis thaliana seedlings following floral dip transformation. *Plant Methods* 2: 19.
28. Earley KW, Haag JR, Pontes O, Opper K, Juehne T, et al. (2006) Gateway-compatible vectors for plant functional genomics and proteomics. *Plant J* 45: 616-629.
29. Desprez T, Juraniec M, Crowell EF, Jouy H, Pochylova Z, et al. (2007) Organization of cellulose synthase complexes involved in primary cell wall synthesis in Arabidopsis thaliana. *Proc Natl Acad Sci U S A* 104: 15572-15577.
30. Weltmeier F, Ehlert A, Mayer CS, Dietrich K, Wang X, et al. (2006) Combinatorial control of Arabidopsis proline dehydrogenase transcription by specific heterodimerisation of bZIP transcription factors. *EMBO J* 25: 3133-3143.
31. Zhang X, Henriques R, Lin SS, Niu QW, Chua NH (2006) Agrobacterium-mediated transformation of Arabidopsis thaliana using the floral dip method. *Nat Protoc* 1: 641-646.
32. Popescu SC, Popescu GV, Bachan S, Zhang Z, Seay M, et al. (2007) Differential binding of calmodulin-related proteins to their targets revealed through high-density Arabidopsis protein microarrays. *PNAS* 104: 4730-4735.
33. Voinnet O, Rivas S, Mestre P, Baulcombe D (2003) An enhanced transient expression system in plants based on suppression of gene silencing by the p19 protein of tomato bushy stunt virus. *Plant J* 33: 949-956.
34. Simon P (2003) Q-Gene: processing quantitative real-time RT-PCR data. *Bioinformatics* 19: 1439-1440.
35. Pfaffl MW (2001) A new mathematical model for relative quantification in real-time RT-PCR. *Nucleic Acids Res* 29: e45.
36. Pfaffl MW, Horgan GW, Dempfle L (2002) Relative expression software tool (REST) for group-wise comparison and statistical analysis of relative expression results in real-time PCR. *Nucleic Acids Research* 30.

37. Kapushesky M, Kemmeren P, Culhane AnC, Durinck S, Ihmels J, et al. (2004) Expression Profiler: next generation online platform for analysis of microarray data. *Nucleic Acids Research* 32: W465-W470.
38. Tamura K, Dudley J, Nei M, Kumar S (2007) MEGA4: Molecular Evolutionary Genetics Analysis (MEGA) Software Version 4.0. *Mol Biol Evol* 24: 1596-1599.
39. Kong H, Landherr LL, Frohlich MW, Leebens-Mack J, Ma H, et al. (2007) Patterns of gene duplication in the plant SKP1 gene family in angiosperms: evidence for multiple mechanisms of rapid gene birth. *Plant J* 50: 873-885.
40. Liu F, Ni W, Griffith ME, Huang Z, Chang C, et al. (2004) The ASK1 and ASK2 genes are essential for Arabidopsis early development. *Plant Cell* 16: 5-20.
41. Smyth DR, Bowman JL, Meyerowitz EM (1990) Early Flower Development in *Arabidopsis*. *The Plant Cell* 2: 755-767.
42. Takahashi N, Kuroda H, Kuromori T, Hirayama T, Seki M, et al. (2004) Expression and interaction analysis of Arabidopsis Skp1-related genes. *Plant Cell Physiol* 45: 83-91.
43. Kong H, Leebens-Mack J, Ni W, Depamphilis CW, Ma H (2004) Highly heterogeneous rates of evolution in the SKP1 gene family in plants and animals: functional and evolutionary implications. *Mol Biol Evol* 21: 117-128.
44. Toufighi K, Brady SM, Austin R, Ly E, Provart NJ (2005) The Botany Array Resource: e-Northerns, Expression Angling, and promoter analyses. *The Plant Journal* 43: 153-163.
45. Winter D, Vinegar B, Nahal H, Ammar R, Wilson GV, et al. (2007) An Electronic Fluorescent Pictography Browser for Exploring and Analyzing Large-Scale Biological Data Sets. *PLoS One* 2: e718.
46. Zimmermann P, Hirsch-Hoffmann M, Hennig L, Gruissem W (2004) GENEVESTIGATOR. Arabidopsis Microarray Database and Analysis Toolbox. *Plant Physiol* 136: 2621-2632.
47. Wang Y, Yang M (2006) The ARABIDOPSIS SKP1-LIKE1 (*ASK1*) protein acts predominately from leptotene to pachytene and represses homologous recombination in male meiosis. *Planta* 223: 613-617.
48. Zhao D, Yang X, Quan L, Timofejeva L, Rigel NW, et al. (2006) ASK1, a SKP1 homolog, is required for nuclear reorganization, presynaptic homolog juxtaposition and the proper distribution of cohesin during meiosis in Arabidopsis. *Plant Mol Biol* 62: 99-110.

49. Chini A, Fonseca S, Fernandez G, Adie B, Chico JM, et al. (2007) The JAZ family of repressors is the missing link in jasmonate signalling. *Nature* 448: 666-671.
50. Diaz-Camino C, Risseuw EP, Liu E, Crosby WL (2003) A high-throughput system for two-hybrid screening based on growth curve analysis in microtiter plates. *Anal Biochem* 316: 171-174.
51. Del Pozo JC, Diaz-Trivino S, Cisneros N, Gutierrez C (2006) The balance between cell division and endoreplication depends on E2FC-DPB, transcription factors regulated by the ubiquitin-SCFSKP2A pathway in *Arabidopsis*. *Plant Cell* 18: 2224-2235.
52. Devoto A, Nieto-Rostro M, Xie D, Ellis C, Harmston R, et al. (2002) *COII* links jasmonate signalling and fertility to the SCF ubiquitin-ligase complex in *Arabidopsis*. *Plant J* 32: 457-466.
53. Dharmasiri N, Dharmasiri S, Weijers D, Lechner E, Yamada M, et al. (2005) Plant development is regulated by a family of auxin receptor F box proteins. *Dev Cell* 9: 109-119.
54. Dieterle M, Zhou YC, Schafer E, Funk M, Kretsch T (2001) EID1, an F-box protein involved in phytochrome A-specific light signaling. *Genes Dev* 15: 939-944.
55. Harmon FG, Kay SA (2003) The F box protein AFR is a positive regulator of phytochrome A-mediated light signaling. *Curr Biol* 13: 2091-2096.
56. Hepworth SR, Klenz JE, Haughn GW (2006) UFO in the *Arabidopsis* inflorescence apex is required for floral-meristem identity and bract suppression. *Planta* 223: 769-778.
57. Jurado S, az-Trivino S, Abraham Z, Manzano C, Gutierrez C, et al. (2008) SKP2A, an F-box protein that regulates cell division, is degraded via the ubiquitin pathway. *Plant J* 53: 828-841.
58. Levin JZ, Meyerowitz EM (1995) *UFO*: An *Arabidopsis* gene involved in both floral meristem and floral organ development. *The Plant Cell* 7: 529-548.
59. Wilkinson MD, Haughn GW (1995) *Unusual Floral Organs* Controls Meristem Identity and Organ Primordia Fate in *Arabidopsis*. *The Plant Cell* 7: 1485-1499.
60. Gagne JM, Downes BP, Shiu SH, Durski AM, Vierstra RD (2002) The F-box subunit of the SCF E3 complex is encoded by a diverse superfamily of genes in *Arabidopsis*. *Proc Natl Acad Sci U S A* 99: 11519-11524.

61. Bennett MD, Leitch IJ (2011) Nuclear DNA amounts in angiosperms: targets, trends and tomorrow. *Ann Bot* 107: 467-590.
62. Bai C, Sen P, Hofmann K, Ma L, Goebel M, et al. (1996) *SKP1* Connects Cell Cycle Regulators to the Ubiquitin Proteolysis Machinery through a Novel Motif, the F-box. *Cell* 86: 263-274.
63. Connelly C, Hieter P (1996) Budding Yeast *SKP1* Encodes an Evolutionarily Conserved Kinetochores Protein Required for Cell Cycle Progression. *Cell* 86: 275-285.
64. Murphy TD (2003) *Drosophila* *skpA*, a component of SCF ubiquitin ligases, regulates centrosome duplication independently of cyclin E accumulation. *J Cell Sci* 116: 2321-2332.
65. Nayak S, Santiago FE, Jin H, Lin D, Schedl T, et al. (2002) The *Caenorhabditis elegans* Skp1-Related Gene Family. Diverse Functions in Cell Proliferation, Morphogenesis, and Meiosis. *Curr Biol* 12: 277-287.
66. Rensing SA, Lang D, Zimmer AD, Terry A, Salamov A, et al. (2008) The Physcomitrella Genome Reveals Evolutionary Insights into the Conquest of Land by Plants. *Science* 319: 64-69.
67. Wagner A (2001) Gene Duplication and Redundancy. In: eLS. John Wiley & Sons, Ltd.
68. Kafri R, Springer M, Pilpel Y (2009) Genetic redundancy: new tricks for old genes. *Cell* 136: 389-392.
69. Gusti A, Baumberger N, Nowack M, Pusch S, Eisler H, et al. (2009) The *Arabidopsis thaliana* F-box protein FBL17 is essential for progression through the second mitosis during pollen development. *PLoS ONE* 4: e4780.
70. Schwab R, Ossowski S, Riester M, Warthmann N, Weigel D (2006) Highly specific gene silencing by artificial microRNAs in *Arabidopsis*. *Plant Cell* 18: 1121-1133.
71. Li X, Zhang Y (2002) Reverse genetics by fast neutron mutagenesis in higher plants. *Funct Integr Genomics* 2: 254-258.
72. Li X, Song Y, Century K, Straight S, Ronald P, et al. (2001) A fast neutron deletion mutagenesis-based reverse genetics system for plants. *Plant J* 27: 235-242.

CHAPTER 3

Functional Characterization of *Arabidopsis SKP1-like* Genes

INTRODUCTION

Gene duplication is thought to be one of the main sources of raw material for genome evolution [1]. Although still under debate, it is widely believed that among duplicated genes one copy of the gene is capable of carrying out its original function leaving the other gene free to mutate and gain one or more novel functions [2]. Recent genetic duplication events are thought to be one of the main contributors to genetic redundancy among duplicated genes [3]. However, it remains to be answered how often duplicated genes compensate for the inactivation of their paralogs [3].

Arabidopsis has undergone at least three rounds of genome duplication throughout its evolution[4], it is estimated that over 41% of *Arabidopsis thaliana* genes possess at least one paralog [5,6]; hence, a high of level of genetic redundancy is expected among these genes. Genes encoding subunits of the SCF class of E3 Ub ligase complexes alone comprise nearly 2% of the protein-coding capacity of the *A. thaliana* genome [7]. The SCF ligase complex consists of four canonical subunits: SKP1 (ASK), CUL1, RBX1 and F-BOX. CUL1 acts as a scaffold protein whose N-terminal and C-terminal domains interact with SKP1 and RBX1, respectively. SKP1 acts as an adaptor protein binding both CUL1 and the substrate specificity-determining F-box protein [7]. F-box proteins interact with SKP1 via its N-terminal 40-aa F-box motif whereas RBX1 interacts with E2 complexes via a RING-finger motif intrinsic to this protein [8–10].

The *Arabidopsis* genome contains approximately 700 *F-BOX* genes, 1 *CUL1* gene, and 21 *ASK* genes [8,9]. Based on the deduced sequence similarity of ASK proteins, a phylogenic tree with seven distinct gene clades can be constructed [7]. The clustering of the *ASK* genes within these clades suggests that the gene family was, in part,

generated by recent gene duplication events, leading to the expectation of a high level of genetic redundancy [7,10].

As discussed in Chapter 2, members of the *ASK* gene family exhibit a variety of expression patterns and are involved in diverse processes in Arabidopsis. Among the twenty-one gene family members, only *ASK1* and *ASK2* have been phenotypically characterized via the analysis of null mutants [11-15]. Single mutants of *ask1* and *ask2* have demonstrated that ASK1 and ASK2 are individually involved in embryogenesis, seedling development, meiosis, organ development and hormonal response. Strong overlapping functional redundancy between these two genes is suggested by the finding that the *ask1/ask2* double mutant exhibits signs of severe developmental delay during early stages of growth and lethality during seedling development [11]. This is further supported by the high similarity in expression and interaction profiles observed between *ASK1* and *ASK2* genes and their protein products, as discussed in Chapter 1. The unique but strongly overlapping protein-protein interaction profile observed between ASK1, ASK2 and several F-box proteins as part of a large Y2H screen provides an explanation and grounds for the mild phenotypes observed for individual *ask1* and *ask2* mutants [6,9].

A combination of data from Chapter 2 and the observed behavior for ASK1 and ASK2 led us to hypothesize that a similar profile of genetic redundancy might be observed within the *ASK* gene family.

To date, functional characterization of genes within the *A. thaliana* genome has heavily relied on exploitation of the T-DNA insertional mutant resource developed as part of a collaborative project between the Crosby and the Ecker labs (the 'SIGnAL Resource (<http://signal.salk.edu/>) [16]. This publicly available resource is known to

harbour insertional mutant alleles with different degrees of genetic penetration for approximately 70% of the protein-coding repertoire of the Arabidopsis genome [16,17]. Characterization of functional redundancy among genes requires the generation of multiple-mutant backgrounds, achievable by employing a simple cross and the facile recovery of double-mutant segregants involving loci that are genetically distant and/or reside on independent linkage groups.

To phenotypically dissect the function of the *ASK* gene family, our lab has utilized two different reverse genetic approaches, namely, T-DNA insertion mutagenesis and fast neutron deletion library screening, where each approach presents benefits and caveats. The T-DNA screen, although powerful, (as shown by our group and others) has proven to be relatively ineffective across large gene families such as in the *ASK* gene family. This is primarily due to the inability to generate multiple mutants for genes that are tightly clustered on small segments of chromosome. This process is further complicated in the *ASK* gene family where the genes are uniformly relatively small (150-aa) with a corresponding reduced probability of identifying random inactivating T-DNA insertions in these gene. To overcome problems associated with the T-DNA screen we performed a set of library screens using pooled DNA from fast neutron deletion lines to identify deletions within the region on chromosome 3 spanning *ASK7/8/9/10* [18]. Although proof-of-principle screens and reconstruction tests appeared to validate the approach, screens of mutant DNA pools failed to identify deletions spanning the *ASK7/8/9/10* gene cluster located on chromosome 3. To overcome the problems associated with the first two approaches, the development and deployment of alternative

and complementary methods were essential. To this end, we employed the ectopic expression of artificial microRNAs (amiRNA) constructs in transgenic plants.

miRNAs are a class of small RNA molecules, 19-24-nt in size, which have been extensively characterized for their role as a gene regulatory mechanism [19]. miRNAs exert their effects on gene expression at three levels; methylation-based regulation of promoter activity, Dicer-mediated control of mRNA stability or control of translational efficiency achieved via direct binding of miRNAs to the target mRNA [19,20]. Although perfectly complementary siRNAs have been extensively used in the animal kingdom as a powerful means to achieve knockdowns of target genes, siRNAs have been shown to affect non-target genes due to its long, double-stranded nature [21-23]. To circumvent this problem, the Arabidopsis community has relied heavily on amiRNAs as a means to knocking down genes of interest [24]. The maximum amount of targets identified for any single miRNA has been 10 genes in *A. thaliana* [25-27]. Thus, miRNAs can provide a level of specificity not afforded by conventional RNAi approaches. Furthermore, our understanding of the miRNA mode of action allows for the prediction of off-target effects, which can be taken into consideration during data analysis. [27].

During the course of this study I generated 18 different amiRNA constructs designed to target select *ASK* genes - either individually or in combination. Transgenic plants harboring all 18 amiRNA constructs were generated and the efficiency of these constructs in reducing the transcript abundance of target genes was measured. This experimental approach was supported by phenotypic analysis of transgenic plants using gross indicators of perturbed patterning, development and hormone response as indicators of altered biological function.

MATERIALS AND METHODS

amiRNA design

amiRNA precursors were designed using the Web MicroRNA Designer (WMD) tool, available at <http://wmd.weigelword.org> [24]. The cDNA sequence of the *ASK* genes (TAIR9) were used as the query input. The optimal amiRNAs (**Table 3.1**) generated by the WMD tool were selected based on the empirically determined criteria.

Once designed, the amiRNA sequences were engineered into the backbone of an endogenous miRNA precursor (miR319a) via site-directed mutagenesis. The amiRNAs were then transferred using the Gateway[®] cloning system and placed behind the cauliflower mosaic virus (CaMV) 35S promoter inherent to the binary vectors, pFK-209 (kanamycin resistance) and pFK-210 (DL-phosphinothricin resistance).

Generation of transgenic plants

Binary plasmids containing the amiRNA precursors were transformed into the *Agrobacterium tumefaciens* strain AGL1 via electroporation. The recombinant plasmids were introduced into *A. thaliana* ecotype Columbia (Col-0), also using the *Agrobacterium* strain AGL1. T1 seeds were harvested from transformed plants and selected on selective MS agar plates (DL-phosphinothricin or kanamycin). Seeds were germinated and plants were allowed to grow and produce siliques in growth chambers. T2 seeds were subsequently harvested from these plants and subjected to a PCR-based allelic content analysis. A complete list of primers used is listed in **Table 3.3**. T3 plants homozygous for the recombinant insertion(s) were subjected to phenotypic survey.

amiRNA	Sequence
amiR- <i>ASK1a</i>	GCACACAACGTTCTACATTAT
amiR- <i>ASK2a</i>	ATCGCGAAAAGTTCGAATTTA
amiR- <i>ASK1/2a</i>	CGCGGCGCTAGAGACACAAAT
amiR- <i>ASK1/2b</i>	TTAGCGCTAGAGTGACAAACT
amiR- <i>ASK3a</i>	CCGCTCCGGGCTCCCAACTTA
amiR- <i>ASK4a</i>	CACCAAGGTTATAGAGTATTA
amiR- <i>ASK3/4a</i>	GAAGCGTAGGTTCCCAATGAT
amiR- <i>ASK3/4b</i>	CCACAGATGCGTGTACTTTT
amiR- <i>ASK7a</i>	AAATCGGTGCCGCAAATCCTT
amiR- <i>ASK10a</i>	GCAGAGCACACTCCCAAATTT
amiR- <i>ASK7/8/9/10a</i>	AAATCGGTGCCGCAAATCCTT
amiR- <i>ASK7/8/9/10b</i>	CGACGCACGCCAAAGCCAGAT
amiR- <i>ASK11/12a</i>	GCCGAGGTTAATGCTATCTCA
amiR- <i>ASK11/12b</i>	AAATCGGTGCCGCAAATCCTT
amiR- <i>ASK20a</i>	CAGCCAGGACGTACAAATATA
amiR- <i>ASK21a</i>	GCCGGGTTCTATCCATAGGAT
amiR- <i>ASK20/21a</i>	GCAGCTAACAGTTAGCAGTTT
amiR- <i>ASK20/21b</i>	TATGATAAGAGGTCATGCATT

Table 3.1. 21-nt amiRNA fragments and their cognate *ASK* gene targets.

Primer	Sequence (5'-3')
AMIR/pFK210	F- CACTCCTGCGGTCCTGC GG
	R- TGCGCAGCCTGAATG GCG AA
pFK209/pFK210	F- CGGTCATTAGAGGCCACG AT
	R- CGGATTCCATTGCCCAGC TA

Table 3.2. Primers used for genotyping of transgenic plants.

Real-time PCR

Total RNA was isolated using a commercial mini-preparation kit (RNeasy™, Qiagen) and contaminating DNA was removed using an immobilized DNase column (RNase-Free DNase Set™, Qiagen). Two micrograms of total RNA was used as template for first strand cDNA synthesis in a 20- μ L reaction using the RevertAid™ synthesis kit (Fermentas). The resulting cDNA was diluted 1:20 and 1.5 μ L of cDNA was used in a standard 20- μ L PCR reaction. Analysis of gene expression employed Maxima™ Sybr-green qPCR master mix (Fermentas) in an Applied Biosystems 7300 RT- PCR System, following the manufacturer's instructions. The primers used in the qRT-PCR analyses are listed in **Table 3.3**.

Name	Sequence (5'-3')
CUL1_Sense	ACAGCAGCCTGGTAAGTAGA
CUL1_Antisense	CAAGTGTGTTGAAGTCTTCA
ASK1_Sense	CAGCCAGAATGAGTTCAAAG
ASK1_Antisense	GAGTATTGCAAGAGGCACGT
ASK2_Sense	CAGCCAGGATAAGATCGAAG
ASK2_Antisense	GCTGAGAAATCCGAAACCAC
ASK3_Sense	AAATAGTTGGCAGCCCGAAG
ASK3_Antisense	CTGGTGGAGACAAGGATTTC
ASK4_Sense	TAGTTCGCAGCCAAGATGAG
ASK4_Antisense	GAGTATTGCAAGAAGCACGT
ASK11-12_Sense	GGTGGAAAGAAGCGGTAGCAA
ASK11-12_Antisense	GAGGGATTCCATCAGCAACG
ASK7_Sense	CTCCCCACAAAGAAAACAA
ASK7_Antisense	CGTACATTTCGGCTTCAATCA
ASK20_Sense	GGCTCTGTGAGTTGACCTCT
ASK20_Antisense	CCTCCTCAGTAAGGTCATCA
ACTIN2_Sense	TCCCTCAGCACATTCCAGCAGAT
ACTIN2_Antisense	AACGATTCTGGACCTGCCTCATC
ASK8_Sense	ACGATCTTTGCTCTCACCAATGCTGC
ASK8_Antisense	AAGAATTCGCGCATCTGCTTCGGA
ASK9_Sense	GCCGCACGCCAATGCCAGATTA
ASK9_Antisense	GCGGCATCGACGTGGTGCTT
ASK10_Sense	GCATGCCAAACCGTCGCGGA
ASK10_Antisense	GTTGAAGAATTTGCGAGTGTGCTCCAC

Table 3.3. Oligonucleotide primers used for qRT-PCR analyses.

RESULTS

To obtain insight into the function of *ASK* genes in *A. thaliana*, amiRNAs targeting various *ASK* genes were designed using online tools available at <http://wmd2.weigelworld.org/> and constructed using an overlapping PCR strategy [24]. . These amiRNAs replaced the original 21-nt miRNA sequence in the miR156a backbone. The amiRNA sequences targeting various *ASK* genes are listed in **Table 3.1**. All amiRNAs were cloned into two vectors, pFK209 and pFK210 [28], between the cauliflower mosaic virus (CaMV) 35S promoter and terminator, conferring resistance to kanamycin and the herbicide bialaphos (Bar), respectively (**Table 3.4**). The availability of two different selection markers served to streamline the process of double transgenic generation. The amiRNAs were transferred into *A. thaliana* Columbia ecotype (Col-0) using *Agrobacterium*-mediated transformation via floral dipping to generate transgenic plants [29]. For each amiRNA multiple independent transgenic plants (n=3) were identified using a PCR-based genotyping assay. To account for any phenotypes arising from off-target effects, two amiRNAs targeting different regions of a given *ASK* mRNA were designed to allow us to compare and contrast various phenotypes arising from independent amiRNA transgenic lines. The levels of target *ASK* mRNAs, as well as mRNAs of *ASK* genes that are closely related to the targets, were investigated in the amiRNA transgenic lines using qRT-PCR.

amiRNA	pDestination
amiR- <i>ASK1a</i>	pFK209-Kanamycin
amiR- <i>ASK2a</i>	pFK210-Bar
amiR- <i>ASK1/2a</i>	pFK209-Kanamycin
amiR- <i>ASK1/2b</i>	pFK210-Bar
amiR- <i>ASK3a</i>	pFK209-Kanamycin
amiR- <i>ASK4a</i>	pFK210-Bar
amiR- <i>ASK3/4a</i>	pFK209-Kanamycin
amiR- <i>ASK3/4b</i>	pFK210-Bar
amiR- <i>ASK7a</i>	pFK210-Bar
amiR- <i>ASK10a</i>	pFK210-Bar
amiR- <i>ASK7/8/9/10a</i>	pFK209-Kanamycin
amiR- <i>ASK7/8/9/10b</i>	pFK210-Bar
amiR- <i>ASK11/12a</i>	pFK209-Kanamycin
amiR- <i>ASK11/12b</i>	pFK210-Bar
amiR- <i>ASK20a</i>	pFK209-Kanamycin
amiR- <i>ASK21a</i>	pFK210-Bar
amiR- <i>ASK20/21a</i>	pFK209-Kanamycin
amiR- <i>ASK20/21b</i>	pFK210-Bar

Table 3.4. amiRNA expression vectors generated throughout this study.

All amiRNAs were cloned into two main vector backbones which harbored either a kanamycin (pFK209) or a bialaphos (pFK210) resistance marker for selection of transgenic plants.

ASK1/2

ASK1 and *ASK2* reside within the first clade, sharing over 83% sequence similarity [7]. *ASK1* and *ASK2* exhibit signs of genetic redundancy and play an essential role in the growth and development of Arabidopsis.[11]. An *ask1* mutant allele was identified as part of a Ds-transposon [30] insertional screen while the *ask2* mutant was identified as part of a T-DNA screen [11]. The *ask1/ask2* double mutant lines were generated by crossing these single mutants. While both *ask1* and *ask2* showed a mild phenotype, the double mutant exhibited delayed embryonic development and lethality at the seedling stage. Due to the lethality of the double mutant [11,30], phenotypic analysis of this mutant has been confined to embryonic stages leading to an incomplete knowledge of the role of the *ASK1* and *ASK2* later in plant development. Since amiRNAs are not 100% penetrant in gene knockdown studies, their use is often seen as a drawback to this type of approach. However, we took advantage of this “drawback” to generate double *ask1/ask2* mutants, which we assumed would be incompletely penetrant and correspondingly viable. Two amiRNA constructs targeting *ASK1* (amiR-*ASK1a* and amiR-*ASK1b*) and *ASK2* (amiR-*ASK2a* and amiR-*ASK2b*) were generated. Additionally, we generated amiRNAs simultaneously targeting both *ASK1* and *ASK2* (amiR-*ASK1/2a* and amiR-*ASK1/2b*).

The transcript abundance of *ASK1* and *ASK2* was measured in all knockdown backgrounds (**Figure 3.1**). amiR-*ASK1a* and amiR-*ASK1b* achieved a relatively efficient knockdown for *ASK1* (~72% and ~67%, respectively), however none of the independent amiRNAs targeting *ASK2* (amiR-*ASK2a* and amiR-*ASK2b*) efficiently knocked down *ASK2*. Interestingly, in both amiR-*ASK1a* and amiR-*ASK1b* backgrounds, the level of

ASK2 transcript is 20% higher than in wildtype. This increase in expression in part can explain the lack of any observed phenotypes for the *ask1* mutant. Among the amiRNAs simultaneously targeting both *ASK1* and *ASK2*, amiR-*ASK1/2a* was more efficient in knocking down the target genes, lowering *ASK1* and *ASK2* transcript levels by ~85% and ~55%, respectively, and these plants were subsequently subjected to gross phenotypic analysis. This mutant plant (amiR-*ASK1/2a*) was viable as expected but exhibited several gross phenotypes such as a smaller stature, delayed transition from vegetative to reproductive development and a smaller silique size (**Figure 3.2**).

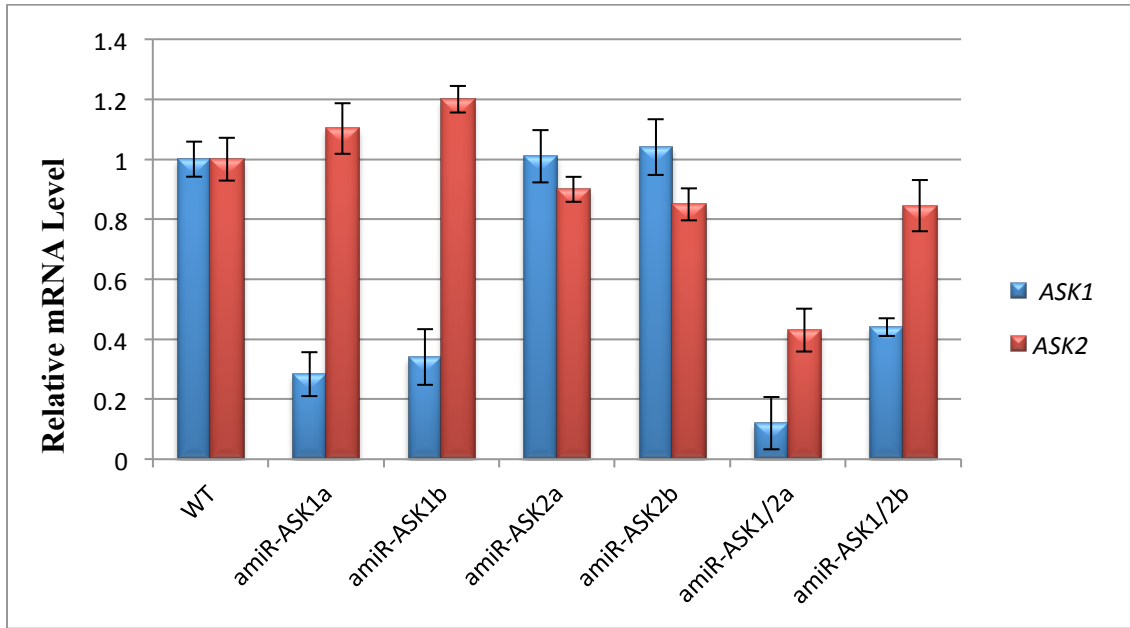


Figure 3.1. mRNA transcript abundance for *ASK1* and *ASK2* in various mutant backgrounds.

RNA was isolated and used to assess *ASK* gene expression as described in the methods. Relative mRNA expression levels in wild type (WT) and different transgenic lines were determined using qRT-PCR. Gene expression is depicted in relative amount after *ACTIN2* normalization. Data depicted is a representative of two independent biological replicates \pm SE from three sample replicates each.

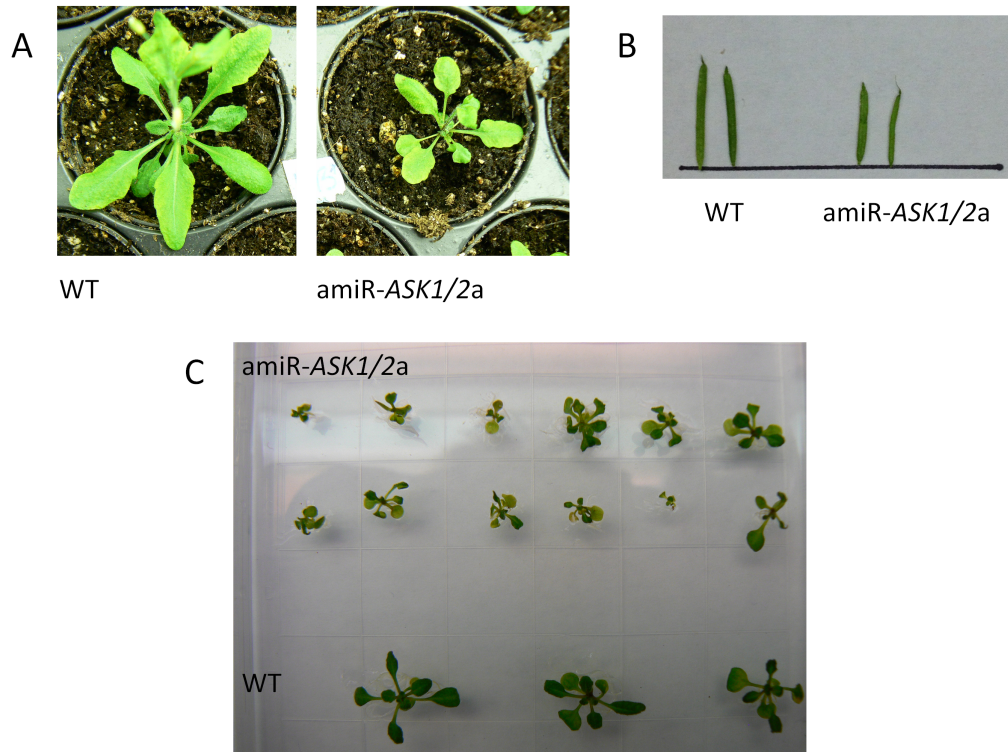


Figure 3.2. Phenotypic characterization of *ask1/ask2* mutant lines

A. The *ask1/2* double mutant line, *amiR-ASK1/2a*, displayed a smaller stature, delayed transition from vegetative to reproductive development. **B.** All double mutants that were viable and reached the flowering stage displayed a smaller silique compared to wildtype plants. **C.** Due to insertional position effect caused by the random nature of T-DNA insertion in the plant genome, *amiRNAs* can exhibit different degrees of penetration thus a wide range of phenotypes can be observed. All *ask1/ask2* double mutant lines generated despite having various insertion sites exhibited a delayed development and smaller stature compared to wild type plants.

ASK3/4

The second clade studied was comprised of *ASK3* and *ASK4*, as two genes bearing a high level of sequence identity at the deduced protein level (94.5%) [7]. Data from chapter one indicates that *ASK3* and *ASK4* share a divergent expression pattern but at the protein level exhibit an almost identical interaction profile. Taken together, this finding indicates that the level of genetic redundancy between *ASK3* and *ASK4* cannot be as high as what was observed for *ASK1* and *ASK2* where a high degree of similarity at the expression and protein-protein interaction levels was observed. In order to understand the phenotypic contribution of these genes to plant development, we designed amiRNAs targeting *ASK3* (amiR-*ASK3a*) and *ASK4* (amiR-*ASK4a*) individually, or two amiRNA constructs targeting both genes simultaneously (amiR-*ASK3/4a* and amiR-*ASK3/4b*). Results of qRT-PCR analyses are presented in **Figure 3.3**. Although amiR-*ASK3a* efficiently knocked down *ASK3* transcript levels by ~85%, amiR-*ASK3a* also non-specifically resulted in a decrease of *ASK4* transcript levels by ~20%. amiR-*ASK3a* mutant transgenic lines did not exhibit any obvious morphological phenotypes. In amiR-*ASK4a* transgenic lines, *ASK3* and *ASK4* mRNA levels were reduced by only 5% and 15%, respectively, and was therefore not subjected phenotypic analysis. amiR-*ASK3/4a* and amiR-*ASK3/4b* mutant lines exhibited a strong reduction in *ASK3* and *ASK4* transcript levels (70-80% and 75-80%, respectively). The strong reduction in transcript levels allowed us to assess the physiological impact of these two genes. However, subsequent phenotypic analysis of these mutants revealed no overt morphological phenotypes. Although *ASK3* and *ASK4* proteins share highly similar interaction profiles,

their divergent expression patterns might partially explain the lack of any observed phenotype for the *ask3/4* double mutant.

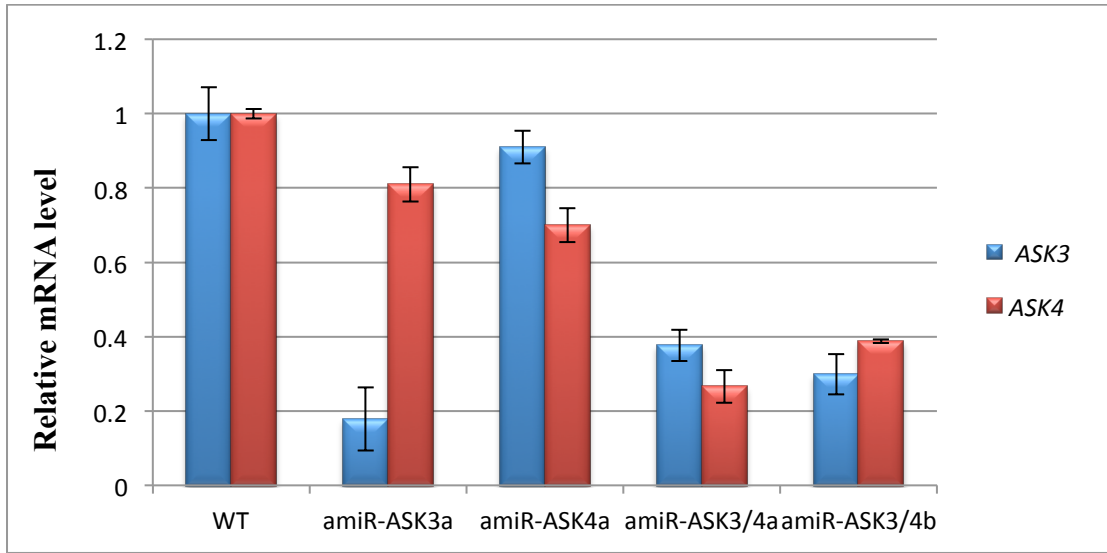


Figure 3.3. mRNA transcript abundance for *ASK3* and *ASK4* in various mutant backgrounds.

RNA was isolated and used to assess *ASK* gene expression as described in the methods. Relative mRNA expression levels in wild type (WT) and different transgenic lines were determined using qRT-PCR. Gene expression is depicted in relative amount after *ACTIN2* normalization. Data depicted is a representative of two independent biological replicates \pm SE from three sample replicates each.

ASK7/8/9/10

This clade is comprised of a set of four tandemly-duplicated genes that are tightly clustered within a 10-kbp span on chromosome 3 [31] [7]. The high sequence similarity between these genes (~85%) raises the possibility of a high level of genetic redundancy within the clade. This hypothesis is further supported by the data gathered in chapter one where expression analysis, along with hierarchical clustering of transcript expression, resulted in a relatively tight clustering of these genes, reminiscent of their phylogenetic clade. Surprisingly, interaction studies performed on genes residing within this clade suggests that although these genes possess a high level of sequence similarity, these gene products present a diverged interaction profile [7,32]. To functionally characterize these genes several attempts were made to design amiRNAs targeting individual genes using various online tools. However, due to the high level of sequence similarity within this gene family, only a single unique amiRNA against *ASK7* (amiR-*ASK7a*) and one against *ASK10* (amiR-*ASK10a*) could be generated. Two amiRNAs were designed to simultaneously knockdown all four genes, amiR-*ASK7/8/9/10a* and amiR-*ASK7/8/9/10b*. In transgenic plants expressing amiR-*ASK7a* and amiR-*ASK10a* constructs, *ASK7* and *ASK10* mRNA transcript levels were significantly lowered, respectively (**Figure 3.4**). The expression of *ASK8*, *ASK9* and *ASK10* was not affected in the amiR-*ASK7* transgenic plant, suggesting that the amiR-*ASK7* construct exhibits a high level of specificity. In the amiR-*ASK10a* transgenic plant the expression of *ASK9* was slightly (~17%) increased, indicative of a potential feedback mechanism and a level of genetic redundancy between *ASK9* and *ASK10*.

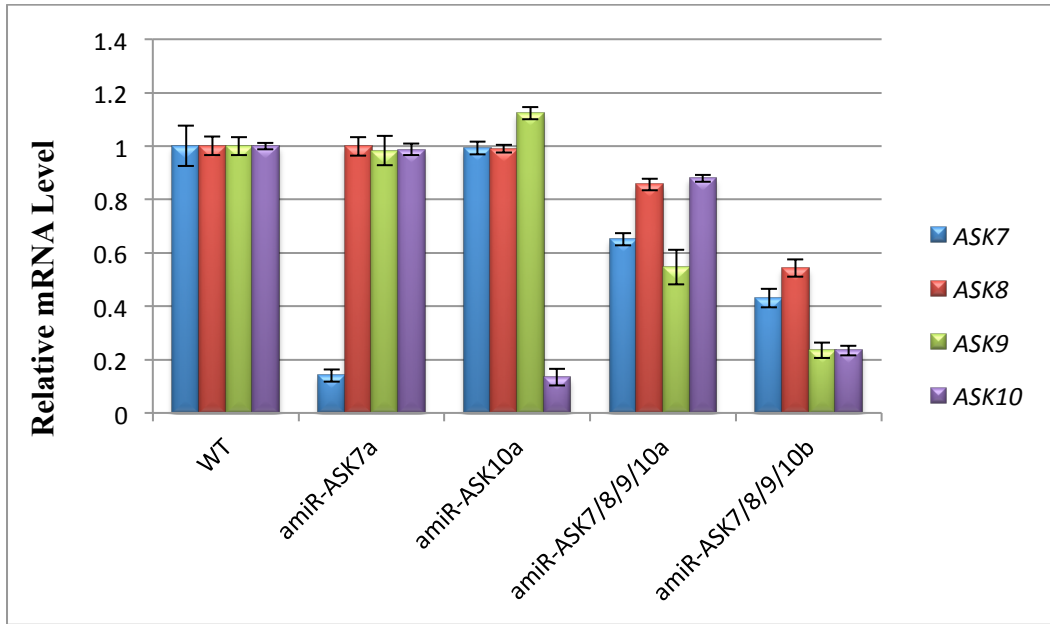


Figure 3.4. mRNA transcript abundance for *ASK7*, *ASK8*, *ASK9* and *ASK10* in various mutant backgrounds.

RNA was isolated and used to assess *ASK* gene expression as described in the methods. Relative mRNA expression levels in wild type (WT) and different transgenic lines were determined using qRT-PCR. Gene expression is depicted in relative amount after *ACTIN2* normalization. Data depicted is a representative of two independent biological replicates \pm SE from three sample replicates.

Phenotypic analysis of the *ask7* mutant plant did not show any overt morphological phenotypes under the lab conditions employed, however *ask10* mutant plants developed smaller siliques and aborted almost 15% of seeds in the silique (**Figure 3.5**). Given the restriction of transcript expression of *ASK10* in siliques [7], the observed phenotype for *ask10* was reassuring. Between the two constructs targeting all four genes within the clade only the amiR-*ASK7/8/9/10b* construct was effective in reducing the transcript levels of all target genes (**Figure 3.4**). Hence, the amiR-*ASK7/8/9/10b* transgenic plant was subjected to phenotypic analysis; this mutant exhibited a smaller silique size and aborted around 20% of seeds within the silique, a phenotype quite similar to that of the *ask10a* mutant plant (**Figure 3.5**). Collectively, these data suggest a mild level of genetic redundancy among the genes within the clade, especially between *ASK9* and *ASK10*.

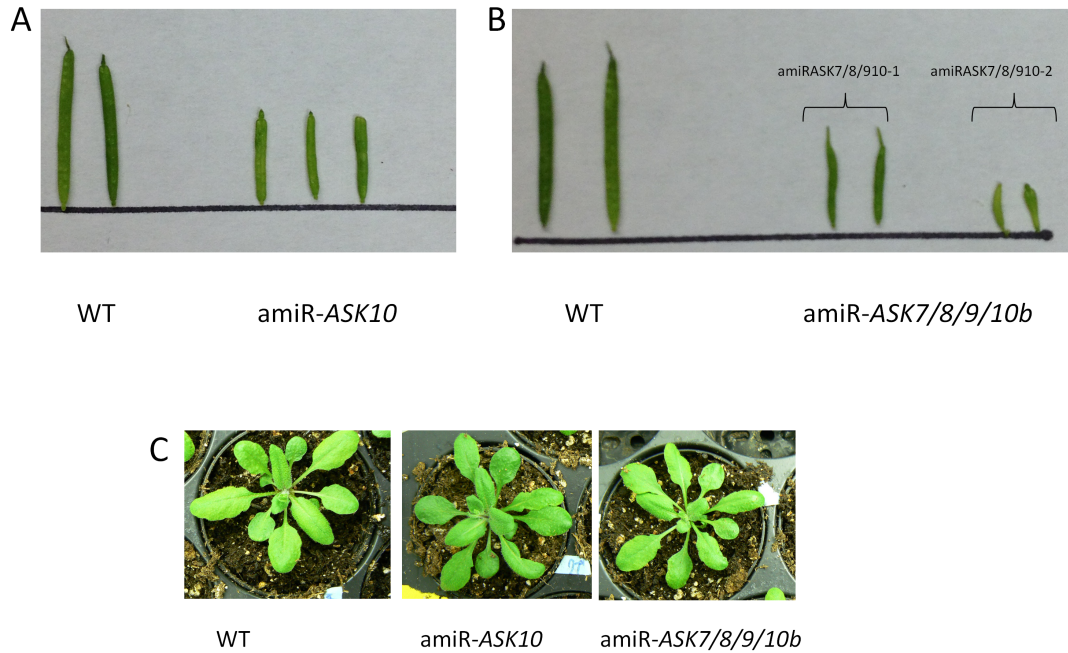


Figure 3.5. Phenotypic characterization of *ask10* and *ask7/8/9/10* mutant lines.

A,B. *ask10* and *ask7/8/9/10b* mutant plants displayed a smaller silique compared to wildtype plants. **C.** *ask10* and *ask7/8/9/10b* mutant plants despite having a smaller silique size did not exhibit any significant phenotype during early of the stages of growth and development.

ASK11/12

ASK11 and *ASK12* are two genes with a DNA sequence similarity of around 99% and are tightly clustered on chromosome 4 [7]. A high level of genetic redundancy can be expected given the corresponding high level of sequence similarity between these two genes. To understand the physiological contribution of these two genes to the growth and development of *A. thaliana* two amiRNAs were designed, simultaneously targeting *ASK11* and *ASK12* (amiR-*ASK11/12a* and amiR-*ASK11/12b*). To measure the mRNA abundance of the target transcripts a single set of primers were designed to amplify the two genes. Mutants independently harboring amiR-*ASK11/12a* and amiR-*ASK11/12b* constructs, significantly down regulated *ASK11* and *ASK12* transcript levels by as much as ~95% (**Figure 3.6**). The availability of two independent amiRNAs targeting different regions of the *ASK11* and *ASK12* mRNA allowed us to assign function, confidently to both genes. Gross phenotypic analysis of the *ask11/12* mutants revealed that both mutants were smaller in stature with mostly pale green leaves (indicating a defect in one of the stages of chloroplast production) and possessed smaller siliques. Interestingly, two recent papers have shown that ASK11 is the SKP1-like protein primarily responsible for the assembly of the SCF^{FBL17} [33,34]. SCF^{FBL17} has been shown to be involved in cell cycle regulation during male gametogenesis via degradation of the CDK inhibitor, KPR6. *fb17* mutations result in seed abortion and smaller silique size [34], thus can in part explain the observed phenotype for *ask11/12* mutants during silique development.

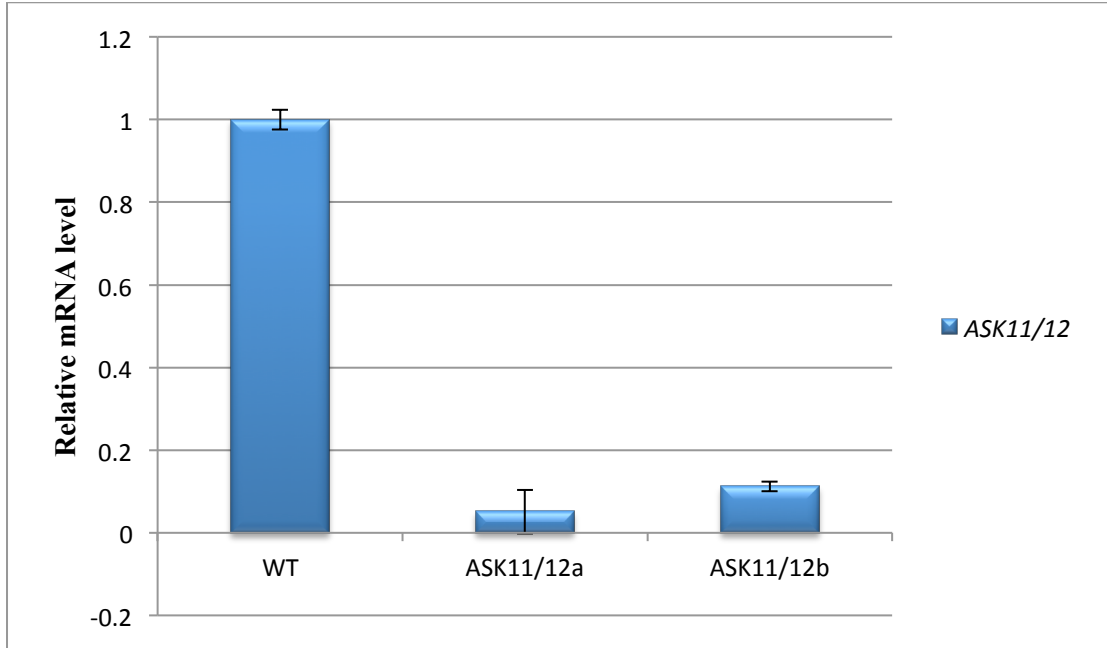


Figure 3.6. mRNA transcript abundance for *ASK11* and *ASK12* in various mutant backgrounds.

RNA was isolated and used to assess ASK gene expression as described in the methods. Due to high level of DNA sequence similarity between the two genes, we designed a single set of primers for both *ASK11* and *ASK12*. Relative mRNA expression levels in wild type (WT) and different transgenic lines were determined using qRT-PCR. Gene expression is depicted in relative amount after *ACTIN2* normalization. Data depicted is representative of 2 independent biological replicates \pm SE from three sample replicates.

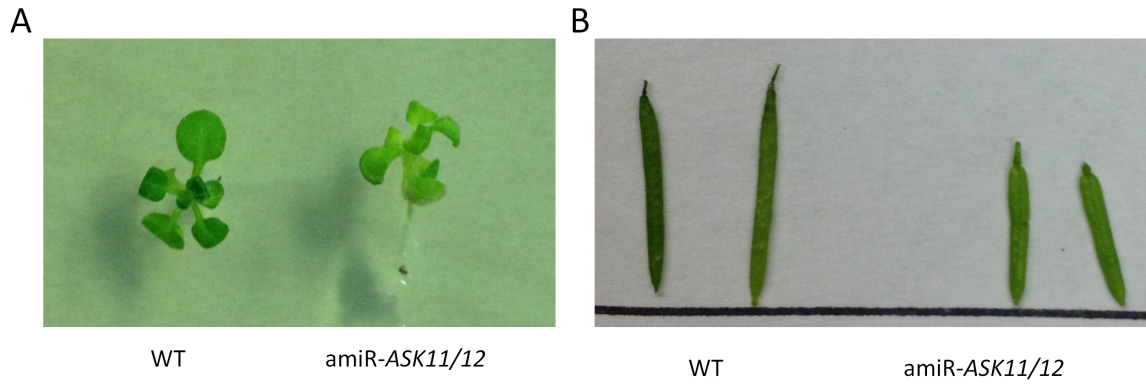


Figure 3.7. Phenotypic characterization of *ask11/12* mutant lines.

A. *ask11/12* mutants both mutants were smaller in stature with mostly pale green leaves.

B. *ask11/12* possessed smaller siliques compared to wild type plants.

ASK20/21

Based on phylogenetic analysis of the deduced protein sequence, *ASK20* and *ASK21* do not possess the characteristics of typical *ASK* genes since both genes are strongly sequence-divergent at their N-termini (the CUL1 interaction domain) [35]. Furthermore, all *ASK* genes in *A. thaliana* or other model species possess either one or no introns, thus can only generate one isoform [7,35,36]. However, both *ASK20* and *ASK21* genes possess multiple introns, and may therefore express several distinct isoforms. Therefore, in light of the degenerate CUL1 binding domain of *ASK20* and *ASK21*, as well as the distinct mRNA splicing patterns of their transcripts, we believe that these two genes have entered the *ASK* gene family through a different evolutionary route than the other *ASK* genes. Collectively these findings denote the possibility of a neo-functionalization for *ASK20* and *ASK21*. To study the functional contribution of the *ASK20* and *ASK21* genes to plant growth and development, 4 amiRNA constructs were designed: amiR-*ASK20a* and amiR-*ASK21a*, which independently target *ASK20* and *ASK21*, respectively; amiR-*ASK20/21a* and amiR-*ASK20/21b*, which simultaneously target both *ASK20* and *ASK21*. The amiR-*ASK20a* and amiR-*ASK21a* constructs both significantly decreased the abundance of *ASK20* and *ASK21*, respectively (**Figure 3.8**). Interestingly, in *ask20* mutant plants the transcript level of *ASK21* was upregulated by 20%. Similarly, in *ask21* mutant plants, *ASK20* transcript levels were upregulated by ~18%. Although at this juncture, the active mechanism behind the observed transcript compensation is unknown, up regulation of a paralog gene strongly indicates genetic redundancy. Between the two amiRNAs designed to target both genes simultaneously, only the amiR-*ASK20/21b* construct achieved a desirable level of transcript reduction for

ASK20 and *ASK21*. Although no interaction-based analysis has been performed on the protein products of these two genes, the expression-based analysis performed presented in chapter one indicate a high correlation among the expression pattern of both genes. Thus it was anticipated that only the double mutants would exhibit phenotypes. Although no in-depth phenotypic analysis is available at this stage of the study, gross phenotypic analysis of the double mutant failed to reveal any significant morphological phenotypes.

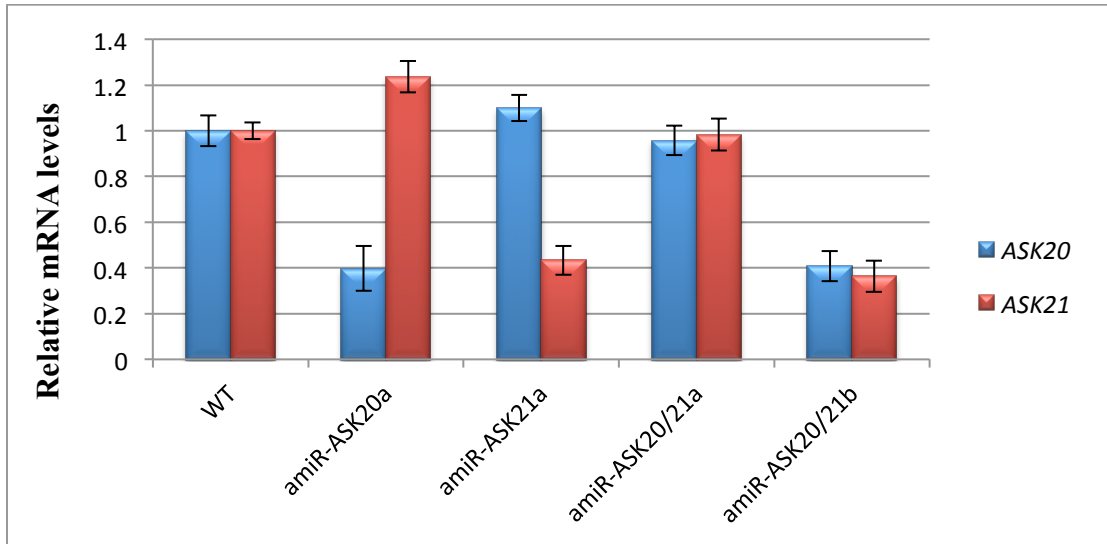


Figure 3.8. mRNA transcript abundance for *ASK20* and *ASK21* in various mutant backgrounds.

RNA was isolated and used to assess ASK gene expression as described in the methods. Due to high level of DNA sequence similarity between the two genes we designed a single set of primers for both *ASK11* and *ASK12*. Relative mRNA expression levels in wild type (WT) and different transgenic lines was determined using qRT-PCR. Gene expression is depicted in relative amount after *ACTIN2* normalization. Data depicted is representative of 2 independent biological replicates \pm SE from three sample replicates.

CONCLUSION

Unbiased genetic surveys have shown that mutations in SCF ligase components affect *A. thaliana* growth and development [37]. *CUL1* null mutations (*cull-1*) are lethal and arrest at the single-cell stage [42,43]. Furthermore, point mutations in the *CUL1* gene (*cull-6* and *cull-7*) result in severe developmental defects [43,44]. Due to the essential role that CUL1 plays during growth and development, it was anticipated that mutations in *ASK* genes should exhibit a similar behavior.

Interestingly, single mutations in *ASK1* did not exhibit any embryonic lethal defects [30]. Furthermore, the *ask2* null mutant did not exhibit any developmental defects at the embryonic stage [11]. The lack of a lethal phenotype for independent *ask1* and *ask2* mutants could have two possible explanations: the remaining, uncharacterized *ASK* genes in *A. thaliana* play an essential role during embryogenesis or a high level of genetic redundancy exists between *ASK1* and *ASK2* during embryogenesis. The *ask1/ask2* double null mutant generated by Liu et al. exhibited severe developmental defects suggestive of the redundant and essential role of *ASK1* and *ASK2* during embryogenesis and seedling growth [11]. The broad expression profile of *ASK1* and *ASK2* during growth and development, along with their general F-Box protein-interaction pattern (shown in chapter two) is suggestive of a major role for *ASK1* and *ASK2* during the later stages of plant development. The generation of the *ask1/ask2a* (*amiR-ASK1/2a*) double mutant, which resulted in a partial knockdown of both genes, has allowed us to assess the contribution of these two genes in plant growth and development. Although an in-depth phenotypic analysis is not available at this stage of the study, gross phenotyping indicates that *ASK1* and *ASK2* play a key role during the transition from vegetative to reproductive stage, flowering and seed generation in *A. thaliana*. Although no significant

morphological phenotypes were observed during embryogenesis among the mutants generated as part of this study, phenotypic analysis of several of these mutants revealed that selected aspects of growth and development are controlled and mediated by *ASK* genes. In instances where mutants exhibited phenotypes (*ask1/2a*, *ask11/12a*, *ask11/12b*, *ask10*, *ask7/8/9/10b*), the observed phenotype was mainly confined to the tissues in which the genes are known to be expressed.

Among duplicated genes, the absence of a phenotype when one of the paralogs is deleted can be the result of an up-regulation of its duplicated paralog. Although the prevalence of this response is not fully understood in plants, in yeast it has been shown that ~12% of the paralogs exhibit such a characteristic [38,39]. To assess whether the absence of overt morphological phenotypes for several of the individual mutants could be the result of such a phenomenon, we assessed the expression of closely related paralogs in various mutant backgrounds. Interestingly, among the six individual mutant lines that achieved a significant level of down-regulation of the target genes, 4 displayed up-regulation of the closely related paralog (*ask1*, *ask10*, *ask20* and *ask21*). Furthermore for genes that reside in clades that show a divergent expression pattern, such as *ASK3* and *ASK4*, we did not observe transcript up-regulation in response to the deletion of the paralog. Moreover, the *ask3/4* double mutant did not exhibit any obvious morphological phenotype under the laboratory conditions assessed, suggesting that *ASK3* and *ASK4* do not genetically interact. Collectively, these data argue that deletion-mediated up-regulation of a paralog gene within the *ASK* family is primarily restricted to genes that are not only genetically interacting, but have also recently diverged.

Although we have only performed gross phenotypic analysis at this stage of the study, the observation of diverse phenotypes (especially in instances that individual mutants exhibited a phenotype) not only argues a high level of sub-functionalization has occurred throughout the *ASK* gene family, but also underscores the breadth of functions that this gene family plays throughout plant development.

Expression-based analysis of the *ASK* genes under various stimuli and conditions performed in the lab have shown that the expression of most *ASK* genes is induced following various biotic and abiotic stimuli (data not shown). Thus, future work will focus on an in-depth morphological phenotypic characterization of these mutants. This phenotypic screen will be further complimented by an in-depth assessment of mutant plant response to a variety of conditions and stimuli that have been previously connected to components of the SCF ligase such as auxin and jasmonate and gibberellin signalling, and pathogenic responses.

At this point in the study we cannot exclude the possibility of neo-functionalization of *ASK* genes. However, if we assume that the phenotypes observed in various *ask* mutant backgrounds are the result of the inability of ASK protein to assemble as part of the SCF ligase, the ubiquitination pattern between wild type and mutant plants should differ. Therefore, assessing the ubiquitination pattern between wild type and *ask* mutant plants should in principle allow us to dissect the molecular mechanism underlying the observed phenotypes. The mutants developed, as part of this study, will allow us to assess the contribution of the various ASK-containing SCF ligases to plant growth and development.

BIBLIOGRAPHY

1. Zhang J (2003) Evolution by gene duplication: an update. *Trends in Ecology & Evolution* 18: 292-298.
2. Prince VE, Pickett FB (2002) Splitting pairs: the diverging fates of duplicated genes. *Nature Reviews Genetics* 3: 827-837.
3. Gu Z, Steinmetz LM, Gu X, Scharfe C, Davis RW, et al. (2003) Role of duplicate genes in genetic robustness against null mutations. *Nature* 421: 63-66.
4. Simillion C, Vandepoele K, Van Montagu MC, Zabeau M, Van de Peer Y (2002) The hidden duplication past of *Arabidopsis thaliana*. *Proc Natl Acad Sci U S A* 99: 13627-13632.
5. Knowles DG, McLysaght A (2006) High rate of recent intron gain and loss in simultaneously duplicated *Arabidopsis* genes. *Molecular biology and evolution* 23: 1548-1557.
6. Duarte JM, Cui L, Wall PK, Zhang Q, Zhang X, et al. (2006) Expression pattern shifts following duplication indicative of subfunctionalization and neofunctionalization in regulatory genes of *Arabidopsis*. *Molecular biology and evolution* 23: 469-478.
7. Dezfulian MH, Soulliere DM, Dhaliwal RK, Sareen M, Crosby WL (2012) The SKP1-Like Gene Family of *Arabidopsis* Exhibits a High Degree of Differential Gene Expression and Gene Product Interaction during Development. *PLoS one* 7: e50984.
8. Vierstra RD (2003) The ubiquitin/26S proteasome pathway, the complex last chapter in the life of many plant proteins. *Trends in Plant Science* 8: 135-142.
9. Vierstra RD (2009) The ubiquitin-26S proteasome system at the nexus of plant biology. *Nat Rev Mol Cell Biol* 10: 385-397.
10. Kong H, Landherr LL, Frohlich MW, Leebens-Mack J, Ma H, et al. (2007) Patterns of gene duplication in the plant SKP1 gene family in angiosperms: Evidence for multiple mechanisms of rapid gene birth. *Plant Journal* 50: 873-885.
11. Liu F, Ni W, Griffith ME, Huang Z, Chang C, et al. (2004) The ASK1 and ASK2 Genes Are Essential for *Arabidopsis* Early Development. *Plant Cell* 16: 5-20.
12. Wang Y, Yang M (2006) The ARABIDOPSIS SKP1-LIKE1 (ASK1) protein acts predominately from leptotene to pachytene and represses homologous recombination in male meiosis. *Planta* 223: 613-617.
13. Yang X, Timofejeva L, Ma H, Makaroff CA (2006) The *Arabidopsis* SKP1 homolog ASK1 controls meiotic chromosome remodeling and release of chromatin from the nuclear membrane and nucleolus. *Journal of Cell Science* 119: 3754-3763.

14. Zhao D, Han T, Risseuw E, Crosby WL, Ma H (2003) Conservation and divergence of ASK1 and ASK2 gene functions during male meiosis in *Arabidopsis thaliana*. *Plant Molecular Biology* 53: 163-173.
15. Zhao D, Yang X, Quan L, Timofejeva L, Rigel NW, et al. (2006) ASK1, a SKP1 homolog, is required for nuclear reorganization, presynaptic homolog juxtaposition and the proper distribution of cohesin during meiosis in *Arabidopsis*. *Plant Molecular Biology* 62: 99-110.
16. Alonso JM, Stepanova AN, Leisse TJ, Kim CJ, Chen H, et al. (2003) Genome-wide insertional mutagenesis of *Arabidopsis thaliana*. *Science Signalling* 301: 653.
17. Alonso JM, Ecker JR (2006) Moving forward in reverse: genetic technologies to enable genome-wide phenomic screens in *Arabidopsis*. *Nature Reviews Genetics* 7: 524-536.
18. Links M, Crosby WL (2007) Organization and evolution of information within eukaryotic genomes. In: Links M, Crosby WL, editors.
19. Cai Y, Yu X, Hu S, Yu J (2009) A brief review on the mechanisms of miRNA regulation. *Genomics, Proteomics & Bioinformatics* 7: 147-154.
20. Meister G, Tuschl T (2004) Mechanisms of gene silencing by double-stranded RNA. *Nature* 431: 343-349.
21. Miyagishi M, Taira K (2002) U6 promoter driven siRNAs with four uridine 3' overhangs efficiently suppress targeted gene expression in mammalian cells. *Nature biotechnology* 20: 497-500.
22. Persengiev SP, Zhu X, Green MR (2004) Nonspecific, concentration-dependent stimulation and repression of mammalian gene expression by small interfering RNAs (siRNAs). *Rna* 10: 12-18.
23. Marques JT, Williams BRG (2005) Activation of the mammalian immune system by siRNAs. *Nature biotechnology* 23: 1399-1405.
24. Schwab R, Ossowski S, Riester M, Warthmann N, Weigel D (2006) Highly specific gene silencing by artificial microRNAs in *Arabidopsis*. *The Plant Cell Online* 18: 1121-1133.
25. Adai A, Johnson C, Mlotshwa S, Archer-Evans S, Manocha V, et al. (2005) Computational prediction of miRNAs in *Arabidopsis thaliana*. *Genome Research* 15: 78-91.
26. Brodersen P, Sakvarelidze-Achard L, Bruun-Rasmussen M, Dunoyer P, Yamamoto YY, et al. (2008) Widespread translational inhibition by plant miRNAs and siRNAs. *Science Signalling* 320: 1185.

27. Voinnet O (2009) Origin, biogenesis, and activity of plant microRNAs. *Cell* 136: 669-687.
28. Mathieu J, Warthmann N, Küttner F, Schmid M (2007) Export of FT Protein from Phloem Companion Cells Is Sufficient for Floral Induction in *Arabidopsis*. *Current Biology* 17: 1055-1060.
29. Zhang X, Henriques R, Lin SS, Niu QW, Chua NH (2006) Agrobacterium-mediated transformation of *Arabidopsis thaliana* using the floral dip method. *Nature Protocols* 1: 641-646.
30. Yang M, Hu Y, Lodhi M, McCombie WR, Ma H (1999) The *Arabidopsis* SKP1-LIKE1 gene is essential for male meiosis and may control homologue separation. *Proceedings of the National Academy of Sciences* 96: 11416-11421.
31. Marrocco K, Lecureuil A, Nicolas P, Guerche P (2003) The *Arabidopsis* SKP1-like genes present a spectrum of expression profiles. *Plant Molecular Biology* 52: 715-727.
32. Kuroda H, Yanagawa Y, Takahashi N, Horii Y, Matsui M (2012) A Comprehensive Analysis of Interaction and Localization of *Arabidopsis* SKP1-LIKE (ASK) and F-Box (FBX) Proteins. *PLoS one* 7: e50009.
33. Gusti A, Baumberger N, Nowack M, Pusch S, Eisler H, et al. (2009) The *Arabidopsis thaliana* F-box protein FBL17 is essential for progression through the second mitosis during pollen development. *PLoS one* 4: e4780.
34. Kim HJ, Oh SA, Brownfield L, Hong SH, Ryu H, et al. (2008) Control of plant germline proliferation by SCFFBL17 degradation of cell cycle inhibitors. *Nature* 455: 1134-1137.
35. Ogura Y, Ihara N, Komatsu A, Tokioka Y, Nishioka M, et al. (2008) Gene expression, localization, and protein-protein interaction of *Arabidopsis* SKP1-like (ASK) 20A and 20B. *Plant Science* 174: 485-495.
36. Risseuw EP, Daskalchuk TE, Banks TW, Liu E, Cotelesage J, et al. (2003) Protein interaction analysis of SCF ubiquitin E3 ligase subunits from *Arabidopsis*. *The Plant Journal* 34: 753-767.
37. Kelley DR, Estelle M (2012) Ubiquitin-mediated control of plant hormone signaling. *Plant Physiology* 160: 47-55.
38. DeLuna A, Springer M, Kirschner MW, Kishony R (2010) Need-based up-regulation of protein levels in response to deletion of their duplicate genes. *PLoS biology* 8: e1000347.
39. Li J, Yuan Z, Zhang Z (2010) The cellular robustness by genetic redundancy in budding yeast. *PLoS genetics* 6: e1001187.

CHAPTER 4

Dimerization of the E3 SCF^{TIR1} Ligase is Essential for Auxin Signaling

INTRODUCTION

The plant hormone auxin is an essential regulator of diverse aspects of plant growth and development [1]. Previous studies have shown that an E3 ubiquitin (Ub) ligase of the SCF class (**SKP1**, **CUL1**, **F-box**) is an essential component of auxin signaling [2-4]. **Transport Inhibitor Response (TIR1)**, is one member of a family of five **Auxin-signaling F-box proteins (AFBs)** and has been shown to act as the receptor for auxin binding and activation of the SCF^{TIR1} complex, leading to targeted protein degradation events involved in auxin perception [5]. **Auxin/INDOLE-3-ACETIC ACID (Aux/IAA)** proteins act as negative regulators of auxin signaling through their interaction with **Auxin Response Factors (ARFs)** [1,4]. In the presence of auxin, these transcription repressors have been biochemically characterized as the prime targets for the SCF^{TIR1} E3 Ub ligase complex in the presence of auxin molecules [2,6]. Thus, in the presence of auxin and a reduced abundance of Aux/IAA proteins, several auxin response genes are activated as part of the generalized auxin response [7-9]. Since auxin plays a central role in many aspects of plant patterning and development, the tight regulation of auxin signaling and response is likewise central to plant growth, particularly at the level of the auxin receptor function of TIR1 and related F-box proteins. To date, all proposed SCF ligase-related auxin regulatory mechanisms mediated by CAND1 and RUB/Nedd8 are described at the level of CUL1 subunit modification [7-9]. Thus, these modifications should be considered as part of the general regulation of SCF ligase homeostasis and function independent of the AFB auxin receptors, with the sole exception of the S-nitrosylation of TIR1 [10]. Substrate recognition by the SCF^{TIR1} complex is thought to be solely dependent on auxin binding to the F-box protein receptor, suggesting that the

SCF^{TIR1} E3 Ub ligase is constitutively active in the presence of auxin [4,8]. However, recent studies have shown that the homo-dimerization of select F-box proteins is required for efficient substrate ubiquitination and subsequent degradation, thus providing a novel perspective of SCF ligase regulation at the level of higher-order SCF complex assembly [11-17]. Accordingly, we have investigated the potential for the homo-dimerization of TIR1 as a major auxin receptor in Arabidopsis, with implications for auxin response and regulation. In this chapter I describe the homo-dimerization of TIR1 protein *in planta* together with a role for TIR1 homo-dimerization in the degradation of Aux/IAA proteins as part of the auxin-signaling pathway.

RESULTS AND DISCUSSION

TIR1 protein lacks a dimerization-domain

Recent reports have shown that select SCF-class E3 Ub ligases can function as a dimer, where dimerization of the complex is mediated through a conserved dimerization domain (D-domain) located immediately N-terminal of the F-box domain within the participating F-box subunit [12,15,16]. As one approach to investigate the potential for the dimerization SCF^{TIR1}, we conducted a thorough bioinformatics survey for the presence of a D-domain within the family of AFB proteins in Arabidopsis. This survey failed to identify a canonical D-domain within TIR1 or any of the other AFB protein sequences (data not shown) suggesting that if TIR1 protein does indeed homo-dimerize, TIR1 homo-dimerization is not mediated by an identifiable D-domain.

It has been suggested that the absence of a canonical D-domain in some F-box proteins, such as the mammalian SKP2, results in the formation of a monomeric SCF ligase complex. However, no experimental data has yet been provided to support that the D-domain is exclusively responsible for mediating SCF homo-dimerization [18]. To experimentally examine the potential for SCF^{TIR1} dimerization *in vivo*, we utilized **Bimolecular Fluorescence Complementation (BiFC)** in a heterologous *Nicotiana benthamiana* leaf expression system, thus allowing for visualization of protein interactions in living plant cells, together with information concerning the sub-cellular localization of the interaction [19-21]. To demonstrate the fidelity of the *Nicotiana* expression system for the recapitulation of TIR1-dependent Aux/IAA protein degradation, we co-expressed IAA7 [8], a member of the Arabidopsis Aux/IAA family of proteins, in the presence and absence of TIR1. As shown in **Figure 4.1A**, IAA7 protein

abundance was markedly reduced when co-expressed with TIR1, suggesting that TIR1 can assemble as part of a Nicotiana SCF ligase and subsequently target IAA7 protein for degradation in the Nicotiana system. To confirm that the observed reduction in protein abundance was consistent with SCF^{TIR1} function and dependent upon 26S proteasome-mediated protein degradation, we treated leaves co-expressing TIR1 and IAA7 proteins with the 26S proteasome inhibitor MG-132 and found that IAA7 abundance was elevated relative to the controls (**Figure 4.1B**). Interestingly, higher molecular weight IAA7 proteins were detected in the presence of MG-132 and TIR1, reminiscent of a ubiquitination pattern. Taken together, the evidence suggests that the Nicotiana transient expression system faithfully recapitulates the function of TIR1-dependent Aux/IAA protein degradation as part of the Arabidopsis auxin-signaling pathway.



Figure 4.1. Arabidopsis Aux/IAA protein abundance is regulated by the SCF^{TIR1} E3 ligase in *N. benthamiana*.

A. IAA7 and TIR1 were visualized using anti-Myc and anti-HA antibodies, respectively. The large subunit of Rubisco was used as a loading control. **B.** Myc:IAA7 and HA:TIR1 were co-expressed and leaves were subjected to MG-132 treatment for 5 h prior to protein extraction.

BiFC constructs expressing components of SCF^{TIR1} were generated and used to assess the homo-dimerization potential of three known subunits of the SCF^{TIR1} complex (**Table 4.1**). Among the three subunits assessed, a homo-dimerization fluorescent signal was observed for TIR1 and Arabidopsis SKP1-like (ASK1), but not for CUL1 (**Figure 4.2D**). Interestingly, the TIR1 homo-dimerization signal was localized to the nucleus, suggesting this F-box protein self-interacts despite lacking a conserved D-domain. The ASK1-ASK1 protein BiFC signal exhibited a pronounced cytoplasmic and weaker nuclear localization, suggesting that ASK1 can also homo-dimerize. All observed interactions were compared to that of TIR1-ASK1 in order to investigate the relative strength of the BiFC signals corresponding to those interactions (**Figure 4.2D**). The sub-cellular behavior of the relatively weak nuclear-localized TIR1-TIR1 interaction was importantly different from that of the predominantly nuclear and weaker cytoplasmic CFP:TIR1 localization (**Figure 4.3**). The exclusively nuclear homo-dimerization of TIR1 is likely biologically relevant, given the demonstrated role of the SCF^{TIR1} complex in the degradation of Aux/IAA transcription factors early in the auxin signaling and response pathway in Arabidopsis.

We used both yeast two-hybrid (Y2H) and co-immunoprecipitation (Co-IP) approaches to validate the BiFC results. Y2H approaches revealed a weak but significant homo-dimerization of TIR1 (**Figure 4.4A**). Similarly, Co-IP experiments involving Myc- and HA-tagged TIR1 fusion-expression constructs co-expressed in the presence of ASK1 in *Nicotiana* leaves show results consistent with TIR1 homo-dimerization (**Figure 4.4B**).

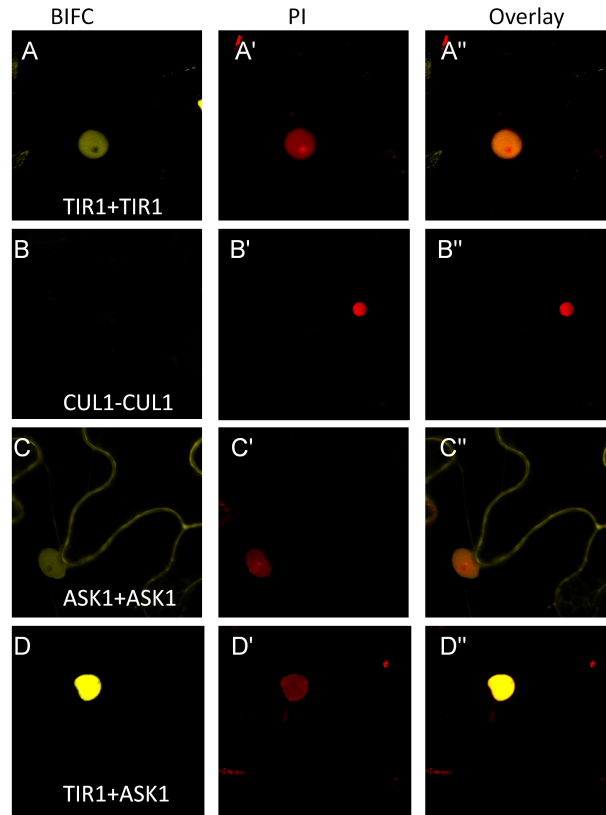


Figure 4.2. BiFC-based evaluation of homo-dimerization potential of SCF^{TIR1} components in *N. benthamiana*.

A. Fluorescent signal confined to the nucleus resulting from a direct interaction of TIR1 proteins fused to complementary fluorescent protein fragments. **B.** No detectable fluorescent signal for CUL1 homo-dimerization following BiFC. **C.** A nuclear and cytoplasmic fluorescent signal distribution resulting from a direct interaction of ASK1 proteins fused to complementary fluorescent protein fragments. **D.** Nuclear fluorescent signal resulting from a direct interaction of ASK1 and TIR1 proteins fused to complementary fluorescent protein fragments. **A'-D'.** PI-stained nuclei. **A''-D''.** Overlay.

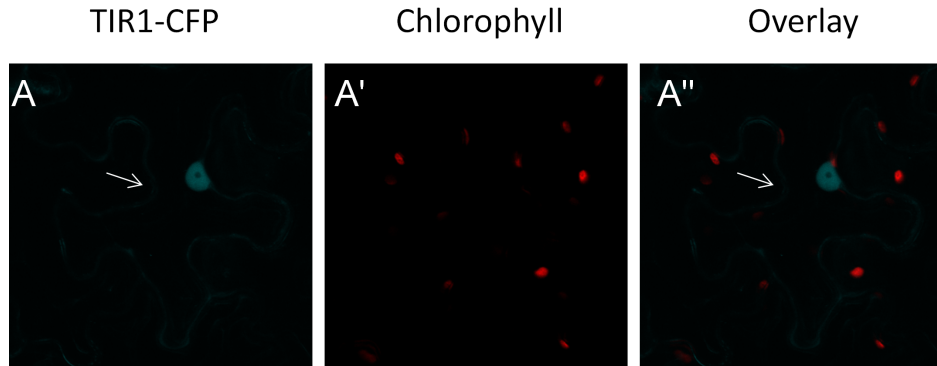
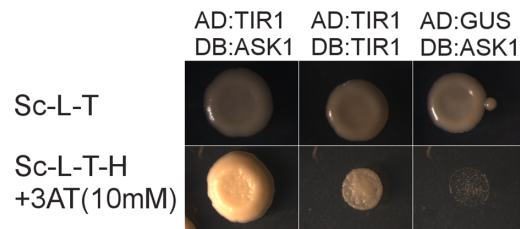


Figure 4.3. Nuclear and cytoplasmic localization of TIR1 following transient expression in *N. benthamiana* leaves.

A. Sub-cellular distribution of CFP-TIR1, following transient expression in *Nicotiana* leaves is indicative of weak cytoplasmic and strong nuclear localization. **A'**. Chlorophyll auto-fluorescence from the leaf mesophyll cell layer. **A''**. Overlay of images A and A'. White arrows indicate CFP-TIR1 localization.

A



B

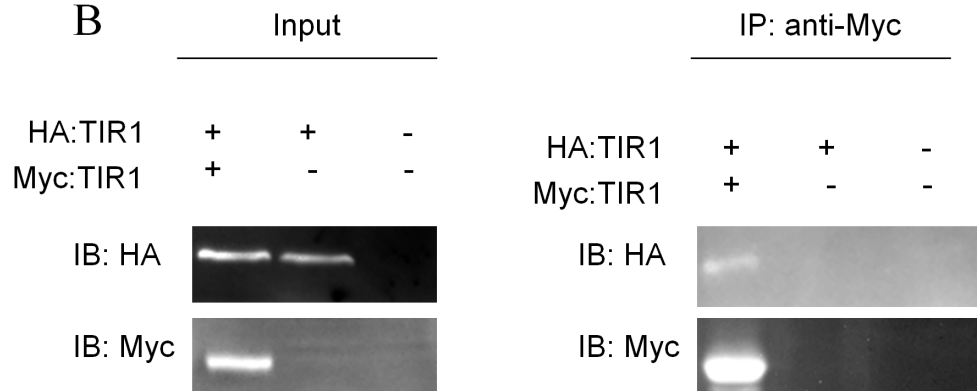


Figure 4.4. Validation of TIR1 homo-dimerization using Co-IP and Y2H.

A. Assessment of TIR1-TIR1 protein interaction and strength relative to ASK1-TIR1 interaction in Y2H assay. Images of single colonies expressing the designated constructs and grown on histidine plates (top panel) and test plates containing 10 mM 3-aminotriazole (3-AT) without histidine (bottom panel). **B.** *In vitro* Co-IP experiments in *Nicotiana* leaves. HA:TIR1 and Myc:TIR1 were co-injected in leaves. Protein extracts were subjected to immunoprecipitation using anti-Myc antibody. The immunoprecipitates were examined by Western blotting using anti-Myc and anti-HA antibody.

TIR1 dimerization is independent of other SCF subunits

The emerging general pattern of homo-dimerization involving F-box proteins has been shown in other systems to be independent of SKP1 subunit binding and interaction [11,15,16]. We assessed the role of ASK1 in TIR1 dimerization by generating a variant allele with the deletion of the degenerate F-box domain – TIR1- Δ F(Δ 10-40) – and assessed the interaction of this deletion variant with both ASK1 and full-length TIR1 using the BiFC system. Interestingly, TIR1- Δ F did not detectably interact with either ASK1 (**Figure 4.5B**) or full-length TIR1 (**Figure 4.5A**), suggesting that ASK1 may be essential in the homo-dimerization of TIR1. The inability of TIR1- Δ F to homo-dimerize could be due to an altered tertiary structure resulting in decreased protein stability. To investigate this, we generated two alleles containing amino acid substitution mutations within the F-box domain of TIR1: Val33 to Glu (V33E-TIR1) and a double mutation of Val33 to Ala and Lys35 to Ala (V33A/K35A-TIR1). When submitted to BiFC interaction analysis, V33E-TIR1 failed both to detectably bind ASK1 (**Figure 4.5F**) as well as to homo-dimerize (**Figure 4.5E**). Alternatively, V33A/K35A-TIR1 retained a partial capacity to associate with ASK1 (**Figure 4.5D**) and also retained the ability to homo-dimerize (**Figure 4.5C**). To further assess the role of ASK1 in TIR1 homo-dimerization, we performed a set of BiFC studies where TIR1 was co-expressed with ASK1 (**Figure 4.5G,H**). The results showed an enhanced fluorescence signal arising from TIR1-TIR1 interaction when co-expressed with ASK1. A parallel set of experiments was carried out in a yeast three-hybrid experiment, where the results supported the finding that TIR1 homo-dimerization was enhanced by co-expression with ASK1 (data not shown).

Previous studies have shown that SKP1 protein can stabilize F-box proteins by interacting with the hydrophobic F-box domain. To assess whether the enhanced TIR1 homo-dimerization was due to protein stabilization in the presence of ASK1, we performed a set of Western blots, which revealed that steady-state TIR1 protein levels are strongly elevated in the presence of ASK1 (**Figure 4.5F**). An alternative explanation for the lack of homo-dimerization by TIR1-ASK1 binding mutants could involve an aberrant sub-cellular localization. Indeed, it has been reported that several F-box proteins retain a nuclear localization signal (NLS) within their F-box domain, such that the deletion of the F-box domain could result in an incorrect localization of the variant protein [22]. In order to investigate the stability and localization of the mutant proteins employed in this study, YFP-tagged variants of each TIR1 mutant were generated and expressed in the *Nicotiana* transient expression system. Upon comparing the localization and stability (signal intensity) of YFP:TIR1 mutants to that of YFP:TIR1, V33A/K35A-TIR1 and V33E-TIR1 mutant proteins retained their nuclear localization (**Figure 4.5J** and **Figure 4.5K**, respectively), although they were relatively unstable as indicated by a marked decrease in fluorescent signal. On the other hand, expression of the YFP:TIR1- Δ F fusion variant resulted in a fluorescent signal that was strongly aggregated and external to the nucleus (**Figure 4.5L**), suggesting the variant was not only mis-localized but also unstable. Taken together, the homo-dimerization experiments involving select TIR1 F-box mutants suggest that the increased stability of TIR1 when co-expressed with ASK1 is effected through the masking of the hydrophobic F-box domain in TIR1 [4], rather than a direct involvement of ASK1 in TIR1 homo-dimerization.

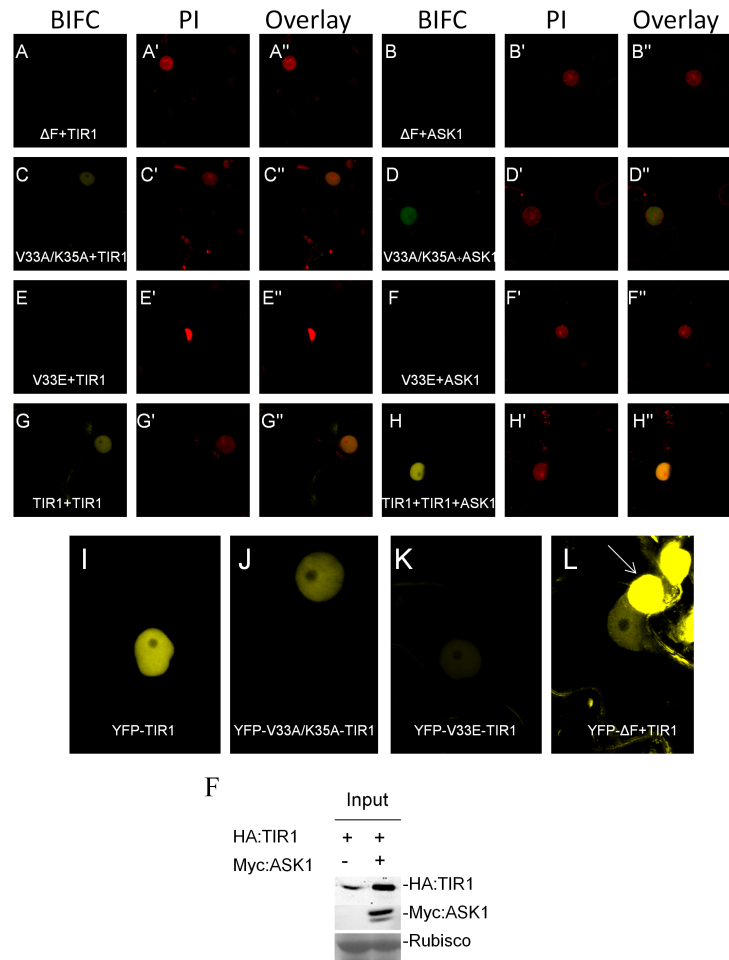


Figure 4.5. TIR1 homo-dimerization is independent of ASK1 homo-dimerization. **A,C,E.** BiFC-based assessment of TIR1 homo-dimerization using ΔF -TIR1, V33A/K35A-TIR1 and V33E-TIR1, respectively. **B,D,F.** BiFC-based assessment of ASK1 binding with ΔF -TIR1, V33A/K35A-TIR1 and V33E-TIR1, respectively. **G,H.** BiFC-based assessment of TIR1 homo-dimerization in the absence and presence of Myc:ASK1, respectively. **A'-H'.** Propidium iodide (PI) staining of the nucleus. **I-L.** Assessment of sub-cellular localization of YFP-TIR1, YFP-V33A/K35A-TIR1, YFP-V33E-TIR1 and YFP- ΔF + TIR1, respectively. **F.** Western blotting on protein cell extracts from *Nicotiana* leaves expressing either TIR1 alone or co-expressing ASK1 and TIR1 in the presence of cycloheximide.

Aux/IAA transcriptional repressors have been shown to be the prime targets of the SCF^{TIR1} complex [2,3]. Following TIR1 binding, Aux/IAA proteins were found to be ubiquitinated and subsequently degraded via the 26S proteasome [2,3,7]. As with most transcription factors, Arabidopsis Aux/IAA proteins have been shown to form hetero- or homo-dimers [23,24]. We considered that the homo-dimerization of Aux/IAA proteins could, in turn, lead to the homo-dimerization of TIR1 while in complex with the SCF ligase. To evaluate this possibility, we assessed the homo-dimerization of IAA7 and IAA3 using the BiFC system. Both proteins exhibited the ability to homo-dimerize within the nucleus (**Figure 4.6A,B**), but the pattern of the homo-dimerization was distinct from that observed for TIR1 homo-dimerization in that the signal was confined to discrete regions within the nucleus. We subsequently examined the localization of YFP:IAA protein fusions and found that both IAA3 and IAA7 exhibited similar localization patterns to that of the BiFC interaction. The differential localization pattern of TIR1 homo-dimerization versus IAA homo-dimerization suggests that the homo-dimerization of the two are spatially – and likely functionally – independent. To further explore this possibility, we developed a set of TIR1 mutants that were previously shown to abolish binding to Aux/IAA proteins. The specific variants included a double mutant where both Ser462 and Ala464 were mutated to Glu (S462E/A464E-TIR1). As shown in (**Figure 4.6C**), the double mutant retained the ability to homo-dimerize, suggesting that the Aux/IAA protein interaction was not obligatory for TIR1 homo-dimerization.

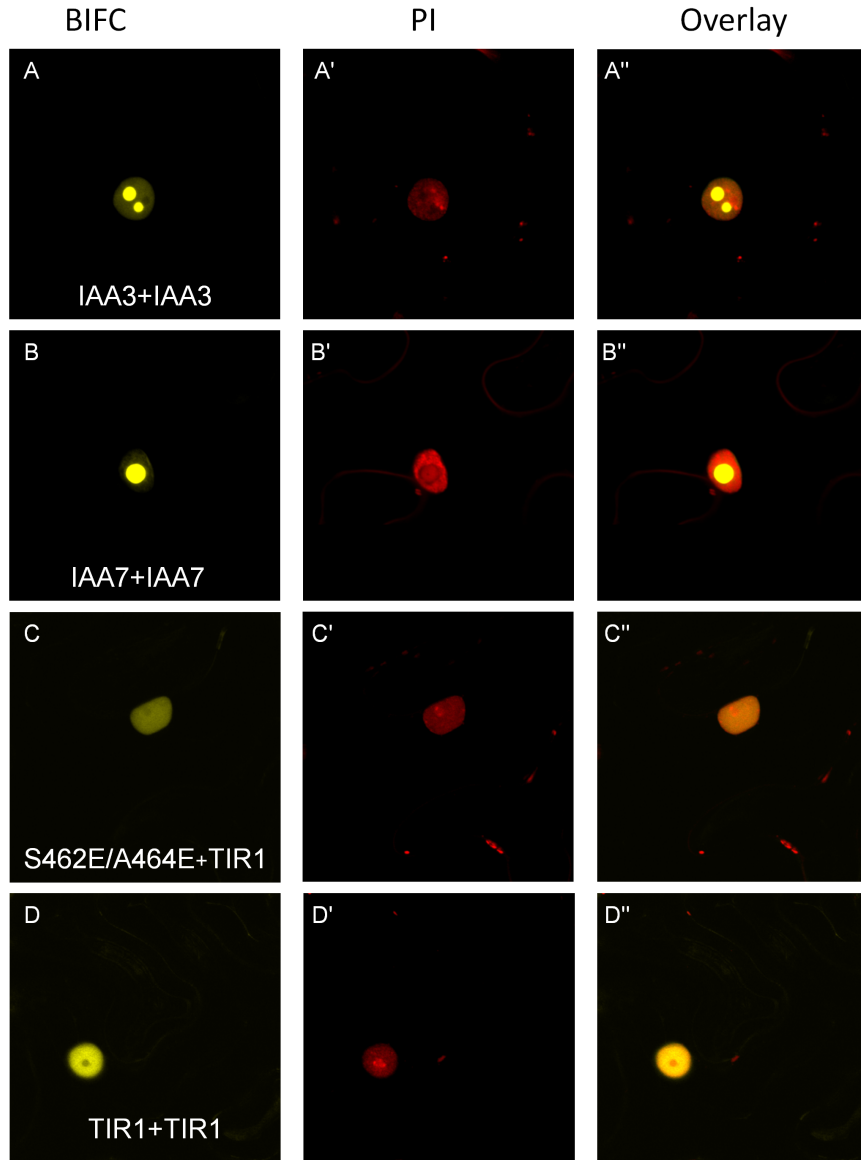


Figure 4.6. TIR1 homo-dimerization is independent of Aux/IAA binding.

A,B. BiFC-based assessment of IAA3 and IAA7 homo-dimerization respectively. **C.** BiFC-based assessment of TIR1 homo-dimerization with S462E/A464E-TIR1. **D.** BiFC-based assessment of TIR1 homo-dimerization. **A'-D'.** Propidium iodide (PI) staining of the nucleus.

Although it cannot be excluded that other Aux/IAA proteins may possibly bind to TIR1 and mediate TIR1-TIR1 self-interaction, the experimental evidence suggests that TIR1 homo-dimerization is independent of Aux/IAA binding, particularly in light of the high degree of sequence similarity within the conserved binding domain of Arabidopsis IAA proteins [25].

Identification of the TIR1 homo-dimerization domain

In order to identify the domain(s) responsible for TIR1 dimerization, a set of deletion mutants were cloned and expressed in BiFC vectors and subsequently assessed for their ability to homo-dimerize. BiFC results show that all the mutant variants failed to dimerize in a manner similar to that of TIR1- Δ F, suggesting that the TIR1 deletion variants possessed a conformational change in the protein structure and a corresponding reduction in stability. To examine the potential effect of the deletions on protein abundance, all TIR1 deletion mutants were cloned in a fusion-expression vector coding for N-terminal HA tags (pEarlygate201) and their steady state abundance was studied using Western blotting following expression in the Nicotiana system. The resulting blots revealed a pronounced reduction in mutant protein abundance in comparison to the wildtype, suggestive of instability of the deletion mutants (data not shown). The results seem consistent with the published tertiary structure for TIR1 that includes a highly hydrophobic core [4]. We suggest that arising from the particular topology of the TIR1 protein, the amino acid deletions made in this study likely significantly alter TIR1's tertiary structure, resulting in the exposure of the hydrophobic core and a corresponding reduction in stability of the protein.

Although the functional relevance of SCF ligase dimerization has not been well understood, one possibility is that F-box protein abundance is stabilized through the masking of otherwise exposed hydrophobic patches on the surface of the protein [15]. To investigate this possibility, we identified several hydrophobic patches in TIR1 that could participate in masking events through protein interaction. A select set of hydrophobic residues within these patches were mutated (Tyr 92 to Glu, Try95 to Ala, Leu441 to Ala, Leu525 to Ala and Leu573 to Ala) and subsequently assessed for homo-dimerization potential using the BiFC approach. All the mutants assessed for homo-dimerization were found to interact (data not shown). Due to the limited number of amino acid substitutions studied to date, the finding that the variant protein set continued to homo-dimerize does not rigorously exclude the possibility of an increased stability arising from homo-dimerization relative to the monomeric form. The results may merely reflect that the above amino acids are not involved in homo-dimerization of TIR1. Further experiments are required to assess the potential contribution of homo-dimerization on the stability of TIR1.

The combination of a weak Y2H interaction as shown in this study and the purification of TIR1 as a monomer following size exclusion chromatography of proteins expressed in insect cells (Dr. N. Zheng, University of Washington, personal communication) led us to investigate the potential role of a post-translational mechanism for the regulation of TIR1 homo-dimerization. To date, the sole post-translational modification reported for TIR1 is *S*-nitrosylation [10]. Although specific modified-amino acid sites have not yet been identified, Cys140 and Cys480 have been suggested to act as the *S*-nitrosylation regulatory site for the function of TIR1. We assessed the role of

Cys140 and Cys480 in TIR1 homo-dimerization by generating mutants (C140A- and C480A-TIR1) and assessing their homo-dimerization potential in the BiFC system. While C480A-TIR1 retained its ability to homo-dimerize, we found that C140A-TIR1 failed to homo-dimerize (**Figure 4.7C**) but retained the ability to interact with ASK1 (**Figure 4.7D**), although the interaction of C140A-TIR1 with ASK1 was relatively weak compared to that involving wildtype TIR1 (**Figure 4.7B**). To verify that the inability of C140A-TIR1 to homo-dimerize did not result from folding defects arising from the mutation of Cys140 to Ala, we mutated Cys140 to Met (C140M-TIR1) and assessed the homo-dimerization of this mutant variant. The results revealed that the C140M-TIR1 mutant failed to dimerize (**Figure 4.7E**), but retained the ability to interact with ASK1 in a manner similar to C140A-TIR1 (**Figure 4.7F**). Although Cys residues can contribute to disulfide bond formation, we noted that no other Cys residues are found within 3Å of Cys140 (the maximum length of a disulfide bond), diminishing the likelihood of intramolecular disulfide bond formation involving this residue. The two amino acids immediately adjacent to Cys140 (Ser139 and Glu141) and two highly conserved and surface-exposed amino acids in close vicinity of Cys140 (Gly142 and Thr145) were mutated to Ala to assess their contribution to TIR1's homo-dimerization. All the variants, with the exception of G142A-TIR1, retained their ability to homo-dimerize (**Figure 4.7G**). G142A-TIR1 interacted with ASK1 in a manner resembling that of C140A-TIR1 (**Figure 4.7H**). These results were confirmed as C140A-TIR1 and G142A-TIR1 did not homo-dimerize in a Y2H experiment, thus validating the BiFC experiment findings.

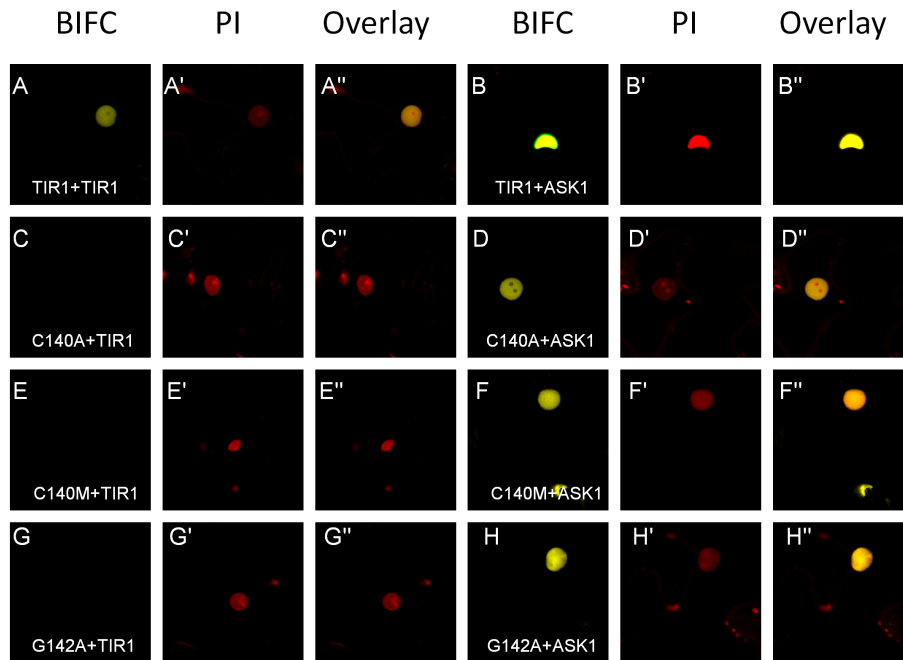


Figure 4.7. Cys140 and Gly142 mediate TIR1 homo-dimerization.

A,C,E,G. BiFC-based assessment of TIR1 homo-dimerization using TIR1, C140A-TIR1, V33E-TIR1 and G142A, respectively. **B,D,F,H.** BiFC-based assessment of ASK1 binding TIR1, C140A-TIR1, V33E-TIR1 and G142A, respectively. **A'-H'.** Propidium iodide staining of the nucleus.

These studies suggest that these two amino acids in close proximity of each other contribute to the homo-dimerization of TIR1 and define a domain necessary for TIR1 homo-dimerization.

TIR1 dimerization contributes to the degradation of IAA7

In order to assess whether TIR1's homo-dimerization is critical for the SCF^{TIR1} ligase-dependent ubiquitination of IAA substrates, we co-expressed wildtype and homo-dimerization-deficient TIR1's (C140A, C140M and G142A) along with IAA7 in the transient Nicotiana system. Interestingly, when we co-expressed IAA7 in the presence of TIR1, IAA7 was completely depleted from the sample. However, IAA7 levels were relatively stable when co-expressed with TIR1 homo-dimerization-deficient mutants (**Figure 4.8**). Thus, homo-dimerization-deficient TIR1 proteins show a reduced rate of substrate turnover.

To evaluate the potential effect of *S*-nitrosylation on TIR1 homo-dimerization, we treated Nicotiana leaves with the NO-donor, sodium nitroprusside (SNP), following injection with BiFC constructs. As shown in (**Figure 4.9B**), following application of SNP on leaves, an obvious increase in the signal intensity arising from the homo-dimerization of TIR1 was observed. To further assess the effect of NO on the homo-dimerization of TIR1, we treated leaves with hemoglobin, a NO scavenger. Interestingly, in the presence of hemoglobin we could not see any TIR-TIR1 BiFC fluorescence signal (**Figure 9C**), establishing the necessity of NO on TIR1's ability to homo-dimerize.

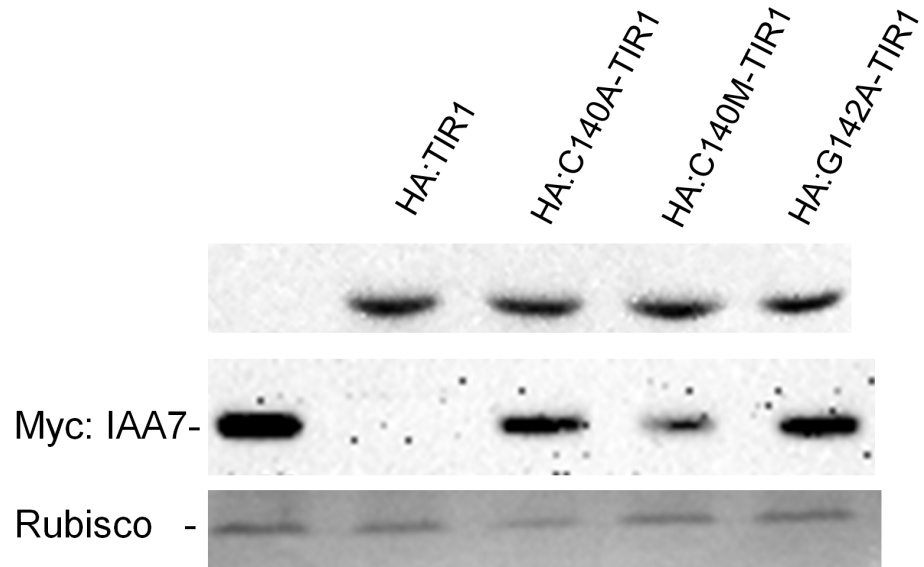


Figure 4.8. TIR1 homo-dimerization is essential for efficient degradation of the Aux/IAA proteins.

Western blotting on protein cell extracts from *Nicotiana* leaves expressing either IAA7 alone or co-expressing IAA7 and TIR1, or IAA7 and TIR1 homo-dimerization-deficient mutants.

To assess whether NO had any effects on TIR1 protein levels, we treated leaves expressing HA-TIR1 with SNP and the *de novo* protein synthesis inhibitor, cycloheximide (CHX), simultaneously. Interestingly, in the presence of SNP, TIR1 was considerably stabilized (**Figure 4.9D**). The increase in the stability of TIR1 following SNP treatment could be the result of enhanced TIR1 homo-dimerization.

To evaluate whether TIR1 homo-dimerization can lead to enhanced stability of TIR1 we treated plants expressing the TIR1 homo-dimerization-deficient mutants (C140A-TIR1 and G142A-TIR1) with SNP.

One possible scenario is that if indeed C140 is the chief residue responsible for *S*-nitrosylation, following SNP treatment we should not see an increase in C140A-TIR1 protein stability. Interestingly, in the presence of SNP and CHX we did not see an increase in C140A-TIR1 protein stability (**Figure 4.9D**). Furthermore, assessment of G142A-TIR1 protein abundance following SNP and CHX treatment did not result in an obvious increase in TIR1 protein levels (**Figure 4.9D**). The availability of the G142A-TIR1 homo-dimerization mutant, which is independent of C140, the potential *S*-nitrosylation site, allowed us to dissect the effect of nitrosylation from homo-dimerization on TIR1 protein stability and establish the necessity of *S*-nitrosylation mediated homo-dimerization on TIR1 protein stability.

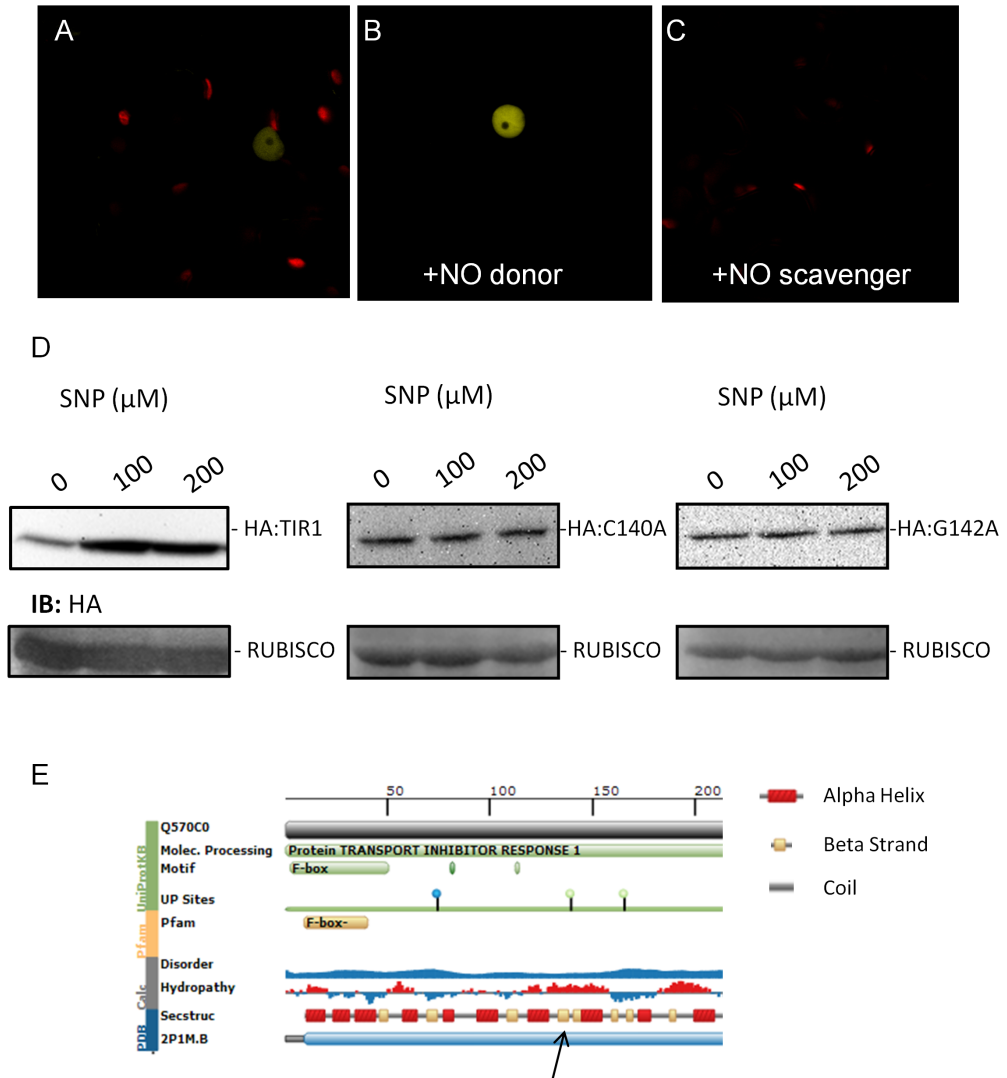


Figure 4.9. *S*-nitrosylation results in an increase in TIR1 protein stability.

A. BiFC-based assessment of TIR1 homo-dimerization. **B,C.** BiFC-based assessment of TIR1 homo-dimerization in the presence of SNP, an NO donor, and hemoglobin, an NO scavenger, respectively. **D.** Western blot of protein cell extracts from *Nicotiana* leaves expressing TIR1 or leaves expressing TIR1 and treated with SNP and cycloheximide 4 h following treatment. **E.** Schematic representation of TIR1 secondary structures along with the corresponding hydrophobicity plot.

CONCLUSION

Our understanding of auxin perception and signaling has been substantially advanced in recent years. Studies have demonstrated that auxin directly binds to TIR1, and in turn increases the affinity of TIR1 for the Aux/IAA protein [3,4,6]. However, despite the broad and essential roles that auxin plays in plant growth and development, the potential for auxin perception regulation at the level of substrate interaction is not clearly understood and remains to be elucidated. Here, we provide evidence for the homo-dimerization of the principal auxin receptor protein, TIR1. Although homo-dimerization among the WD-class of F-box proteins has been described [11-13,15-17,26], no corresponding evidence has been provided for the LRR class of F-box proteins. Thus, the self-interaction of TIR1 reported here is the first example of homo-dimerization involving a member of the LRR-class of F-box proteins in any species. Data presented here indicates that two amino acids, C140 and G142, play an essential role in the homo-dimerization of TIR1, since three mutants (C140A, C140M and G142A) are deficient in their ability to undergo homo-dimerization. We also assessed the degradation of Aux/IAA proteins in the presence of wildtype and mutant TIR1's and showed that the homo-dimerization of TIR1 is correlated with the efficient degradation of Aux/IAA proteins. Hence, these mutants are significantly incapacitated for the ubiquitination of Aux/IAA proteins in comparison to wildtype TIR1 protein. Furthermore, we have provided evidence that NO can result in an increase in the abundance of TIR1. The data provided here indicate that the increase in TIR1 abundance is mediated via an increase in the homo-dimerization of TIR1. We believe, given that residues mediating the homo-dimerization of TIR1 (C140 and G142) are residing within a highly hydrophobic and

surface exposed patch of TIR1 (**Figure 4.9E**), the homo-dimerization is potentially resulting in the burial of this hydrophobic patch within the interaction interface of TIR1-TIR1, resulting in an increase in TIR1 protein stability. The increase in TIR1 protein stability, in turn, results in more efficient degradation of the Aux/IAA proteins, allowing the plant to more competently respond to the presence of auxin.

Future work will primarily focus to address the molecular mechanism behind TIR1 stabilization and whether SCF^{TIR1} is subjected to auto-ubiquitination. Furthermore, a more in-depth understanding of the mechanism behind the deficiency in Aux/IAA protein degradation is required. Two potential scenarios that can be postulated is a decrease in the ubiquitination level of the substrate by SCF^{TIR1} or a decrease in the affinity of TIR1 towards Aux/IAA protein. Finally, assessment of TIR1's ability to homo-dimerize during development will provide a more in-depth understanding of the role auxin plays in the regulation of plant growth and development.

MATERIALS AND METHODS

***N. benthamiana* transient expression system**

Plasmids to be introduced in *N. benthamiana* were transformed into the AGL1 strain of *Agrobacterium tumefaciens* via electroporation. Successful introduction of transgenes were verified by *in situ* colony PCR. *Agrobacterium* cultures were infiltrated individually or co-infiltrated with cultures transformed with other expression constructs on the abaxial surface of 3-4-week-old *N. benthamiana* leaves. All *Agrobacterium* cultures were co-infiltrated with tomato bushy stunt virus p19 to suppress gene silencing.

Protein extraction and Western blotting

Proteins were extracted from *N. benthamiana* leaves transiently expressing indicated expression constructs 3 days post-infiltration. Leaves were flash frozen and ground in liquid nitrogen and mixed with 100 μ L of extraction buffer [100 mM TRIS-HCl (pH 7.5), 150 mM NaCl, 5 mM EDTA, 10 mM 2-mercaptoethanol, 10% glycerol, 0.1% Triton X-100, 1X EDTA-free Complete protease inhibitors (Roche, St. Louis, MO)] per 100 mg of ground tissue. Lysates were cleared by centrifugation at 14,000 *g* for 15 min and proteins were resolved by 12% SDS-PAGE. Proteins were subsequently transferred to a PVDF membrane using a TransBlot SD Semi-Dry Transfer unit (BioRad) and Bjerrum and Shaefer-Nielsen buffer (48 mM TRIS, 39 mM glycine, 0.00375% SDS, 20% methanol). Blots were then incubated in either anti-HA or Myc antibody overnight at 1:1,000 in 1% skim milk/TBST at 4°C overnight. Blots were then washed with TBST 3 times at 10 min intervals and incubated with secondary antibody (Santa Cruz Biotechnology), 1:10,000 in 2% skim milk/TBST for 1 h at room temperature. Blots were washed as previously described prior to exposure using Pico West Reagent (Fisher

Scientific) and visualized with an AlphaImager (Alpha Innotech Corp., San Leandro, CA).

Confocal imaging

Imaging of BiFC signals *in planta* was performed using an Olympus Model FV1000 point-scanning/point-detection laser scanning confocal microscope. Cyan Fluorescent Protein (CFP), Yellow fluorescent Protein (YFP) and propidium iodide (PI) were excited using 440, 512 and 543 nm laser lines, respectively. When using multiple fluorophores simultaneously, images were acquired sequentially in order to reduce excitation and emission overlaps. Olympus water immersion PLAPO60XWLSM (NA 1.0) and UPLSAPO 20x (NA 0.75) objectives were employed. Image acquisition was conducted at a resolution of 512 x 512 pixels, with a scan rate of 10 ms per pixel. Olympus FLUOVIEW v1.5 software was used for image acquisition and the export of TIFF files. Figures were assembled using GIMP 2.0 (<http://www.gimp.org/>).

BIBLIOGRAPHY

1. Mockaitis K, Estelle M (2008) Auxin receptors and plant development: a new signaling paradigm. *Annual review of cell and developmental biology* 24: 55-80.
2. Dharmasiri N, Dharmasiri S, Estelle M (2005) The F-box protein TIR1 is an auxin receptor. *Nature* 435: 441-445.
3. Kepinski S, Leyser O (2005) The Arabidopsis F-box protein TIR1 is an auxin receptor. *Nature* 435: 446-451.
4. Tan X, Calderon-Villalobos LI, Sharon M, Zheng C, Robinson CV, et al. (2007) Mechanism of auxin perception by the TIR1 ubiquitin ligase. *Nature* 446: 640-645.
5. Villalobos LIAC, Lee S, De Oliveira C, Ivetac A, Brandt W, et al. (2012) A combinatorial TIR1/AFB1/Aux/IAA co-receptor system for differential sensing of auxin. *Nature chemical biology* 8: 477-485.
6. Dharmasiri N, Dharmasiri S, Weijers D, Lechner E, Yamada M, et al. (2005) Plant development is regulated by a family of auxin receptor F box proteins. *Developmental cell* 9: 109-119.
7. Chapman EJ, Estelle M (2009) Mechanism of auxin-regulated gene expression in plants. *Annu Rev Genet* 43: 265-285.
8. Calderon-Villalobos LI, Tan X, Zheng N, Estelle M (2010) Auxin perception--structural insights. *Cold Spring Harb Perspect Biol* 2: a005546.
9. Kelley DR, Estelle M (2012) Ubiquitin-mediated control of plant hormone signaling. *Plant Physiol* 160: 47-55.
10. Terrile MC, Paris R, Calderón-Villalobos LIA, Iglesias MJ, Lamattina L, et al. (2012) Nitric oxide influences auxin signaling through S-nitrosylation of the Arabidopsis TRANSPORT INHIBITOR RESPONSE 1 auxin receptor. *The Plant Journal* 70: 492-500.
11. Barbash O, Diehl JA (2008) SCFFbx4 B-crystallin E3 ligase: When one is not enough. *Cell Cycle* 7: 2983-2986.
12. Barbash O, Zamfirova P, Lin DI, Chen X, Yang K, et al. (2008) Mutations in Fbx4 Inhibit Dimerization of the SCFFbx4 Ligase and Contribute to Cyclin D1 Overexpression in Human Cancer. *Cancer cell* 14: 68-78.
13. Li Y, Hao B (2010) Structural Basis of Dimerization-dependent Ubiquitination by the SCF^{Fbx4} Ubiquitin Ligase. *Journal of Biological Chemistry* 285: 13896-13906.

14. McMahon M, Thomas N, Itoh K, Yamamoto M, Hayes JD (2006) Dimerization of Substrate Adaptors Can Facilitate Cullin-mediated Ubiquitylation of Proteins by a "Tethering" Mechanism. *Journal of Biological Chemistry* 281: 24756-24768.
15. Merlet J, Burger J, Gomes JE, Pintard L (2009) Regulation of cullin-RING E3 ubiquitin-ligases by neddylation and dimerization. *Cellular and molecular life sciences* 66: 1924-1938.
16. Tang X, Orlicky S, Lin Z, Willems A, Neculai D, et al. (2007) Suprafacial Orientation of the SCFCdc4 Dimer Accommodates Multiple Geometries for Substrate Ubiquitination. *Cell* 129: 1165-1176.
17. Welcker M, Clurman BE (2007) Fbw7/hCDC4 dimerization regulates its substrate interactions. *Cell Div* 2.
18. Deshaies RJ, Joazeiro CAP (2009) RING domain E3 ubiquitin ligases. *Annual review of biochemistry* 78: 399-434.
19. Kerppola TK (2008) Bimolecular fluorescence complementation (BiFC) analysis as a probe of protein interactions in living cells. *Annu Rev Biophys* 37: 465-487.
20. Kerppola TK (2006) Visualization of molecular interactions by fluorescence complementation. *Nat Rev Mol Cell Biol* 7: 449-456.
21. Waadt R, Kudla J (2008) In Planta Visualization of Protein Interactions Using Bimolecular Fluorescence Complementation (BiFC). *CSH Protoc* 2008: pdb prot4995.
22. Nelson DE, Laman H (2011) A Competitive binding mechanism between Skp1 and exportin 1 (CRM1) controls the localization of a subset of F-box proteins. *J Biol Chem* 286: 19804-19815.
23. Kim J, Harter K, Theologis A (1997) Protein-protein interactions among the Aux/IAA proteins. *Proc Natl Acad Sci U S A* 94: 11786-11791.
24. Ouellet F, Overvoorde PJ, Theologis A (2001) IAA17/AXR3: biochemical insight into an auxin mutant phenotype. *Plant Cell* 13: 829-841.
25. Ramos JA, Zenser N, Leyser O, Callis J (2001) Rapid degradation of auxin/indoleacetic acid proteins requires conserved amino acids of domain II and is proteasome dependent. *Plant Cell* 13: 2349-2360.
26. Kirk R, Laman H, Knowles PP, Murray-Rust J, Lomonosov M, et al. (2008) Structure of a conserved dimerization domain within the F-box protein Fbxo7 and the PI31 proteasome inhibitor. *Journal of Biological Chemistry* 283: 22325-22335.

VITA AUCTORIS

NAME: Mohammad Haj Dezfulian

PLACE OF BIRTH: Dezfool, Iran

YEAR OF BIRTH: 1983

EDUCATION: Chamran University of Ahvaz, Ahvaz, Iran
2002-2006 B.Sc.